

DISSERTATION  
*IN VIVO* DIRECT MEASUREMENT OF MYOCARDIAL OXYGEN CONSUMPTION  
IN DIFFERENT ANIMAL MODELS

Submitted by  
Catriona M. MacPhail, DVM  
Department of Clinical Sciences

In partial fulfillment of the requirements  
for the Degree of Doctor of Philosophy  
Colorado State University  
Fort Collins, Colorado  
Spring, 2007

UMI Number: 3266355

### INFORMATION TO USERS

The quality of this reproduction is dependent upon the quality of the copy submitted. Broken or indistinct print, colored or poor quality illustrations and photographs, print bleed-through, substandard margins, and improper alignment can adversely affect reproduction.

In the unlikely event that the author did not send a complete manuscript and there are missing pages, these will be noted. Also, if unauthorized copyright material had to be removed, a note will indicate the deletion.

**UMI**<sup>®</sup>

---

UMI Microform 3266355

Copyright 2007 by ProQuest Information and Learning Company.

All rights reserved. This microform edition is protected against unauthorized copying under Title 17, United States Code.

ProQuest Information and Learning Company  
300 North Zeeb Road  
P.O. Box 1346  
Ann Arbor, MI 48106-1346

COLORADO STATE UNIVERSITY

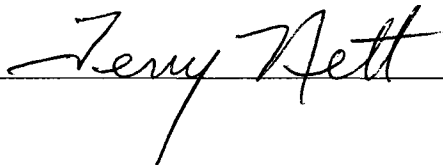
March 29, 2007

WE HEREBY RECOMMEND THAT THE DISSERTATION PREPARED UNDER OUR SUPERVISION BY CATRIONA M. MACPHAIL, DVM, ENTITLED *IN VIVO* DIRECT MEASUREMENT OF MYOCARDIAL OXYGEN CONSUMPTION IN DIFFERENT ANIMAL MODELS, BE ACCEPTED AS FULFILLING IN PART REQUIREMENTS FOR THE DEGREE OF DOCTOR OF PHILOSOPHY.

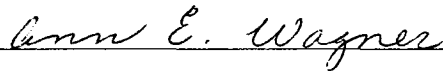
Committee on Graduate Work



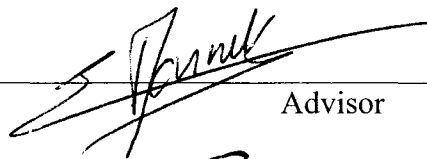
---



---



---



---

Advisor



---

Department Head

ABSTRACT OF DISSERTATION  
*IN VIVO* DIRECT MEASUREMENT OF MYOCARDIAL OXYGEN CONSUMPTION  
IN DIFFERENT ANIMAL MODELS

Myocardial oxygen consumption ( $MVO_2$ ) is an important indicator of cardiac performance reflecting oxygen supply and demand. It is a valuable physiological tool as  $MVO_2$  provides a quantifiable link between myocardial performance and total metabolism. Indirect measurement of  $MVO_2$  relies on extrapolation of hemodynamic parameters, as a reasonable correlation exists between  $MVO_2$  and measurements based on the left ventricular pressure-volume relationship. However, multiple factors influence oxygen consumption and must be taken into account when  $MVO_2$  is estimated. Major determinants of  $MVO_2$  include myocardial mass, heart rate, contractility, and wall stress, with minor influences from preload, basal oxygen requirement, and activation energy.  $MVO_2$  can be directly determined from a variety of methods, but requires measurement of myocardial blood flow by some process. Microsphere technology allows calculation of myocardial blood flow, but requires organ harvest. Direct catheterization of the coronary sinus allows determination of coronary sinus blood flow and  $MVO_2$  is then calculated as the product of coronary blood flow and coronary arterio-venous oxygen content difference, which is divided by heart rate to yield  $MVO_2$  per beat.

Myocardial oxygen consumption was calculated through measurement of myocardial blood flow using colored microsphere technology to determine the effect of sevoflurane on cardiac performance in ferrets. A dose-dependent decrease in arterial blood pressure, left ventricular pressure, systemic vascular resistance, aortic flow, and  $dp/dt$  (an index of contractility) was detected as expired concentration of sevoflurane increased. Heart rate, central venous pressure, coronary vascular resistance, myocardial oxygen extraction ratio, and  $\tau$  (the time constant of relaxation) were unchanged. Cardiac external work decreased, as did myocardial oxygen consumption, causing increased cardiac efficiency at higher concentrations of sevoflurane. Sevoflurane caused minimal and predictable cardiovascular effects in ferrets without increasing myocardial metabolic demands. Data obtained from this study have not been previously reported for a species that is being commonly used in cardiovascular research.

Colored microsphere technology was also used to determine myocardial oxygen consumption in a canine model of altered splanchnic blood flow. A model was developed for this study to examine the direct cardiovascular effects of two pathophysiological events (gastric ischemia and portal hypertension) that occur during gastric dilatation-volvulus (GDV), a severe clinical syndrome of the canine patient, independent of the effect of other events that overtly influence hemodynamics (caudal vena cava occlusion and thoracic impingement). The hypothesis of this study is that the alterations in splanchnic blood flow that occur early in the course of GDV cause early intrinsic cardiac damage due to interference with myocardial energy transfer. This damage may make the heart more susceptible to injury from further hemodynamic and hypoxic insults. It was found that portal hypertension and gastric ischemia caused an

increase in  $MVO_2$ , while cardiac external work was maintained. Therefore, a less efficient transfer of energy occurred in the myocardium following alteration of splanchnic blood flow. We speculate that reduction of cardiac efficiency could be an early event that occurs in GDV that may predispose these dogs to further cardiac dysfunction.

The use of  $MVO_2$  is of considerable value in determining the effectiveness of medical and surgical interventions for the treatment of heart failure. Numerous heart failure models in a variety of species have been developed, all with their unique advantages and disadvantages. However, none of the models are the ideal reproduction of the human cardiac failure. Anthracycline-induced cardiac injury is most commonly performed using Adriamycin. This model not only replicates the clinical occurrence of doxorubicin-induced cardiotoxicity observed in cancer patients, but also causes severe dilated cardiomyopathy and heart failure that is seen in clinical dilated cardiomyopathy of various etiologies. A previously established protocol for Adriamycin-induced cardiomyopathy was altered in an effort to create a more consistent and less lethal model of heart failure. Adjustments that were enacted included a decrease in the cumulative dose of Adriamycin, reduction in number of intracoronary injections, and distribution of Adriamycin injection between the descending branch and the circumflex branch of the left coronary artery. The protocol of 22.5mg Adriamycin in 60mL saline administered intracoronary weekly for 2 weeks with concurrent administration of verapamil resulted in a predictable and severe model of dilated cardiomyopathy with reduced overall mortality compared to a previously published protocol. This protocol for induction of heart failure

described here is relatively fast, technically simple, well tolerated by the animal, and has an acceptable mortality rate.

Previous studies have demonstrated that in dogs with Adriamycin-induced cardiomyopathy, an unstimulated skeletal muscle wrap placed around the heart maintains cardiac efficiency and cardiac functional reserve while allowing reverse ventricular remodeling by preventing further ventricular dilatation, reducing afterload, and preserving diastolic function. As there is significant morbidity associated with latissimus dorsi muscle harvest, the objective of the last experiment was to determine whether a prosthetic cardiac wrap would have the same function as an unstimulated muscle wrap. The hypotheses were that in a canine model of cardiomyopathy, prosthetic cardiac binding would provide a myocardial sparing effect, preserve cardiac functional reserve, and would not interfere with diastolic function.

Twelve normal adult large-breed dogs were used in this study and cardiomyopathy was induced in all dogs by the protocol described above. Three weeks after the last injection of Adriamycin, left and right heart catheterization was performed and echocardiography was repeated. Dogs were then randomly split into two groups with one group to undergo prosthetic cardiac binding (treatment group) and the other group to have no treatment (control group). Treatment dogs underwent surgery one week after baseline cardiac catheterization. Through a median sternotomy, the pericardium was resected at the level of the atrioventricular groove and replaced with polypropylene mesh. The mesh was sutured to the remaining pericardium and was in direct contact with the epicardium of the right and left ventricles. Echocardiography was performed three and six weeks after surgery and a terminal cardiac catheterization was performed at six weeks

postoperatively. Left ventricular dimensions were unchanged in the treatment group from the time of surgery until 6 weeks postoperatively compared to control dogs whose parameters significantly increased during that same time frame ( $p = 0.005$ ). However, no difference in cardiac function was found between treatment and control dogs. Therefore, while prosthetic cardiac binding may limit progressive cardiac dilatation, no improvement in cardiac function is attained with this procedure in dogs with Adriamycin-induced cardiomyopathy.

Catriona M. MacPhail, DVM  
Department of Clinical Sciences  
Colorado State University  
Fort Collins, Colorado  
Spring 2007

## ACKNOWLEDGEMENTS

I would like to express my sincere gratitude to the following individuals:

My advisor and mentor, Dr. Eric Monnet.

The members of my committee, Dr. Scott Earley, Dr. Terry Nett, and Dr. Ann Wagner.

Dr. Jamie Gaynor, Dr. David Getzy, Ms. June Boon, Ms. Denise Parker, and Ms. Tara Raske for their advice and assistance in the various experiments.

Dr. Paul Lunn and Dr. Peter Dorhout for their guidance and encouragement.

Dr. Howard Seim and Dr. Martha Tissot Van Patot for their unconditional support.

My parents, Dr. and Mrs. Donald C. MacPhail, for always being there.

Dr. Michael Lappin for his unwavering love, support, and encouragement.

## DEDICATION

*For Dr. Alan Tucker  
(1947 – 2004)*

## TABLE OF CONTENTS

Abstract	iii
Acknowledgements	vii
Dedication	ix
List of Tables	xi
List of Figures	xii
Introduction and Literature Review	1
Epidemiology of Heart Failure	2
Pathophysiology of Heart Failure	3
Medical Management of Heart Failure	9
Surgical Treatment of Heart Failure	10
Experimental Induction of Cardiac Dysfunction	24
Evaluation of Cardiac Function	30
Aims, Rationale, and Objectives	44
Bibliography	47
CHAPTER 1	
Evaluation of sevoflurane on hemodynamic and cardiac energetic parameters in normal ferrets	59
CHAPTER 2	
Evaluation of cardiac performance in the dog after induction of portal hypertension and gastric ischemia	82
CHAPTER 3	
Adjustments in protocol for induction of canine heart failure by intracoronary Adriamycin injection decreases untimely mortality	105
CHAPTER 4	
Evaluation of prosthetic cardiac binding as an interventional treatment in a canine model of Adriamycin-induced dilated cardiomyopathy	128
CONCLUSIONS AND FUTURE DIRECTIONS	
Effect of ascending versus descending dynamic aortomyoplasty on hemodynamic and cardiac energetic parameters of normal dogs	162

## LIST OF TABLES

### Introduction & Literature Review

1. Reported causes and associations with dilated cardiomyopathy pg. 6
2. Comparison of characteristics between restrictive cardiomyopathy and constrictive pericarditis pg. 9
3. Factors affecting diastolic distensibility of the left ventricle. pg. 41

### Chapter 1

- 1-1. Mean  $\pm$ SD values for hemodynamic parameters at various expired concentrations of sevoflurane in 7 ferrets. pg. 77
- 1-2. Mean  $\pm$  SD values for calculated hemodynamic and energetic parameters at varying levels of sevoflurane concentration. pg. 78
- 1-3. Mean  $\pm$  SD values for blood gas parameters at various expired concentrations of sevoflurane in 7 ferrets. pg. 79

### Chapter 2

- 2-1. Hemodynamic parameters at baseline, following induction of portal hypertension, and following creation of portal hypertension and gastric ischemia. LV, left ventricle; SVR, systemic vascular resistance; CVR, coronary vascular resistance. pg. 102

### Chapter 3

- 3-1. Echocardiographic data presented as mean  $\pm$  standard deviation for dogs receiving 22.5mg Adriamycin weekly for two weeks. pg. 125
- 3-2. Hemodynamic data presented as mean  $\pm$  standard deviation for dogs receiving 22.5mg Adriamycin weekly for two weeks. pg. 125

### Chapter 4

- 4-1. Selected echocardiographic and hemodynamic data from control and treatment dogs at 12 weeks presented as mean  $\pm$  standard deviation. P-values less than 0.05 were considered significant. pg. 153

## LIST OF FIGURES

### Introduction & Literature Review

1. Law of LaPlace:  $T$  (tension) =  $(P \times \text{radius } [r]) / (2 \times \text{wall thickness } [\mu])$  pg. 5
2. Single pressure-volume loop demonstrating the cardiac cycle. pg. 33
3. Multiple pressure-volume loops demonstrating the end-systolic and end-diastolic pressure-volume relationships. pg. 34
4. Diagram of the time-varying elastance model demonstrating the pressure-volume area (PVA), which consists of the area with the pressure-volume loop, external work (EW) plus the area underneath the ESPVR line and to the left of the isovolumic relaxation segment, the potential energy (PE). pg. 35
5. A left and upward shift of the curve of the EDPVR indicates less ventricular compliance. pg. 40

### Chapter 1

- 1-1. Effect of increasing expired concentration of sevoflurane on cardiac energetic parameters: A) myocardial oxygen consumption ( $P = 0.04$ ), B) cardiac external work ( $p = 0.0002$ ), and C) cardiac efficiency ( $P = 0.02$ ). pg. 80

### Chapter 2

- 2-1. Comparison of myocardial oxygen consumption (mean  $\pm$  standard deviation;  $n=5$ ) obtained at baseline, 30 minutes after induction of portal hypertension ( $P = 0.003$ ), and 30 minutes after creation of gastric ischemia ( $P = 0.024$ ). pg. 103
- 2-2. Comparison of cardiac efficiency (mean  $\pm$  standard deviation;  $n=5$ ) obtained at baseline, 30 minutes after induction of portal hypertension, and 30 minutes after creation of gastric ischemia. pg. 104

### Chapter 3

- 3-1a. Actuarial survival curve dogs receiving 22.5mg intracoronary Adriamycin weekly for 2 weeks. pg. 126
- 3-1b. Actuarial survival curve from Monnet et al,<sup>4</sup> for dogs receiving 15mg intracoronary Adriamycin weekly for 4 weeks. pg. 126
- 3-2. Representative section of normal canine myocardium (40x). pg. 127
- 3-3. Representative section of canine myocardium (40x) following intracoronary administration of Adriamycin. pg. 127

## Chapter 4

- 4-1. Intraoperative photographs following completion of prosthetic cardiac binding in 6 dogs. pg. 154
- 4-2. Variably loaded pressure-volume loops for Dog #3. pg. 155
- 4-3. Comparison of ESPVR in Dog #3 at 6 weeks and 12 weeks. pg. 155
- 4-4. Ejection fraction of the control group (■) and treatment group (■) at baseline, 5 weeks, and 12 weeks. pg. 156
- 4-5. Fractional shortening of the control group (■) and treatment group (■) at baseline, 5 weeks, and 12 weeks. pg. 157
- 4-6. Comparison of ejection fraction of individual dogs; Control dogs = C# (--◇--); Treatment dogs = T# (—□—). pg. 158
- 4-7. Comparison of fractional shortening of individual dogs; Control dogs = C# (--◇--); Treatment dogs = T# (—□—). pg. 158
- 4-8. Left ventricular diastolic volume index (LVDVI) of the control group (■) and treatment group (■) at baseline, 5 weeks, and 12 weeks. pg. 159
- 4-9. Left ventricular end-diastolic pressure of the control group (■) and treatment group (■) at 5 weeks and 12 weeks (P-value = NA). pg. 160
- 4-10. Comparison of LVEDP of individual dogs; Control dogs = C# (--◇--); Treatment dogs = T# (—□—). pg. 160
- 4-11. Representative section of epicardium (10x). Clear spaces (arrows) are areas of mesh dropout. These areas are surrounded by a mild to moderate inflammatory reaction. pg. 161
- 4-12. Representative section of epicardium (10x). Fragments of mesh can be seen in the clear spaces (black arrow). A moderate inflammatory reaction with multinucleated giant cells white arrow) surrounds these clear spaces. pg. 161

## Conclusions & Future Directions

- 5-1. Comparison of cardiac efficiency over time for control dogs and dogs undergoing dynamic cardiomyoplasty, adynamic cardiomyoplasty, and prosthetic cardiac binding. A significant improvement of cardiac efficiency was only present in the dogs receiving dynamic cardiomyoplasty. pg. 163

5-2. Intraoperative photograph of ascending dynamic aortomyoplasty. pg. 176

5-3. Intraoperative photograph of descending dynamic aortomyoplasty. pg. 176

## INTRODUCTION & LITERATURE REVIEW

### *Epidemiology of Heart Failure*

According to the World Health Organization (WHO) an estimated 16.7 million people in the world die from cardiovascular disease each year (Mackay and Mensah, 2004). The WHO also estimates that by the year 2020, cardiovascular disease will cause 25 million deaths a year. Cardiovascular disease is the leading cause of death in Europe with over 4 million deaths per year, accounting for almost 50% of all deaths (British Heart Foundation, 2000). The latest figures from the American Heart Association document that cardiovascular disease affects 79,400,000 people, or 33.3% of the population of the United States (American Heart Association, 2007). Cardiovascular disease was also responsible for 36.3% of all deaths in the United States in 2004 (Minino et al, 2006). Cardiovascular disease causes an average of 1 death every 34 seconds with nearly 2,600 people dying each day, which is more than the next 5 leading causes of death. The estimated direct and indirect cost of cardiovascular disease and stroke for 2007 is \$431.8 billion (American Heart Association, 2007).

Overall mortality from cardiovascular disease has declined in the last twenty years; however death specifically from heart failure has substantially increased (Dec, 2004). Reasons for this increase are uncertain, but improvements in recognition and treatment of coronary artery disease are thought to have contributed to the increase in patients that go on to develop chronic left ventricular dysfunction and subsequent congestive heart failure (Starling, 1998). Heart failure is the primary cause of death of 40,000 to 45,000 people a year in the United States and is a contributory factor in an additional 200,000 deaths (Massie and Shah, 1997). One year mortality rates based on New York Heart Association (NYHA) classification have been estimated at 10%, 20%,

and 40% for heart failure classes II, III, and IV, respectively (Guyatt and Devereaux, 2004). The cost to care for people in heart failure accounts for 5% of the national health care budget (Westaby, 2003) with direct and indirect costs estimated for 2004 at \$33.2 billion (American Heart Association, 2007). Yearly hospitalization rates average from 2,000 per million for patients under 65 to 18,000 per million for those over 65 years old; 29% to 47% of patients are readmitted within 6 months of the initial hospital discharge. Over the last 10 years, hospitalizations for heart failure have increased by 70% (Lloyd-Jones, 2001). Median survival following onset of symptoms and diagnosis of heart failure is only 2.5 years with 80% of men and 70% of women under the age of 65 dying within 8 years of diagnosis (American Heart Association, 2007). Death due to heart failure has increased 155% since 1979 with sudden cardiac death 6 to 9 times more likely to occur in people with heart failure versus the general population. Although medical management of heart failure has made great strides within the last several years, it is still believed that 1 out of 3 patients with heart failure gain no symptomatic relief from standard medical care (Westaby, 2003).

### ***Pathophysiology of Heart Failure***

Heart failure used to be simply characterized as a loss of left ventricular contractile function. However, current understanding is that heart failure is an extremely complex process that involves systolic and/or diastolic dysfunction, structural changes of ventricular chambers, and peripheral vascular responses mediated by neuroendocrine processes. Ventricular remodeling is the term used to describe the pathologic change in shape of the left ventricle that occurs secondary to contractility impairment. Remodeling

is best defined as the change in chamber volume and shape unrelated to preload-mediated increase in sarcomere length (Cohn, 1995). The left ventricle changes from its normal elliptical shape to a dilated sphere that has limited contractile function and filling capacity (Westaby, 2003). Structural changes in the myocardium are most commonly due to infarction, as in ischemic cardiomyopathy, or myocyte hypertrophy, as in dilated cardiomyopathy. A change in left ventricular shape typically leads to increase in chamber volume that will increase systolic load. The consequence is systolic dysfunction as chamber volume increases out of proportion to ventricular mass, resulting in significant increases in wall stress (Pfeffer, 2002). Ventricular remodeling is thought to be a progressive process even when patients with heart failure appear clinically stable. It is also thought to be potentially reversible if recognized and treated early (Pfeffer, 2002).

There are multiple causes of heart failure. Most applicable to this dissertation is a discussion of primary myocardial disease, or cardiomyopathy. Cardiomyopathies are traditionally classified by anatomic manifestation: dilated, hypertrophic, and restrictive. Dilated cardiomyopathy is the most common form and has a variety of underlying causes. Dilated cardiomyopathy is characterized by systolic dysfunction resulting in left ventricular or biventricular dilatation; it is the primary indication for heart transplantation. Hypertrophic cardiomyopathy is the inappropriate thickening of the ventricular wall and interventricular septum. Restrictive cardiomyopathy is characterized by impaired diastolic function due to abnormal rigidity of the ventricular walls that impede filling, while systolic function remains intact. It can be difficult to clinically differentiate restrictive cardiomyopathy from constrictive pericarditis.

## DILATED CARDIOMYOPATHY

Dilated cardiomyopathy has an incidence of 36.5 cases per 100,000 (Codd et al, 1989). It accounts for nearly 10,000 deaths each year in the United States (Manolio et al, 1992). However, the actual incidence is probably much higher as the disease is typically asymptomatic in initial stages and many cases may go unrecognized (Dec and Fuster, 1994). There are multiple causes of dilated cardiomyopathy including viral infection, bacterial infection, or a variety of toxins (Table 1). However, the majority of dilated cardiomyopathy patients will have no obvious underlying cause (Hosenpud, 1988).

Asymptomatic systolic dysfunction is the first stage of dilated cardiomyopathy, but the rate of progression is unknown. Due to the reduction in myocardial contractility, the heart dilates out of proportion to the degree of hypertrophy resulting in an increased radius:wall thickness ratio. Cardiac function is further compromised due to an increase in myocardial wall stress and a decrease in subendocardial coronary blood flow. According to the Law of LaPlace, wall stress, or tension, directly depends on the pressure (P) produced in the ventricles, as well as the size and shape of the heart (Figure 1).

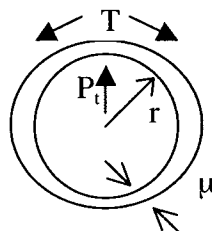


**Figure 1. Law of LaPlace:  $T$  (tension) =  $(P \times \text{radius } [r]) / (2 \times \text{wall thickness } [\mu])$**

The diameter of the ventricle increases to compensate for the decrease in cardiac output, but it also causes an increase in systolic wall stress. Increased wall stress induces a degree of ventricular hypertrophy, but it is not typically enough to compensate for the ventricular dilatation. Increased wall stress also eventually causes a reduction in ejection fraction and cardiac output (McElroy et al, 1989).

**Table 1. Reported causes and associations with dilated cardiomyopathy (Hosenpud, 1994)**

---

1. Idiopathic	d. Diabetes mellitus
2. Infectious	e. Beriberi
a. Viral	f. Selenium deficiency
i. Coxsackievirus	g. Kwashiorkor
ii. Echovirus	5. Collagen vascular disease
iii. Adenovirus	a. Lupus erythematosus
iv. Arbovirus	b. Dermatomyositis
b. Bacterial	6. Polyarteritis nodosa
i. Diphtheria	7. Neuromuscular disease
ii. Tuberculosis	a. Duchenne's disease
iii. Leptospirosis	b. Fredreich's ataxia
c. Rickettsial	c. Limb girdle
i. Typhus	d. Neurofibromatosis
ii. Q fever	e. Myasthenia gravis
d. Protozoal	8. Toxins
i. Chagastic	a. Alcohol
ii. Malarial	b. Arsenic
iii. Leishmaniasis	c. Cobalt
3. Granulomatous	d. Lead
a. Idiopathic	e. Carbon tetrachloride
b. Sarcoidosis	f. Carbon monoxide
c. Giant cell	g. Catecholamines
d. Wegner's	h. Amphetamines
4. Metabolic / Endocrine	i. Cocaine
a. Acromegaly	j. Anthracyclines
b. Hypothyroidism	k. Cyclophosphamide
c. Pheochromocytoma	

Once patients become symptomatic, prognosis dramatically worsens; progressive heart failure is the cause of death in 75% of dilated cardiomyopathy patients, while most others die suddenly from arrhythmias (Dec and Fuster, 1994).

#### RESTRICTIVE CARDIOMYOPATHY

Restrictive cardiomyopathy is an abnormality of diastolic relaxation resulting in restricted ventricular filling, high filling pressures, and reduced stroke volume in the face of normal systolic function due to reduction of total ventricular volume. The impairment of diastolic function arises from a reduction in ventricular compliance due to a number of causes revolving around infiltrative disease of the myocardium (amyloidosis, radiation injury, fibrosis); however idiopathic restrictive cardiomyopathy, where the myocardium is intrinsically abnormal, appears to be most common. The diseased myocardium resists stretching during ventricular filling

#### CONSTRICTIVE PERICARDITIS

Although not a primary disease of the myocardium, a discussion of constrictive pericarditis is warranted due to the nature of the main project (Chapter 4: Evaluation of prosthetic cardiac binding as an interventional treatment in a canine model of Adriamycin-induced dilated cardiomyopathy). Constrictive pericarditis and restricted cardiomyopathy share some functional resemblance. Constrictive pericarditis occurs when the pericardium becomes thickened and fibrotic resulting in restriction of diastolic filling. It is typically a symmetrical process that uniformly affects all cardiac chambers. Tuberculosis used to be the most common cause of constrictive pericarditis. However, currently idiopathic and viral etiologies are most common (Cameron et al, 1987; Mehta et

al, 1999). Constrictive pericarditis is also a major complication following cardiac surgery (D’Cruz et al, 1992). The treatment of choice is pericardiectomy.

#### RESTRICTIVE CARDIOMYOPATHY VERSUS CONSTRICTIVE PERICARDITIS

It can be very difficult to differentiate constrictive pericarditis from restrictive cardiomyopathy (Table 2). The conditions are hemodynamically similar as right and left ventricular diastolic pressures are elevated, stroke volume and cardiac output are depressed, left ventricular end-diastolic volume is normal or decreased, and diastolic filling is impaired (Lorell and Grossman, 2000). Both constrictive pericarditis and restrictive cardiomyopathy have characteristic left and right ventricular filling pressure tracings. The “dip and plateau” or “square root” sign reflects early and rapid ventricle filling that levels early in diastole as the limits of pericardial or ventricular compliance is reached. In constrictive pericarditis there is elevation and equilibrium of diastolic pressures in all four cardiac chambers. This is in contrast to restrictive cardiomyopathy where filling pressures in the right and left ventricles are elevated, but not equalized. Assessment of diastolic filling through traditional angiography, radionuclide angiography, or Doppler echocardiography may also help differentiate between these two conditions (Tyberg et al, 1981; Aroney et al, 1989) . In constrictive pericarditis, 80% of diastolic filling occurs in the first half of diastole, whereas in restrictive cardiomyopathy, early diastolic filling is slow and sluggish. Ultimately, endomyocardial biopsy is required to distinguish constrictive pericarditis from restrictive cardiomyopathy if other tests have not been helpful (Schoenfeld et al, 1987).

**Table 2. Comparison of characteristics between restrictive cardiomyopathy and constrictive pericarditis (Hosenpud 1994, Lorell 1997).**

---

	<b>RESTRICTIVE</b>	<b>CONSTRICTIVE</b>
<b>Pericardial knock</b>	Absent	May be present
<b>Valvular murmurs</b>	Possible	Absent
<b>Kussmaul's sign</b>	Absent	May be present
<b>Imaging studies (CT, MRI)</b>	Normal pericardium	Thickened pericardium
<b>Left ventricular filling rate</b>	Delayed	Rapid and early
<b>Ventricular pressures</b>	Disparate LV vs. RV filling	Equal RV and LV filling
<b>Endomyocardial biopsy</b>	Abnormal	Normal

***Medical Management of Heart Failure***

Medical management of heart failure primarily is directed at improving systolic function. Standard practice often employs diuretics, angiotensin converting enzyme (ACE) inhibitors, and beta-blockers. The main objective of the use of ACE inhibitors and beta-blockers in patients with heart failure is to block the neuroendocrine processes. Numerous studies have demonstrated the consistent improvement in clinical signs and reduction in mortality and hospitalizations associated with use of ACE inhibitors in a wide variety of patients (Garg and Yusuf, 1995). ACE-inhibitors have been shown to be beneficial in both the short and long term for reasons that extend beyond the basic vasodilating properties of these drugs. Angiotensin II blockade allows for reversal of vasoconstriction, limits sodium retention and potassium excretion, and inhibits

angiotensin II-mediated myocyte hypertrophy. The use of beta-blockers used to be considered contraindicated in heart failure patients (Bristow, 2000). However, significant clinical data has been accumulated to support the use of beta-blockers to treat patients with systolic dysfunction (Krum, 1999). Beta-blockers consistently improve left ventricular function by a mechanism that is not well understood (Bristow et al, 1996). One theory is that chronic adrenergic bombardment that the myocardium suffers when in failure is a main contributor to the progression of ventricular remodeling and that interference by beta-blockers with the chronic sympathetic stimulation can slow or halt that progression. In spite of marked improvements in pharmacologic therapy for heart failure, medical management is still associated with progression of clinical signs, further ventricular remodeling, and high intermediate-term mortality rates (Dec, 2004).

### ***Surgical Treatment of Heart Failure***

Aside from the gold standard treatment of heart transplantation, there are several distinct approaches of surgical treatment of heart failure that are currently undergoing clinical and experimental trials. Simply, the goal of surgical therapy for heart failure is to replace, resect, or support the failing left ventricle.

#### **SURGICAL REPLACEMENT**

Replacement is best exemplified by cardiac transplantation, which is considered the only established and widely accepted surgical treatment of heart failure. The prognosis following transplantation has improved with 1, 5, and 10 year survival estimated at 85%, 70%, and 60%, respectively with over 90% of patients returning to NYHA Class I (Hosenpud et al, 2001). Despite this positive outlook, only 2,202 heart

transplants were performed in the United States in 2001, with over 25,000 patients on the waiting list. In addition, it is estimated that 45,000 to 70,000 patients per year would benefit from this course of treatment (American Heart Association, 2007). This is primarily due to lack of availability of donor hearts and increase in number of potential candidates.

The total artificial heart is an optimistic alternative to transplantation, however postoperative complications and size limitations have limited its use. The most recent model is the Abiomed Abiocor™ (Abiomed Inc., Danvers, MA) replacement heart that was recently implanted for the 14<sup>th</sup> time ([www.abiomed.com/Fabiocar.html](http://www.abiomed.com/Fabiocar.html)). An exciting alternative to the Abiocor artificial heart is the Arrow Lionheart™ (Arrow International Inc., Reading, PA), which is a completely implantable total electric artificial heart, with no wires or tubes protruding externally through the skin. The Lionheart is currently in Phase I clinical trials in the United States. In contrast to the total artificial heart, removal of the patient's native heart is not necessary for implantation of the Lionheart. The Lionheart is touted as a permanent left ventricular assist system (LVAS) for patients with severe heart failure ineligible for transplantation ([www.arrowintl.com/products/card\\_assist/](http://www.arrowintl.com/products/card_assist/)). Other types of left ventricular assist devices (LVAD) are primarily considered to be "bridges", either to recovery or transplantation. However, newer LVAD are being used as permanent methods for treatment of heart failure. It has been shown that long-term LVAD support allows for reversal of ventricular remodeling through considerable unloading of the left ventricle (Dec, 2004). Complications associated with artificial hearts, LVAS, and LVAD are hemorrhage,

infection, thromboembolism, renal failure, and neurological problems (Hunt and Frazier, 1998).

#### SURGICAL RESECTION

Resection of the affected part of the ventricle is considered the most direct method of addressing ventricular dilatation. The two most famous procedures to accomplish this goal are the Batista procedure and the Dor procedure. The Batista procedure is a partial left ventriculectomy that reduces the size of the ventricular chamber and therefore decreases wall stress as predicted by the Law of LaPlace. However after initial enthusiasm, this surgery has recently fallen out of favor. It is thought that any benefit gained from the procedure is temporary, as the ventricle will continue to dilate in the long-term. Short- and mid-term clinical outcomes have been disappointing (Batistia et al, 1997; Starling et al, 2000). Also, there is a considerable early mortality rate that is not appreciated with other methods of surgical treatment of heart failure. Surgical mortality is approximately 15% with one-year survival estimated at 56% (Stolf et al, 1998).

The Dor procedure is a patch aneurysmectomy in which the size and shape of the ventricle are altered by removal of a noncontracting portion of the ventricular wall and reconstruction to a normal geometry by a synthetic patch. Initial results have demonstrated improvement in NYHA class and an increase in ejection fraction of 8 to 12% (Dor et al, 1998; McCarthy, 1999). Secondary procedures, especially coronary revascularization, are often performed in conjunction with the Dor procedure. Mitral valve repair or replacement is also occasionally performed. The benefits seen with the

Dor procedure could be attributable to the concurrent procedures although the results reported thus far are promising.

#### VENTRICULAR SUPPORT

##### **Dynamic Cardiomyoplasty**

Support of the failing left ventricle has been performed primarily through skeletal muscle assistance, epitomized by dynamic cardiomyoplasty. Dynamic cardiomyoplasty is a surgical procedure for dilated cardiomyopathy that involves using the patient's own skeletal muscle to augment ventricular contraction. The major advantage of dynamic cardiomyoplasty touted over other surgical procedures is that this surgical technique could be performed without cardiopulmonary bypass. It also provides a biologic, native power source to support cardiac function. In the procedure, the latissimus dorsi muscle is mobilized and wrapped circumferentially around both ventricles. After a period of rest and a period of training, the muscle is paced with burst stimulation synchronized to cardiac systole. Chronic repetitive stimulation of the latissimus dorsi muscle is thought to induce changes in the skeletal muscle that are more consistent with the qualities of cardiac muscle, such as fatigue resistance (Kass et al, 1995). Proposed benefits of cardiomyoplasty include improvement of stroke volume and cardiac output, reduction in wall stress allowing ventricular remodeling, prevention of further cardiac dilatation, and provision of collateral blood supply to ischemic myocardium (Carpentier et al, 1993; Jatene et al, 1991; Kawaguchi et al, 1994; Mannion et al, 1996; Schreuder et al, 1995).

Although some clinical and hemodynamic benefit of dynamic cardiomyoplasty has been documented, the overall effectiveness of cardiomyoplasty is controversial (Astra and Stephenson, 2000). Most studies have shown clinical improvement and enhanced

physical capacity in human patients with little objective data to explain how. One of the more recent long-term studies analyzed outcomes in 43 patients that underwent dynamic cardiomyoplasty (Benicio et al, 2003). Hospital mortality was 2.2% with 1-, 2-, 5-, and 9-year survival determined to be 81%, 65%, 35%, and 11%, respectively. Patients died from either progressive heart failure or sudden cardiac death due to arrhythmia.

In 2001, dynamic cardiomyoplasty was excluded as a surgical option in the American College of Cardiology and American Heart Association guidelines for evaluation and management of chronic heart failure (Hunt et al, 2001). This was due to the poor long-term results and failure of most authors to demonstrate improvements in hemodynamic parameters and systolic function despite real improvements in NYHA class. Disappointing long-term results have mostly been blamed on degeneration of the latissimus dorsi muscle over time. Progressive muscle damage and fibrosis has been documented in failed cases of dynamic cardiomyoplasty (Lucas, 1993). Muscle damage and degeneration is thought to be caused by surgical dissection, chronic electrical stimulation, muscle ischemia, and loss of resting tension (Arpesella et al, 1998; el Oakley et al, 1995; Ianuzzo et al, 1996a). Even the postoperative delay to rest the muscle before electrical stimulation has been theorized to contribute to muscle atrophy and loss of function (Ianuzzo et al, 1996b).

New interest in dynamic cardiomyoplasty stems from the development of a stimulation protocol that allows the muscle to rest for a period of time each day (Arpesella et al, 1998). Periodic interruption of electrical stimulation will decrease damage to the muscle without impairment of hemodynamic benefits (Chekanov et al, 2000). Furthermore, intermittent stimulation has been shown to increase left ventricular

stroke volume, stroke work, and peak pressure (Kashem et al, 2001). An activity-rest protocol (“demand stimulation”) based on a heart rate cut-off avoids full transformation of the latissimus dorsi, which consequently results in improved systolic assistance as skeletal muscle properties are preserved. This protocol has been shown to improve NYHA class, increase ejection fraction, and prolong survival (Rigatelli et al, 2003). Also of interest is the use of growth factors or other substances to increase muscle perfusion or angiogenic potential. Basic fibroblast growth factor that was administered during vascular delay following latissimus dorsi mobilization was shown to augment muscle perfusion and function (Carroll et al, 2000). Application of autologous biological glue between the heart and muscle flap resulted in significant new blood vessel growth and improved revascularization of the ischemic myocardium (Chekanov et al, 1998). These and other adjustments in the harvest and stimulation of the latissimus dorsi muscle may help renew interest and improve success in dynamic cardiomyoplasty.

### **Adynamic Cardiomyoplasty**

What improvement in cardiac function is seen from dynamic cardiomyoplasty is thought to result from two main mechanisms. The first mechanism is systolic compression. There is enhancement of left ventricular systolic function by direct contraction of the wrapped muscle in concert with ventricular contraction. Myocardial stress is thought to decrease during systole as determined by a reduction in transmural pressure gradient (Chen et al, 1995). The second mechanism is passive constraint. The presence of the latissimus dorsi muscle around the ventricles prevents further ventricular dilatation and slows any further increase in myocardial oxygen tension associated with a larger radius of the ventricular cavity. This is known as the “girdling

effect” in that the presence of the wrap without stimulation may modulate or reverse the remodeling process of the failing heart (Kawaguchi et al, 1996). The surgical procedure in which the heart is wrapped with skeletal muscle without muscle stimulation is known as adynamic cardiomyoplasty. Patients with dynamic cardiomyoplasty have major improvements in clinical symptoms and in NYHA functional class patients, despite consistent lack of evidence of systolic assistance; thus the girdling effect has been proposed has the major benefit of dynamic cardiomyoplasty.

In 1993, Capouya et al were the first to describe positive results from a nonstimulated muscle wrap (Capouya et al, 1993). In a canine rapid-pacing model it was found that wrapped and unstimulated hearts developed less chamber enlargement and a less severe decline in ejection fraction when compared to control dogs. Kass in 1995, found evidence of the girdling effect serendipitously in one human patient that was having mechanical problems with the cardiomyostimulator following dynamic cardiomyoplasty for DCM (Kass et al, 1995). Despite the absence of any demonstrable systolic assistance from the muscle wrap, this patient had chronic lowering of end-diastolic volume and increased ejection fraction. Serial pressure-volume loop studies found shifting of the end-systolic pressure-volume relationship (ESPVR) to the left, which is consistent with reverse ventricular remodeling. A constrictive effect of the muscle wrap was also ruled out, as there was minimal alteration of the end-diastolic pressure-volume relationship (EDPVR). These authors made similar findings in two other patients and then speculated that the benefit of dynamic cardiomyoplasty may derive from the passive mechanism of an external elastic constraint to the epicardial surface by the latissimus dorsi muscle. They also theorized that the skeletal muscle wrap

acted differently than an intact pericardium as it is more compliant and would stiffen more gradually when lengthened, thereby better accommodating cardiac filling without dramatically altering diastolic pressures.

Monnet and Orton in 1998 also found evidence of a positive effect of an unstimulated muscle wrap (Monnet and Orton, 1998). In a canine model of Adriamycin-induced cardiomyopathy, myocardial oxygen consumption was less in dogs that had undergone dynamic cardiomyoplasty when compared to control dogs. Myocardial oxygen consumption was also unaffected by acute changes in the cardiosynchronization ratio including when the cardiomyostimulator was turned off. The adynamic effect was not clear as the muscle had been conditioned and chronically stimulated in this experiment, but it did suggest that electrical stimulation of the muscle in cardiomyoplasty may not be necessary for a myocardial sparing effect.

Several experimental studies have since then gone on to demonstrate a positive effect of adynamic cardiomyoplasty. Mott et al used a canine rapid-pacing model to compare the passive girdling effect and the dynamic systolic squeezing effect of cardiomyoplasty (Mott et al, 1998). After one month of rapid ventricular pacing, left ventricular ejection fraction was significantly higher in both dogs with adynamic or dynamic cardiomyoplasty versus control dogs that received no surgery. Likewise, there was less ventricular dilatation in the treatment groups versus the controls. DeAngelis et al used a rat model in which myocardial infarction was induced by coronary ligation (DeAngelis et al, 2001). This study returned data that supported the findings that adynamic cardiomyoplasty prevents further cardiac dilatation and stabilized left ventricular end-diastolic pressure (LVEDP) and diastolic function. In 2002, Ootaki et al

used a canine model of Adriamycin-induced cardiomyopathy to further delineate the potential benefit of adynamic cardiomyoplasty (Ootaki et al, 2002). They found that the unstimulated skeletal muscle wrapped around the heart resulted in a mild girdling effect in a progressive heart failure model. Ejection fraction of the left ventricle was also preserved. Using a similar model, Monnet evaluated the effect of adynamic cardiomyoplasty on cardiac efficiency and contractile reserve (Monnet, 2002). Six weeks after surgery, dogs with adynamic cardiomyoplasty had better preservation of myocardial oxygen consumption, an increase in mechanical cardiac efficiency, and a reduction in left ventricular end-diastolic dimensions when compared to the control group. During dobutamine stress testing,  $dP/dt_{max}$  increased to a larger degree in the treated dogs when compared to untreated dogs. No constrictive pathology of adynamic cardiomyoplasty was observed as indices of diastolic function ( $dP/dt_{min}$  and tau) were preserved.

Left ventricular dilatation and remodeling are valuable compensatory mechanisms that allow a heart in the early stages of failure to achieve near normal systolic function at increased but tolerable diastolic pressure. However, progressive ventricular dilatation will result in increased myocardial wall tension according to the law of LaPlace. The positive benefits of the girdling effect of adynamic cardiomyoplasty are mostly attributed to mechanisms based on the law of LaPlace (Capouya et al, 1993; Cho et al, 1993; Kass et al, 1995; Nakajima et al, 1994; Schreuder et al, 1995; Shirota et al, 2000; Shirota et al, 2002). The presence of an unstimulated muscle wrap around the heart is thought to decrease ventricular wall stress as progressive dilatation is prevented. Also, heart wall thickness is effectively increased by the presence of the wrap thereby decreasing wall stress.

## **Prosthetic Cardiac Binding**

A major problem associated with adynamic cardiomyoplasty is that the harvest of the latissimus dorsi muscle is complex and invasive. Dissection alone may take 1 to 2 hours, which is of concern for patients with heart failure under general anesthesia. Another concern about adynamic cardiomyoplasty is that an unstimulated muscle may be detrimental in the long-term if the muscle becomes fibrotic and uncompliant. Over time, large areas of the muscle appear to be replaced by fatty degeneration and myofibrillolysis. Early studies investigating dynamic cardiomyoplasty found there to be a severely negative effect of placement of an unstimulated muscle wrap around the heart as both ejection fraction and cardiac output were decreased (Cheng et al, 1992; Cheng et al, 1993; el Oakley et al, 1995; Magovern et al, 1993). Since there is a fair amount of evidence that positive benefits derived from cardiomyoplasty may not require chronic electrical stimulation, the next logical step was to determine whether a nonbiologic material could be used in place of the muscle and serve the same function.

Prosthetic cardiac binding is the term used to describe the technique in which a polypropylene or a polytetrafluoroethylene (PTFE) mesh is wrapped around the ventricles similar to how the latissimus dorsi muscle is placed in cardiomyoplasty. Proposed advantages to cardiac binding when compared to adynamic cardiomyoplasty include avoidance of the burden and inertia of the muscle, fibrosis of the muscle and loss of compliance, and an invasive and prolonged operative procedure. It has also been proposed that prosthetic cardiac binding could be performed by thoracoscopy, thus further minimizing surgical morbidity (Oh et al, 1998).

Vaynblat et al, were the first to describe prosthetic cardiac binding. A PTFE mesh was used in a canine model of Adriamycin-induced heart failure (Vaynblat et al, 1997). Cardiac binding prevented biventricular dilatation and significantly attenuated the anticipated increase in LVEDP. However no improvement in systolic function was achieved when compared to an untreated group. From this study it was concluded that if no significant advantage of muscle stimulation in cardiomyoplasty can be proven, then an equivalent girdling effect may be achieved through artificial means rather than through muscle harvest.

Oh and co-workers directly compared the effects of adynamic cardiomyoplasty versus cardiac binding in a canine model of rapid-pacing induced heart failure (Oh et al, 1998). This study found that both adynamic cardiomyoplasty and cardiac binding reduce cardiac enlargement and functional deterioration although adynamic cardiomyoplasty appeared to be more effective. The ejection fraction of control dogs after four weeks of rapid pacing was 17.5% compared to cardiac binding dogs that had an EF of 30.1% and adynamic cardiomyoplasty dogs that had an EF of 27%. Both cardiac binding and adynamic cardiomyoplasty reduce ventricular dilatation, as LVEDV and LVESV were significantly less in treated dogs versus control dogs. However, adynamic cardiomyoplasty appeared to be overall more effective than cardiac binding. This finding was attributed to the adaptiveness of the skeletal muscle. Canine diaphragm has been shown to have nonlinear passive stress-stretch behavior with the muscle becoming stiffer as stress increases (Oh et al, 1998). The ability of the muscle to both yield and support the ventricle is an advantage over prosthetic materials as ventricular dilatation is limited but diastolic filling is not compromised. It is also thought that prosthetic materials will

induce a fibrotic reaction in the epicardium that may result in a detrimental effect.

However, the concern of prosthetic cardiac binding causing a constrictive physiology has not been demonstrated. In the above study, no evidence of epicardial constriction by the mesh, as manifested by equalization of LVEDP, was noted. The authors concluded that the passive restraint from prosthetic cardiac binding was not sufficient to reverse ventricular remodeling, but proposed that it could be used as an adjunct to other procedures.

In 2000, an attempt was made to address the concern that prosthetic cardiac binding may cause cardiac constriction (Shah et al, 2000). In a canine model of Adriamycin-induced cardiomyopathy, a flap of pericardium was interposed in the wrap. Treated dogs had longer survival and attenuation of left ventricular dilatation and increases in LVEDP. However, this study did not have a cardiac binding group without an interposed pericardial flap. Also, diastolic function was not thoroughly evaluated; therefore the claim that pericardial interposition in the wrap would prevent cardiac constriction cannot be validated.

Device-based left ventricular reshaping is a derivative of prosthetic cardiac binding in which a patented device is used to alter the shape of the left ventricle. The Corcap Cardiac Support Device® (CSD) by Acorn Cardiovascular, Inc. (St. Paul, MN) is a knitted polyester-mesh jacket designed to return the dilated left ventricle to an ellipsoid shape and provide functional support particularly during diastole. Restraint of ventricular dilatation reduces myocardial wall stress according the law of LaPlace. Multiple experimental studies have shown that the CSD limits progressive left ventricular dilatation and improves left ventricular function as reflected by an increase in fractional

shortening (Power et al, 1999a; Chaudhry et al, 2000). Long-term implantation results in complete encapsulation of the mesh by a thin layer of fibrous tissue with no evidence of myocardial constriction (Chaudhry et al, 2000). Evaluation of an experimental model of acute myocardial infarction found that the CSD attenuated infarction development, reducing the akinetic area when compared to controls (Pilla et al, 2003). This was thought to be due to the alleviation of pathologic wall stresses. The advantage to both the CSD and prosthetic cardiac binding is the procedure itself, as it is relatively inexpensive and simple to perform. The only overt difference between the CSD and prosthetic cardiac binding is that CSD does mildly constrain the heart at the time of application (typically to a 10% reduction in left ventricular end-diastolic diameter), whereas prosthetic cardiac binding does not attempt to cause any constraint. Clinical evaluation of the CSD was performed in 34 human patients with no serious device-related complications (Konertz et al, 2001; Raman et al, 2001). Other clinical reports describe structural, functional, and clinical improvements in patients receiving CSD, as ventricular chamber dimensions decrease, ejection fraction increases, and patient functional status improves (Oz et al, 2003; Livi et al, 2005). However, recently an FDA advisory panel did not recommend approval of the CSD in the United States and requested additional statistical evidence of benefit of the device ([www.acorncv.com](http://www.acorncv.com)).

The Myosplint® (Myocor Inc., Plymouth, MN) is a three-part device that is implanted through the left ventricle, drawing the opposing walls together. Two epicardial pads are connected by a flexible transventricular rod made of braided polyethylene. These pads are covered with PTFE to encourage endothelialization and inhibit thrombus formation. The dilated left ventricle is effectively divided into two chambers with a

reduced effective radius. Again, according to the law of LaPlace, reduction in radius correlates linearly with myocardial wall stress. The size of the device is chosen to reduce the left ventricular radius by 20%, which should reduce wall stress by 20%. In contrast to the CSD, the Myosplint has more of an effect on systolic function (Takagaki et al, 2002a). It has also been demonstrated that the Myosplint had a significant improvement in left ventricular performance as a result of significant reduction in ventricular volume and significant increase in ejection fraction (Fukamachi et al, 2003). In addition, the Myosplint results in improved myocardial energetics, as myocardial oxygen consumption is significantly reduced (Fukamachi et al, 2003). The Myosplint can be implanted quickly and relatively easily without involving cardiopulmonary bypass. In an acute feasibility study, the Myosplint was implanted in a small group of transplant patients immediately before excision of the native heart resulting in a reduction of end-systolic wall stress by 27% and decreasing left ventricular volume by approximately 25% (McCarthy et al, 2001). As of November 2002, the Myosplint has been implanted in 9 patients as a solo procedure and in 12 patients in combination with mitral valve repair (Schenk et al, 2001). It is thought that both the CSD and Myosplint have a place in the management of patients with end-stage yet compensated heart failure (Schenk and Reichenspurner, 2003). Preexisting diastolic dysfunction may be a contraindication to device implantation, however interference of these devices with diastolic function has not been documented.

While studies performed to date have provided invaluable information, care must be taken not to overestimate positive or negative findings because of the small sample sizes in each of the studies. The final experiment of this degree program focused on the

evaluation prosthetic cardiac binding in an established model of heart failure. This was natural progression of the work already performed at Colorado State University. In addition, multiple modalities to assess cardiac function, specifically myocardial oxygen consumption, were utilized.

### *Experimental Induction of Cardiac Dysfunction*

Differences in results among studies evaluating the various surgical techniques for heart failure are typically attributed to variations in surgical technique, chosen end-points, animal model, heart failure model, and methods for evaluating cardiac function. Numerous heart failure models in a variety of species have been developed, all with their unique advantages and disadvantages. However, none of the models are the ideal reproduction of the human cardiac failure. Currently available models typically fail in their ability to reflect clinical heart failure, because the cause and course of human heart failure is so variable. If an ideal animal model existed, it would reflect a common human cardiac condition, mimic the clinical course of human heart failure, have consistent and predictable hemodynamic alterations, induce neurohumoral activation, and be practical, simple, and inexpensive to create (Arnolda et al, 1999; Muders and Elsner, 2000; Power and Tonkin, 1999). Evaluation of surgical treatments for heart failure generally requires the use of large animal models with hearts of similar size to that of a human. Such species include dogs, sheep, and swine, rather than the traditional rat or rabbit model. Some classic models of heart failure in larger animals include rapid ventricular pacing, coronary microembolization, and intracoronary Adriamycin administration. The animal

model chosen is usually based on the objectives of the study and the resources available to the researcher (Power and Tonkin, 1999).

Rapid ventricular pacing in dogs is the most commonly used heart failure model. It results in either acute biventricular failure or a less severe but more stable and sustainable degree of cardiac dysfunction, depending on the pacing protocol chosen. This is a popular model because it is relatively easy to create, the researcher has ability to intervene and adjust the rate of pacing, it reliably creates a repeatable severe dilated cardiomyopathy, and it is reversible. The reversibility of this model is also its major disadvantage, as continual pacing often interferes with the treatment being evaluated. Therefore, it is impossible to attribute an improvement in function and decrease in heart size to the treatment imposed if pacing is also discontinued. This problem is often circumvented by performing the surgery of interest before heart failure is induced. Obviously, this does not correspond to the clinical course of events. Adjustments to pacing protocols have recently been described to induce a chronic model of heart failure (Patel et al, 2000; Takagaki et al, 2002b). These alterations include longer duration of pacing and varying rates of pacing. Another problem with this model is whether the alterations that occur are relevant to the most common cause of human heart failure, ischemic cardiomyopathy (Todaka et al, 1997).

Coronary artery microembolization is a technique used to create a stable model of left ventricular dysfunction that results in diffuse ischemic injury to the myocardium. It has been shown to cause ventricular remodeling similar to that seen in human heart failure (Huang et al, 1997). Microembolization has been performed in both canine and ovine models with repeatable and predictable results (He et al 2004; Huang et al, 2004;

Monreal et al, 2004; Todaka et al, 1997). Unlike rapid ventricular pacing, coronary artery microembolization causes a progressive and irreversible form of heart failure. Disadvantages to this model lie in the need for multiple procedures to create left ventricular dysfunction. Microspheres are repeatedly injected into the anterior descending or circumflex branch of the left coronary artery until LVEDP reaches approximately 20mmHg. Recently, alterations to the microembolization model (delivery of a relatively small amount of microspheres) allowed a scenario that mimicked a small myocardial infarction that elevated end-diastolic pressure but preserved systolic function (He et al, 2004). There was neurohormonal activation and expansion of intravascular blood volume with clinical evidence of heart failure.

Anthracycline-induced cardiac injury is most commonly achieved using Adriamycin. This model not only replicates the clinical occurrence of doxorubicin-induced cardiotoxicity seen in cancer patients, but also causes severe dilated cardiomyopathy and heart failure that models dilated cardiomyopathy of various etiologies. Adriamycin (doxorubicin) is an anthracycline antibiotic that is isolated from cultures of *Streptomyces* spp. that is used to treat numerous forms of cancer in both human and veterinary patients. Adriamycin intercalates into DNA, interfering with both DNA and RNA polymerase activity thereby inhibiting protein synthesis. Numerous adverse reactions are associated with Adriamycin, including gastrointestinal upset and bone marrow hypoplasia. However, cardiotoxicity is a particular concern with this agent. In clinical patients, cardiotoxicity is seen with increased total cumulative exposure. The exact mechanism of Adriamycin-induced cardiomyopathy is unclear. However, the prevailing theory is that Adriamycin causes free radical formation that stimulates lipid

peroxidation and destabilizes cellular membrane integrity (Doroshov, 1983). Another proposed mechanism is that Adriamycin causes a dose-dependent and irreversible decrease in mitochondria calcium-loading capacity (Zhou et al, 2001). Other explanations of cardiotoxicity implicate platelet-activating factor, prostaglandins, histamine, and C-13 hydroxy anthracycline metabolites (Olson and Mushlin, 1990). Adriamycin is also thought to interfere with calcium release from the sarcoplasmic reticulum through inhibition of the sodium-calcium exchange or inhibition of the sodium-potassium ATPase pump resulting in calcium overload and further impairment of mitochondrial function (Kusuoka et al, 1991; Olson and Mushlin, 1990; Azuma et al, 1981). Regardless of the exact mechanism Adriamycin-induced cardiotoxicity, cardiac dysfunction is thought to occur due to a profound disruption of calcium homeostasis (Olson and Mushlin, 1990).

Classic histologic changes associated with Adriamycin-induced cardiotoxicity include degeneration and atrophy of myocytes with myofibril disruption and loss of myofilaments (Bristow et al, 1978). There is also loss of subcellular structural elements, dissociation of tight junctions, mitochondrial degeneration, and cytoplasmic vacuolization secondary to sarcoplasmic reticulum swelling (Billingham et al 1978, Ferrans 1978).

Adriamycin-induced cardiomyopathy was first achieved in a rabbit model by Jaenke et al in 1976, which demonstrated that the cardiotoxic effects of Adriamycin are cumulative and irreversible (Jaenke, 1976). The cardiotoxic properties of Adriamycin have since been well described, however the use of Adriamycin to create an animal model of heart failure in order to evaluate the effects of new therapies was first reported

in 1992 (Magovern et al, 1992). Experimental administration of Adriamycin induces a repeatable, progressive, and irreversible pattern of left ventricular dysfunction.

There are several ways to administer Adriamycin to induce cardiomyopathy. The first and easiest method is intravenous administration. However, the systemic doses of Adriamycin necessary to cause cardiac damage are associated with significant toxic effects of other organ systems, particularly the gastrointestinal tract and bone marrow. Intracoronary administration allows application of a lower Adriamycin dose because it is not diluted in the systemic circulation allowing the heart to be directly affected without secondary systemic adverse effects. Access to the coronary vasculature can be performed through surgical placement of an intracoronary catheter, with a subcutaneous access port, or through repeated cardiac catheterization through the femoral artery.

The original description of surgical catheter placement was by Magovern (Magovern et al, 1992). Following thoracotomy for catheter positioning in the left coronary artery, dogs were given 5 weekly infusions of 10 mg doxorubicin. There were problems with catheter occlusion, and overt heart failure occurred in only 1 of 6 dogs, yet all dogs survived the 3-month study period. Repeated intracoronary injection through nonsurgical cardiac catheterization has also been described (Monnet and Orton, 1999; Toyoda et al, 1998). A Judkins catheter is used to selectively infuse the left main coronary artery. The obvious advantage to this method is the avoidance of a major surgical procedure. The disadvantage is the necessity for repeated femoral artery puncture under general anesthesia, which may become increasingly difficult with weekly injections (Christiansen et al, 2002). However, surgically placed catheters still require the animal to be sedated during Adriamycin infusion. The implanted catheters are also

prone to occlusion and may contribute to thrombosis of the coronary artery and major ventricular infarction.

A variety of Adriamycin doses and dosing protocols for induction of cardiomyopathy have been described. The pilot protocol described by Magovern (10mg intracoronary infusions of Adriamycin weekly for 5 weeks) resulted in a significant decrease in left ventricular ejection fraction, cardiac output, and dP/dt with a significant increase in end-diastolic volume (Magovern et al, 1992). Histological changes were consistent with previous descriptions of Adriamycin-induced cardiotoxicity. This same protocol was used recently by Christiansen in a project to further evaluate partial left ventriculectomy (Christiansen et al, 2002; Christiansen et al, 2003). Adriamycin administration resulted in a severe dilated cardiomyopathy as determined by a significant increase in central venous pressure, mean pulmonary artery pressure, pulmonary wedge pressure, and ventricular dimensions with a significant drop in cardiac output and ejection fraction. Toyoda et al used a protocol of 0.7 mg/kg weekly for 5 weeks in Beagles (8-12 kg in body weight) that produced a reliable dilated cardiomyopathy. A dose of 1.0-1.5 mg/kg was found to repeatedly result in premature death. Monnet and Orton describe using a total dose of 15 mg administered weekly for 4 weeks in 30 kg dogs (Monnet and Orton, 1999). This study also resulted in a repeatable dilated cardiomyopathy with a significant decrease in cardiac efficiency.

Unique to Monnet's study was the use of verapamil to potentiate the cardiotoxic effects of Adriamycin and allow the use of a lower total overall dose (Monnet and Orton, 1999). This was done based on a study by Bright and Buss that showed that dogs receiving both doxorubicin and verapamil had a shorter survival time when compared to

dogs receiving only doxorubicin (Bright and Buss, 1990). Multiple other experimental studies have also demonstrated an increase in severity of heart failure and a reduction in survival with concurrent administration of Adriamycin and calcium channel blockers (Klugmann et al, 1981; Ozols et al, 1987; Rabkin et al, 1983). It is postulated that a heart injured by Adriamycin may need a higher calcium concentration to maintain function therefore the presence of calcium channel blockers may contribute to further deterioration of cardiac function (Rabkin, 1985). An additional mechanism that has been suggested is that both Adriamycin and calcium channel blockers may interfere with intracellular calmodulin-regulated calcium-dependent mechanisms (Katoh et al, 1981). Calcium channel blockers also block G protein and increase intracellular concentration of Adriamycin (Tsuruo et al, 1983). Increased levels of myocardial cell calcium concentrations have been repeatedly shown to accompany Adriamycin cardiotoxicity, which leads to calcium overload.

For the main project of this dissertation, a canine model of Adriamycin-induced cardiomyopathy was utilized. Adjustments in the protocol were instituted in an effort to simplify the process and to decrease untimely mortality. Concurrent verapamil administration was also utilized.

### ***Evaluation of Cardiac Function***

Heart failure has been classically defined as the clinical syndrome that occurs when heart disease decreases cardiac output, increases venous pressures, and produces molecular aberrations that lead to progressive deterioration of heart function and untimely myocardial cell death. The diagnosis of heart failure is typically made when

there are characteristic alterations in echocardiogram findings and hemodynamic parameters.

Echocardiography provides useful information about cardiac function in a noninvasive manner. Two-dimensional echocardiography allows visual assessment of all chambers and valves, while M-mode echocardiography provides information on left ventricular function through determination of chamber dimensions at varying phases of the cardiac cycle. Doppler echocardiography evaluates both systolic and diastolic function by recording velocities of intracardiac blood flow.

Right heart catheterization allows measurement of central venous, right atrial, right ventricular, pulmonary artery, and pulmonary capillary wedge pressures as well as determination of cardiac output. It is most commonly performed using a balloon-tipped, flow-directed (Swan-Ganz) catheter. A small thermistor is incorporated into the tip of a Swan-Ganz catheter to allow measurement of cardiac output by a thermodilution technique. Iced saline is injected through the proximal port into the cranial vena cava or right atrium with the thermistor positioned in the pulmonary artery. A curve of the change in temperature over time is generated as the saline passes the thermistor tip, similar to an indicator-dilution curve generated from indocyanine green dye technique. A normal curve has a rapid upstroke with a slower downstroke. The area under the curve (a function of mean indicator concentration), as well as the curve duration, are calculated. Cardiac output is inversely related to the area under the thermodilution curve, plotted as a function of temperature versus time. The advantages of this technique over other methods of cardiac output determination are that it does not require blood withdrawal or arterial puncture, the indicator is inert and inexpensive, and that there is virtually no

recirculation. Problems arise in cases of severe tricuspid regurgitation or low cardiac output. Tricuspid regurgitation causes loss of the saline due to turbulent and backward blood flow through the tricuspid valve. The downslope of the curve is artificially prolonged resulting in a falsely low cardiac output reading. Low cardiac output causes a slow downslope of the curve with resulting difficulty in detecting the onset of recirculation. This results in an overestimation of cardiac output.

Left heart catheterization is typically performed to determine left ventricular systolic and end-diastolic pressures and as well as to perform left heart angiography. LVEDP is the pressure achieved within the ventricle at maximal filling volume just prior to the onset of contraction. In other words, LVEDP is a reflection of preload on the left ventricle. Taking LVEDP with the thickness of the left ventricular wall and radius of the left ventricular chamber, left ventricular myocardial wall stress can be estimated according to the Law of LaPlace. Wall stress is the force or tension per unit of cross-sectional area of the ventricular wall. The Law of LaPlace states that the tension on the ventricular wall is directly proportional to the pressure and radius of the left ventricle and indirectly proportional to wall thickness. As the failing heart dilates and increases the chamber radius and as the wall becomes thinner from the increase in left ventricular volume, myocardial wall stress increases. Several surgical methods that were discussed earlier in this section are directed at decreasing the radius of curvature within the left ventricle, thereby decreasing myocardial wall stress and improving cardiac function.

If a multielectrode micromanometer catheter (Mikro-tip multi-segment pressure-volume transducer catheter SPC-550, Millar Instruments, Dallas TX) is used for left heart

catheterization, left ventricular pressure and volume can be measured simultaneously (Figure 2).

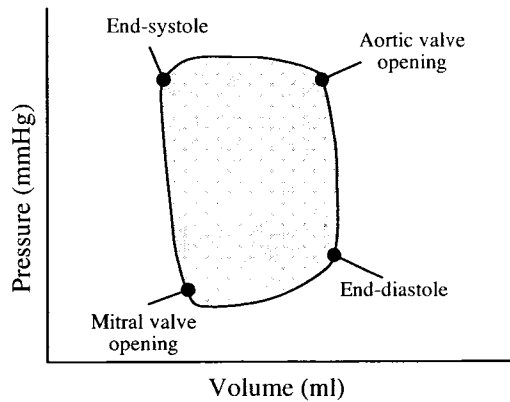


**Figure 2. Single pressure-volume loop demonstrating the cardiac cycle.**

Left ventricular volume is measured through generation of an electrical field within the left ventricle from an electrode placed at the tip of the apex and an electrode just above the aortic valve. Sensing electrodes are spaced evenly along the length of the catheter within the ventricle to allow measurement of the potential produced by the electrical current. The conductance between electrode pairs is calculated and the sum of conductances is proportional to ventricular volume. However, to achieve a more accurate reflection of ventricular volume, parallel conductance (loss of current through the ventricular wall, right ventricle, and pericardium) must be corrected for. The placement of muscle or prosthetic material around the left ventricle will also contribute to parallel conductance. By injecting hypertonic saline into the pulmonary artery, there is a transient alteration of blood conductivity without changing ventricular volume. This technique allows for calculation of parallel conductance and therefore a more accurate calculation of ventricular volume. This method has been validated in both isolated heart preparations and open-chest anesthetized dogs (Burkhoff et al, 1984; Kass et al, 1986).

Myocardial contractility can also be assessed through the determination of the maximum rate of rise of left ventricular systolic pressure:  $dP/dt$ . This index is highly sensitive to abrupt changes in contractility and preload, but it is relatively unaffected by changes in afterload (Little WC, 1985). It is also influenced by ventricular hypertrophy. The parameter  $dP/dt_{max}$  is best utilized to reflect acute inotropic changes in an individual. Increases in maximal  $dP/dt$  occur during exercise, with tachycardia, or from administration of inotropic agents. There is reduced usefulness for comparisons between individuals.

The pressure-volume relationship is a very effective method for evaluating left ventricular performance. This modality also allows separate evaluation of systolic and diastolic function at different loading conditions (Figure 3).

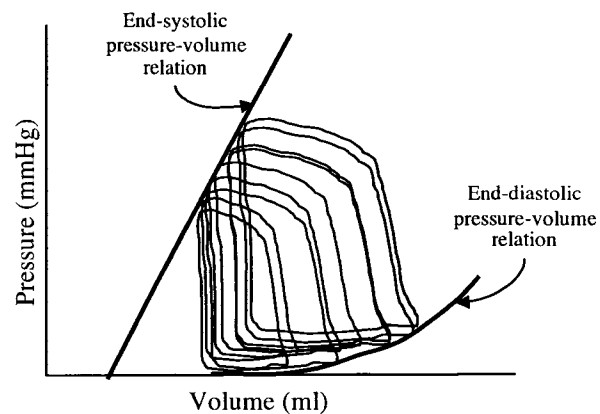


**Figure 3. Multiple pressure-volume loops demonstrating the end-systolic and end-diastolic pressure-volume relationships.**

The creation of pressure-volume loops is considered to be the gold-standard diagnostic test for assessment of left ventricular function and is also an excellent method for determining the efficacy of a therapeutic or surgical intervention (Sagawa et al, 1977). Pressure-volume loops simultaneously provide information of cardiac passive and active properties, loading properties, and energetic parameters (Pak and Kass, 1995). The end-

systolic pressure-volume relation (ESPVR) is an index of global ventricular contractility (Foex and Leone, 1994; Hedayati et al, 2002; Pak and Kass, 1995; Sagawa et al, 1977). The slope of the ESPVR defines chamber stiffness at end-systole (Ees) and the left ventricular contractile state. It has also been suggested that a leftward shift of ESPVR is an indication of reversal of ventricular remodeling (Kass et al, 1995).

The pressure-volume diagram also provides important information about left ventricular energetics. Determination of cardiac efficiency provides a more global evaluation of cardiac function and is considered one of the most important measures of left ventricular pump performance (Kameyama et al, 1992; Silvestry et al, 1997). Suga describes the time-varying elastance model in which the total energy created by each contraction is represented by the total area under the ESPVR and the systolic segment of the pressure-volume trajectory (Suga et al, 1993) (Figure 4). This is the pressure-volume area (PVA), which is made up of external work (EW, the area within the PV loop) and potential energy (PE, the area to the left of the isovolumic relaxation line).

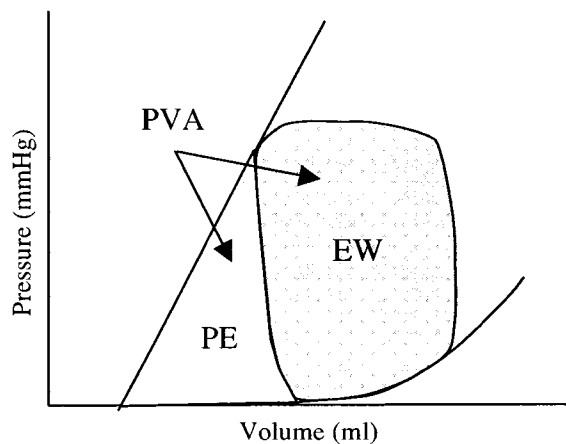


**Figure 4. Diagram of the time-varying elastance model demonstrating the pressure-volume area (PVA), which consists of the area with the pressure-volume loop, external work (EW), plus the area underneath the ESPVR line and to the left of the isovolumic relaxation segment, the potential energy (PE).**

A strong correlation has been demonstrated between PVA and myocardial oxygen consumption ( $MVO_2$ ) and the reciprocal of the slope of the linear  $MVO_2$ -PVA relation has been considered to represent the efficiency with which oxygen is utilized to generate ME. Cardiac efficiency can then be determined by the ratio of external work, calculated from cardiac output and left ventricular end-diastolic pressure, to  $MVO_2$ .

Myocardial oxygen consumption is an important indicator of cardiac performance reflecting oxygen supply and demand. It is a valuable physiological tool as  $MVO_2$  provides a quantifiable link between myocardial performance and metabolism. When assessing the effectiveness of interventional treatments of the failing heart, determination of  $MVO_2$  can delineate a protective, or oxygen sparing, effect versus an oxygen wasting effect. Cardiac efficiency is also an extremely valuable parameter for assessing the effect of treatment on failing hearts and has been found to be a powerful mortality predictor in patients with moderate heart failure due to DCM (Kim et al, 2002). Improvement in the efficiency of energy transfer is thought to be an important factor in the improvement of patient's clinical signs particularly when other hemodynamic parameters are relatively unaffected (Suga et al, 1993).

Instead of indirect estimation of  $MVO_2$  from the PVA in the pressure-volume relation,  $MVO_2$  can also be directly calculated if myocardial or coronary sinus blood flow is known. There are a variety of invasive and noninvasive methods that can be employed to measure myocardial blood flow including positron emission topography, radiolabeled microsphere technology, Doppler flowmetry, and electromagnetic flowmetry. Methods that were utilized in the various projects described in this dissertation included colored microsphere technology and direct measurement by

thermodilution. The continuous thermodilution technique employs a dual-thermistor thermodilution catheter (Baim Coronary Sinus Flow Catheter, Wilton Webster Labs Inc., Altadena, CA) that is fed from the jugular vein to the level of the coronary sinus. Placement is confirmed by fluoroscopy and infusion of nonionic iodinated contrast. Iced saline solution is then injected through the coronary sinus catheter at a constant rate and blood temperature, saline temperature, and mixture of blood and saline temperature are measured continuously during injection. Change in temperature of blood flowing over the thermistor is proportional to the indicator infusion rate and the coronary sinus blood flow:

$$\text{Coronary Blood Flow} \approx \frac{T_M - T_I}{T_B - T_M} \times \text{injectate flow} \times C$$

where  $T_M$  = temperature of blood-injectate mixture;  $T_I$  = injectate temperature;  $T_B$  = blood temperature;  $C$  = derived constant.

Specific coronary sinus blood flow is then calculated by a Baim coronary sinus flow analyzer (CF 300A Flowmeter; Wilton Webster Labs Inc., Altadena, CA). Direct measurement by this method is a sensitive and useful determinant of left ventricular coronary blood flow (Bradley and Baim, 1985). Concerns regarding this method are that accuracy is dependent on catheter position within the coronary sinus and that only large changes (greater than 30%) in coronary blood flow are likely to be accurate (Marcus et al, 1987). Other fundamental drawbacks to this methodology are that rapid changes in blood flow may be missed due to the slow frequency response of this procedure and that right-sided perfusion is not evaluated because venous drainage does not occur through the coronary sinus (Bradley and Baim, 1985).

Colored microsphere technology is an accurate, straight-forward, and reproducible technique for regional blood flow measurement. This method has been validated in several animal models as well as for determination of myocardial blood flow and has been recognized as the gold standard for measurement of capillary blood flow (Hakkinen et al, 1995; Hale et al, 1988; Kowallik et al, 1991). To perform this technique, different colored microspheres are injected into the left atrium at each time point of interest while simultaneously retrieving a blood sample from the descending aorta or femoral artery. Following completion of the study, samples are harvested from the right and left ventricle. The sample is then digested and the resulting solution is filtered and centrifuged. Extraction of the dye from the microspheres is accomplished by adding dimethylformamide. Spectrophotometry is then performed to allow calculation of the number of microspheres in each sample by comparison of sample wavelength absorption to a reference sample. Calculation of myocardial blood flow is determined by comparing the number of microspheres in each tissue sample to the number of microspheres in the blood sample with the following equation: Myocardial blood flow (mL/min/g) = Total tissue spheres/tissue weight (g) x 1/total reference spheres (mL/min).

The use of colored or fluorescent microspheres for chronic blood flow measurement up to 2 months has been described and is superior to radioactive microsphere due to leaching of the radioactive label (Kowallik et al, 1991; Van Oosterhout et al, 1998). A potential disadvantage is that in situations of low blood flow, there will be low concentrations of microspheres and/or aggregations of microspheres. This problem can be avoided by the use of a high number of microspheres or the use of Tween 80 to prevent aggregation. However, a recent study described using four types of

colored microspheres to perform repeated blood flow measurements in the same rat and detect small changes in low blood flow tissues (DeAngelis et al, 2005).

When evaluating cardiac performance, it is not only critical to assess the ability of the ventricle to contract, but also the ability of the ventricle to fill. Assessment of diastolic function is also essential when evaluating new therapies for heart failure. Diastolic dysfunction is often clinically diagnosed by a means of exclusion. In other words, if there is evidence of heart failure in the presence of normal systolic function, diastolic abnormalities likely exist. Diastolic dysfunction can occur in conjunction or in the absence of systolic dysfunction. When it occurs alone, it is frequently due to interference of left ventricular filling due to increased myocardial stiffness or impaired relaxation. Left ventricular filling is driven by left atrial and pulmonary venous pressures. Left atrial pressure is most often approximated from measurement of pulmonary capillary wedge pressure determined from right heart catheterization. Elevation of left atrial pressure implies resistance to ventricular filling or mitral regurgitation.

Compliance is the reciprocal of stiffness. Alteration of myocardial stiffness is best determined from pressure-volume loops and the end-diastolic pressure-volume relation (EDPVR) (Figure 3). The position of the EDPVR suggests the passive characteristics of the left ventricle, in particular the distensibility of the chamber (Figure 5).

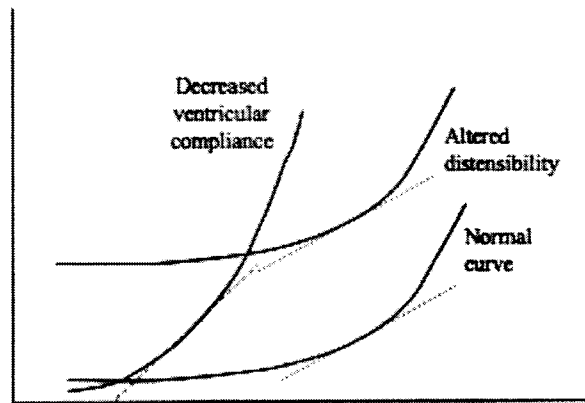


**Figure 5. A left and upward shift of the curve of the EDPVR indicates less ventricular compliance (Gibson and Francis, 2003). Increasingly higher pressures are then required to distend the left ventricle enough to accommodate a normal left ventricular volume.**

Since ventricular compliance is represented by the slope of a curve, it is not possible to calculate a single value. Also, it has not been found that quantifying ventricular compliance is a clinically useful measurement due to the complexity of pressure-volume relations (Gibson and Francis, 2003). There are multiple factors that can influence the distensibility of the left ventricle (Table 3).

The active properties of ventricular relaxation are determined through measures of isovolumetric relaxation. Echocardiographic measurements can assist in the diagnosis of impaired relaxation, but are not completely sufficient to definitively diagnose a diastolic problem. Evidence of impaired relaxation can be assessed by measurement of isovolumic relaxation time (IVRT) and determination of the E:A ratio.

IVRT is the time between aortic valve closure and mitral valve opening: the time during diastole when there is no change in volume and the myocardium is relaxing. It is measured by M-mode echocardiography. The length of IVRT is dependent not only on the rate of ventricular relaxation, but also the difference in pressures between the pressures of the aorta and left atrium at the time of aortic valve closure and mitral valve

**Table 3. Factors affecting diastolic distensibility of the left ventricle (Grossman W, 2000).**

---

Extrinsic Factors:

Pericardial restraint

Constrictive pericarditis

Cardiac tamponade

Right ventricular loading

Coronary vascular engorgement

Extrinsic compression

Tumor

Pleural pressure

Intrinsic Factors:

Altered passive elasticity

Amyloidosis

Edema

Fibrosis

Altered active elasticity

Myocardial ischemia

Ventricular hypertrophy

opening, respectively. A prolonged IVRT may imply impaired myocardial relaxation, while a shortened IVRT indicative of a restriction to filling. A significantly prolonged IVRT has also been shown to be a sensitive and specific indicator of Adriamycin-induced cardiotoxicity (Stoddard et al, 1992; Monnet and Orton, 1999).

Echocardiographic phases of ventricular filling are described as early (E), and late, or atrial (A), when filling is dependent on atrial contraction. The E:A ratio reflects mitral inflow velocities during left ventricular filling. Normally the E:A ratio is greater than 1.0. If the ratio is reversed, impaired relaxation is suggested. When diastolic dysfunction is present, typically a greater portion of end-diastolic volume is the result of late filling (A) rather than early filling (E). However, severe diastolic dysfunction can result in a significantly elevated E:A ratio where there is an increased rate of early filling with little to no filling from atrial contraction. This restriction to filling typically can occur in cases of constrictive pericarditis or restrictive cardiomyopathy.

The energy-consuming process of isovolumic relaxation can also be determined from left heart catheterization. The three main determinants of isovolumic relaxation are load, inactivation, and uniformity of load. The maximal rate of left ventricular pressure decline is  $dP/dt_{\min}$ , and is abnormal in conditions associated with impaired myocardial relaxation. However,  $dP/dt_{\min}$  is greatly influenced by the pressure at the time of aortic valve closure and is not a good reflection of the rate of isovolumetric relaxation (Little and Braunwald, 1997). Tau ( $\tau$ ) is the time constant of the exponential decline of pressure. It was first described in 1976 as the negative inverse of the semilogarithmic slope of the left ventricular pressure decay from  $\max dP/dt_{\min}$  to LVEDP (Weiss et al, 1976). Since then multiple other mathematical methods have been proposed, primarily to

minimize the effects of external pressure (such as pericardial constraint). Classically,  $\tau$  is determined from linear regression analysis of  $dp/dt$  versus left ventricular pressure, specifically the calculation of the slope of the regression plot during diastole (Craig and Kurgo, 1980). The normal value in humans has been reported to range from 25 to 40 msec (Grossman, 2000; Hirota, 1980). A monoexponential decay model has been described, however this method is problematic in cases of ventricular dilatation, such as DCM (Thompson et al, 1982; Kass, 2000). When plotting  $dP/dt$  against simultaneous left ventricular pressure in a patient DCM, monoexponential decay is linear when the actual data is curvilinear. A minimal change in end-diastolic pressure could result in a significant shift in  $\tau$ , which may not accurately reflect the true pressure decay (Kass, 2000). Increases in  $\tau$  are typically associated with slow relaxation and asynchrony of the relaxation process. This can be due to abnormal activation in the presence of bundle-branch block, myocardial hypertrophy, or regional wall motion abnormalities due to myocardial ischemia. Shortening of  $\tau$  occurs from acceleration of the rate of active relaxation due to increases in heart rate or sympathetic stimulation. Tau is not completely independent of loading conditions, but the interference from changes in load is thought to be small. Increases in left ventricular peak systolic pressure, mean aortic pressure, or left ventricular end-systolic pressure are generally accompanied by an increase in  $\tau$ , while increases in arterial pressure or end-diastolic volume are thought to minimally increase  $\tau$  (Gaasch WH, et al, 1986; Grossman W, 2000). There are technical limitations to the measurement of  $\tau$ , particularly the large beat-to-beat variability of  $\tau$  due to the limited number of data points that can be collected.

### ***Aims, Rationale, and Objectives***

During the course of my PhD work, four major experiments were performed that relate to the assessment of cardiac function with the primary focus being the direct determination of myocardial oxygen consumption. The information derived from these experiments is presented in journal style chapters:

Chapter 1: Evaluation of sevoflurane on hemodynamic and cardiac energetic parameters in normal ferrets

Chapter 2: Evaluation of cardiac performance in the dog after induction of portal hypertension and gastric ischemia

Chapter 3: Adjustments in protocol for induction of canine heart failure by intracoronary Adriamycin injection decreases untimely mortality

Chapter 4: Evaluation of prosthetic cardiac binding as an interventional treatment in a canine model of Adriamycin-induced dilated cardiomyopathy

The experiments described in the first two chapters in this dissertation reflect my introduction to the technical aspects of cardiac instrumentation and assessment of cardiac energetic parameters. Completion of these experiments also allowed me to gain experience in the interpretation of the large volume of data that can be easily collected once instrumentation is applied correctly. The work describes a variety of methods used to evaluate cardiac performance and particularly emphasizes the value of determining myocardial oxygen consumption. In addition, information was garnered about the usefulness of the ferret as an animal model for cardiovascular research as well as further insight to the etiology of cardiac dysfunction in dogs with gastric dilatation-volvulus syndrome.

Chapter 3 describes the refinements made to the canine model of Adriamycin-induced cardiomyopathy used in chapter 4. The animal and model chosen to evaluate

surgical treatment of heart failure in an experimental setting is critical. Large animal models are challenging and induced heart failure should mimic the clinical course of human disease as much as possible. The economics surrounding the utilization of large animal models make it crucial for untimely mortality to be limited in heart failure scenarios. Adjustments to a previously published protocol were made and the subset of control dogs was evaluated using echocardiography and cardiac catheterization. Myocardial oxygen consumption was determined directed through measurement of coronary sinus blood flow.

The objective of the main project that is described in Chapter 4 is to further investigate prosthetic cardiac binding in a canine model of Adriamycin-induced cardiomyopathy. Although the basic methodology of my project has been performed (Oh et al, 1998; Vaynblat et al, 1997), most studies create heart failure after the intervention has already been made. We chose to perform the surgery relative to clinical course of human heart failure and when it is felt that dynamic cardiomyoplasty might be most useful. This is during the time hemodynamic indices and systolic function parameters have been affected, but clinical symptoms are minimal (Astra and Stephenson, 2000).

As described in the literature review that chronicles the progression of the surgical treatment of heart failure, prosthetic cardiac binding has its advantages and disadvantages. However, the attractiveness of this procedure is in its simplicity. Is the limitation of progressive left ventricular dilatation and remodeling by prosthetic cardiac binding enough to improve long-term outcome and quality of life in patients with moderate to severe heart failure? Even if the answer to that question is yes, have the potential negative aspects of this technique been adequately investigated? The impetus

for this project was that we felt that the following questions have been left unanswered from the work that has already been published:

1. Does prosthetic cardiac binding limit progression of already established heart failure?
2. Is prosthetic cardiac binding beneficial or detrimental to diastolic function?
3. Is there a significant enough epicardial reaction that could result in a constrictive or restrictive pathology?

Therefore the objective of this experiment was to assess the effect of prosthetic cardiac binding on a canine model of Adriamycin-induced cardiomyopathy through various methods of cardiac performance assessment, in particular myocardial oxygen consumption. The hypothesis is that prosthetic cardiac binding improves function in a canine model of cardiomyopathy without interfering with diastole.

The dissertation ends with a summary that describes the main conclusions from the results of this project and the future directions of the continued work in this area at Colorado State University.

## BIBLIOGRAPHY

American Heart Association. Heart Disease and Stroke Statistics – 2007 Update. *Circulation* 2007;115:e69-e171

Arnolda LF, Llewellyn-Smith IJ, Minson JB. Animal models of heart failure. *Aust N Z J Med* 1999;29:403-409

Aroney CN, Ruddy TD, Dighero H et al. Differentiation of restrictive cardiomyopathy from pericardial constriction. *J Am Coll Cardiol* 1989;13:1007-1014

Arpesella G, Carraro U, Mikus PM, et al. Activity-rest stimulation of latissimus dorsi for cardiomyoplasty: 1-year results in sheep. *Ann Thorac Surg* 1998;66:1983-1990

Astra LI, Stephenson LW: Skeletal muscle as a myocardial substitute. *Proc Soc Exp Biol Med* 2000;224:133-140

Azuma J, Sperelakis N, Hasegawa H, et al. Adriamycin cardiotoxicity: Possible pathogenic mechanisms. *J Mol Cell Cardiol* 1981;13:381-397

Batista RJ, Verde J, Nery P. Partial left ventriculectomy to treat end-stage heart disease. *Ann Thorac Surg* 1997;64 :634-638

Benicio A, Moreira LF, Bacal F, et al. Reevaluation of long-term outcomes of dynamic cardiomyoplasty. *Ann Thorac Surg* 2003;76:821-827

Billingham ME, Mason JW, Bristow MR, et al. Anthracycline cardiomyopathy monitored by morphologic changes. *Cancer Treat Rep* 1978;62:865-872

Bradley AB, Baim DS. Measurement of coronary blood flow in man: Methods and implications for clinical practice. *Cardiovasc Clin* 1985;15:67-82.

Bright JM, Buss D. Effects of verapamil on chronic doxorubicin-induced cardiotoxicity in dogs. *J Natl Cancer Inst* 1990;82:963-964.

Bristow MR, Mason JW, Billingham ME, et al. Doxorubicin cardiomyopathy: Evaluation by phonocardiography, endomyocardial biopsy, and cardiac catheterization. *Ann Intern Med* 1978;88:168-175

Bristow MR, Gilbert EM, Abraham WT, et al. Carvedilol produces dose-related improvements in left ventricular function and survival in subjects with chronic heart failure. MOCHA Investigators. *Circulation* 1996;94:2807-2816

Bristow MR. Beta-adrenergic receptor blockade in chronic heart failure. *Circulation* 2000;101:558-569

British Heart Foundation. European Cardiovascular Disease Statistics, 2000

- Burkhoff D, Van der Velde E, Kass D, et al. Accuracy of volume measurement by conductance catheter in isolated, ejecting canine hearts. *Circulation* 1984;72:440-447
- Cameron J, Oesterle SN, Baldwin JC, et al. The etiologic spectrum of constrictive pericarditis. *Am Heart J* 1987;113:354-360
- Capouya ER, Gerber RS, Drinkwater DC, et al. Girdling effect of nonstimulated cardiomyoplasty on left ventricular function. *Ann Thorac Surg* 1993;56:867-870
- Carpentier A, Chachques JC, Acar C, et al: Dynamic cardiomyoplasty at seven years. *J Thorac Cardiovasc Surg* 1993;106:42-52
- Carroll SM, Carroll CM, Stremel RW, et al. Vascular delay and administration of basic fibroblast growth factor augment latissimus dorsi muscle flap perfusion and function. *Plast Reconstr Surg* 2000;105:964-971
- Chaudhry PA, Mishima T, Sharov VG, et al. Passive epicardial containment prevents ventricular remodeling in heart failure. *Ann Thorac Surg* 2000;70:1275-1280
- Chekanov VS, Nikolaychik VV, Reider MA, et al. Autologous biological glue and aprotinin prevent ischemia in latissimus dorsi muscle after mobilization. *Basic Appl Myol* 1998;8:211-219
- Chekanov VS, Kararozov P, Reider M, et al. Effects of electrical stimulation post-cardiomyoplasty in a model of chronic heart failure: hemodynamic results after 12-hour cessation versus a nonstop regimen. *PACE* 2000;23:1094-1102
- Chen F, Aklog L, deGuzman BJ, et al. New technique measures decreased transmural myocardial pressure in cardiomyoplasty. *Ann Thorac Surg* 1995;60:1678-1682
- Cheng W, Justicz AG, Soberman MS, et al. Effects of dynamic cardiomyoplasty on indices of left ventricular systolic and diastolic function in a canine model of chronic heart failure. *J Thorac Cardiovasc Surg* 1992;103:1207-1213
- Cheng W, Michele JJ, Spinale FG, et al. Effects of cardiomyoplasty on biventricular function in canine chronic heart failure. *Ann Thorac Surg* 1993;55:893-901
- Cho PW, Levin HR, Curtis WE, et al. Pressure-volume analysis of changes in cardiac function in chronic cardiomyoplasty. *Ann Thorac Surg* 1993;56:38-45
- Christiansen S, Redmann K, Scheld HH, et al. Adriamycin-induced cardiomyopathy in the dog – an appropriate model for research on partial left ventriculectomy? *J Heart Lung Transplant* 2002;21:783-790

- Christiansen S, Stypmann, Jahn UR, et al. Partial left ventriculectomy in modified Adriamycin-induced cardiomyopathy in the dog. *J Heart Lung Transplant* 2003;22:301-308
- Codd MB, Sugrue DD, Gersh BJ, et al. Epidemiology of idiopathic dilated and hypertrophic cardiomyopathy. *Circulation* 1989;80:564-572
- Cohn JN. Structural basis for heart failure. Ventricular remodeling and its pharmacological inhibition. *Circulation* 1995;91:2504-2507
- Craig WE, Murgo JP : Evaluation of isovolumic relaxation in normal man during rest, exercise and isoproterenol infusion. *Circulation* 1980 ;62(suppl III)III-22
- D’Cruz IA, Overton DH, Pai GM. Pericardial complications of cardiac surgery: Emphasis on the diagnostic role of echocardiography. *J Cardiac Surg* 1992;7:257-268
- De Angelis K, Leirner AA, Irigoyen MC, et al. Nonstimulated cardiomyoplasty improves hemodynamics in myocardial-infarcted rats. *Artificial Organs* 2001;25:939-943
- De Angelis K, Gama VM, Farah VAM, et al. Blood flow measurements in rats using four color microspheres during blockade of different vasopressor systems. *Braz J Med Bio Res* 2005;38:119-125
- Dec GW, Fuster V. Idiopathic dilated cardiomyopathy. *N Engl J Med* 1994;331:1564-1575
- Dec GW. Management of heart failure: crossing boundary over to the surgical country. *Surg Clin North Am* 2004;84:1-25
- Dor V, Sabatier M, Di Donato M, et al. Efficacy of endoventricular patch plasty in large postinfarction akinetic scar and severe left ventricular dysfunction: comparison with a series of large dyskinetic scars. *J Thorac Cardiovasc Surg* 1998;116:50-59
- Doroshov JH. Effect of anthracycline antibiotics on oxygen radical formation in the rat heart. *Cancer Res* 1983;43:460-472
- el Oakley RM, Jarvis JC, Barman D, et al. Factors affecting the integrity of latissimus dorsi muscle grafts: implications for cardiac assistance from skeletal muscle. *J Heart Lung Transplant* 1995;14:359-365
- Ferrans VJ. Overview of cardiac pathology in relation to anthracycline cardiotoxicity. *Cancer Treat Rep* 1978;62:857-864
- Foëx P and Leone BJ. Pressure-volume loops: a dynamic approach to the assessment of ventricular function. *J Cardiothorac Vasc Anesth* 1994;8:84-96.

Fukamachi K, Inoue M, Doi K, et al. Device-based left ventricular geometry change for heart failure treatment: developmental work and current status. *J Card Surg* 2003;18 Suppl 2:S43-47

Gaasch WH, Carroll JD, Blaustein AS, et al. Myocardial relaxation: Effects of preload on the time course of isovolumic relaxation. *Circulation* 1986;73:1037-1041

Garg R, Yusuf S. Overview of randomized trials of angiotensin-converting enzyme inhibitors on mortality and morbidity in patients with heart failure. Collaborative Groups on ACE Inhibitor Trials. *JAMA* 1995;273:1450-1456

Gibson DG, Francis DP. Clinical assessment of left ventricular diastolic function. *Heart* 2003;89:231-238

Grossman W. Evaluation of systolic and diastolic function of the ventricles and myocardium. In Baim DS and Grossman W (eds.): *Cardiac Catheterization, Angiography, and Intervention*. 6<sup>th</sup> ed. Philadelphia, Lippincott Williams and Wilkins, 2000, pp 367-390

Guyatt GH, Devereaux PJ. A review of heart failure treatment. *Mt Sinai J Med* 2004;71:47-54

Hakkinen JP, Miller MW, Smith AH, et al. Measurement of organ blood flow with coloured microspheres in the rat. *Cardiovasc Res* 1995;29:74-79

Hale SL, Alker KJ, Kloner RA. Evaluation of nonradioactive, colored microspheres for measurement of regional myocardial blood flow in dogs. *Circulation* 1988;78:428-434

He KL, Dickstein M, Sabbah HN, et al. Mechanisms of heart failure with well preserved ejection fraction in dogs following limited coronary microembolization. *Cardiovasc Res* 2004;64:72-83

Hedayati N, Sherwood JT, Schomisch SJ, et al. Circulatory benefits of diastolic counterpulsation in an ischemic heart failure model after aortomyoplasty. *J Thorac Cardiovasc Surg* 2002;123:1067-1073

Hirota Y. A clinical study of left ventricular relaxation. *Circulation* 1980;62:756-

Hosenpud JD. Chronic idiopathic myocarditis: controversies in causes and therapies. *Cardiovasc Rev Rep* 1988;9:31-37

Hosenpud JD. The Cardiomyopathies. In Hosenpud JD and Greenberg BH (eds.): *Congestive Heart Failure. Pathophysiology, Diagnosis, and Comprehensive Approach to Management*. Springer-Verlag, New York, 1994, pp 196-222

Hosenpud JD, Bennett LE, Keck BM, et al. The registry of the international society for heart and lung transplantation: eighteenth official report – 2001. *J Heart Lung Transplant* 2001;20:805-815

Huang Y, Kawaguchi O, Zeng B, et al. A stable ovine congestive heart failure model. A suitable substrate for left ventricular assist device assessment. *ASAIO* 1997;43:M408-413

Huang Y, Hunyor SN, Jiang L, et al. Remodeling of the chronic severely failing ischemic sheep heart after coronary microembolization: functional, energetic, structural, and cellular responses. *Am J Physiol* 2004;286:H2141-2150

Hunt SA, Frazier OH. Mechanical circulatory support and cardiac transplantation. *Circulation* 1998;97:2079-2090

Hunt SA, Baker SW, Chin MH, et al. ACC/AHA Guidelines for the evaluation and management of chronic heart failure in the adult. *J Am Coll Cardiol* 2001;38:2101-2113

Ianuzzo CD, Ianuzzo SE, Carson N, et al. Cardiomyoplasty: degeneration of the assisting skeletal muscle. *J Appl Physiol* 1996;80:1205-1213

Ianuzzo CD, Ianuzzo SE, Locke M, et al. Preservation of the latissimus dorsi muscle during cardiomyoplasty surgery. *J Card Surg* 1996;11:99-108

Jaenke RS. Delayed and progressive myocardial lesions after Adriamycin administration in the rabbit. *Cancer Res* 1976;36:2958-2966

Jatene AD, Moreira LF, Stolf NA, et al. Left ventricular function changes after cardiomyoplasty in patients with dilated cardiomyopathy. *J Thorac Cardiovasc Surg* 1991;102:132-139

Kameyama T, Asanoi H, Ishizaka S, et al. Energy conversion efficiency in human left ventricle. *Circulation* 1992;85:988-996.

Kashem A, Santamore WP, Chiang B, et al. Vascular delay and intermittent stimulation: keys to successful latissimus dorsi muscle stimulation. *Ann Thorac Surg* 2001;71:1866-1873

Kass DA, Yamazaki T, Burkhoff D, et al. Determination of left ventricular end-systolic pressure-volume relationships by the conductance (volume) catheter technique. *Circulation* 1986;73:586-595

Kass DA, Baughman HL, Pak PH, et al. Reverse remodeling from cardiomyoplasty in human heart failure. External constraint versus active assist. *Circulation* 1995;91:2314-2318

- Kass DA. Assessment of diastolic dysfunction. Invasive modalities. *Cardiol Clin* 2000;18:571-583
- Katoh N, Wise BC, Wrenn RW, et al. Inhibition by Adriamycin of calmodulin-sensitive and phospholipids-sensitive calcium dependent phosphorylation of endogenous protein from heart. *Biochem J* 1981;198:199-205
- Kawaguchi O, Goto Y, Futaki S, et al: The effects of dynamic cardiac compression on ventricular mechanics and energetics. Role of ventricular size and contractility. *J Thorac Cardiovasc Surg* 1994;107:850-859
- Kim IS, Izawa H, Sobue T, et al. Prognostic value of mechanical efficiency in ambulatory patients with idiopathic dilated cardiomyopathy in sinus rhythm. *J Am Coll Cardiol* 2002;39:1264-1268.
- Klugmann S, Bartoli Klugmann F, Decroti G, et al. Adriamycin experimental cardiomyopathy in Swiss mice. Different effects of two calcium antagonistic drugs on ADM-induced cardiomyopathy. *Pharmacol Res Commun* 1981;13:769-776
- Konertz WF, Shapland JE, Hotz H, et al. Passive containment and reverse remodeling by a novel textile cardiac support device. *Circulation* 2001;104[suppl 1]:I207-I275
- Kowallik P, Schulz R, Guth BD, et al. Measurement of regional myocardial blood flow with multiple colored microspheres. *Circulation* 1991;83:974-982
- Krum H. Beta-blockers in heart failure. The 'new wave' of clinical trials. *Drugs* 1999;58:203-210
- Kusuoka H, Futaki S, Koretsune Y, et al. Alterations of intracellular calcium homeostasis and myocardial energetics in acute Adriamycin-induced heart failure. *J Cardiovasc Pharmacol* 1991;18:437-444
- Little WC. The left ventricular  $dP/dt_{max}$ -end diastolic relation in closed chest dogs. *Circ Res* 1985;56:808-815
- Little WC, Braunwald E. Assessment of cardiac function. In Braunwald E (ed.): *Heart Disease: A Textbook of Cardiovascular Medicine*. 5<sup>th</sup> ed. Philadelphia, WB Saunders Co., 1997, pp 421-444
- Livi U, Alfieri O, Vitali E, et al. One-year experience with the Acorn CorCap cardiac support device: results of a limited market release safety study in Italy and Sweden. *Ital Heart J* 2005;6:59-65
- Lloyd-Jones DM. The risk of congestive heart failure: sobering lessons from the Framingham Heart Study. *Curr Cardiol Rep* 2001;3:184-190

Lorell BH. Pericardial diseases. In Braunwald E (ed.): *Heart Disease: A Textbook of Cardiovascular Medicine*. 5<sup>th</sup> ed. Philadelphia, W.B. Saunders, 1997, pp 1478-1534

Lorell BH, Grossman W. Profiles in constrictive pericarditis, restrictive cardiomyopathy, and cardiac tamponade. In Baim DS and Grossman W (eds.): *Cardiac Catheterization, Angiography, and Intervention*. 6<sup>th</sup> ed. Philadelphia, Lippincott Williams and Wilkins, 2000, pp 829-850

Lucas CM, Van der Veen FH, Cherlex EC. Long-term follow-up (12 to 35 weeks) after dynamic cardiomyoplasty. *J Am Coll Cardiol* 1993;22:78-767

Mackay J, Mensah G. *The Atlas of Heart Disease and Stroke*. World Health Organization, 2004

Magovern JA, Christleb IY, Badylak SF, et al. A Model of left ventricular dysfunction caused by intracoronary Adriamycin. *Ann Thorac Surg* 1992;53:861-863

Magovern JA, Park SE, Cmolik BL, et al. Early effect of right latissimus dorsi cardiomyoplasty on left ventricular function. *Circulation* 1993;88:II298-303

Manolio TA, Baughman KL, Rodeheffer R, et al. Prevalence and etiology of idiopathic dilated cardiomyopathy (summary of a National Heart, Lung, and Blood Institute workshop). *Am J Cardiol* 1992;69:1458-1466

Mannion JD, Blood V, Bailey W, et al: The effect of basic fibroblast growth factor on blood flow and morphologic features of a latissimus dorsi cardiomyoplasty. *J Thorac Cardiovasc Surg* 1996;111:19-28

Marcus ML, Wilson RF, White CW. Methods of measurement of myocardial blood flow in patients: a critical review. *Circulation* 1987;76:245-253.

Massie BM, Shah NB. Evolving trends in the epidemiologic factors of heart failure: rationale for preventive strategies and comprehensive disease management. *Am Heart J* 1997;133:703-712

McCarthy PM. New surgical options for the failing heart. *J Heart Valve Dis* 1999;8:471-475

McCarthy PM, Takagaki M, Ochiai Y, et al. Device-based change in left ventricular shape: a new concept for the treatment of dilated cardiomyopathy. *J Thorac Cardiovasc Surg* 2001;122:482-490

McElroy PA, Shroff SG, Weber KT. Pathophysiology of the failing heart. *Cardiology Clinics* 1989;7:25-37

Mehta A, Mehta M, Jain AC. Constrictive pericarditis. *Clin Cardiol* 1999;22:334-344

Minino AM, Heron MP, Smith BL. Deaths: preliminary data for 2004. *Natl Vital Stat Rep* 2006;54(19):1-49

Monnet E, Orton EC. Myocardial oxygen consumption is affected by dynamic cardiomyoplasty in dogs with Adriamycin-induced cardiomyopathy. *J Card Surg* 1998;13:475-483

Monnet E, Orton EC. A Canine model of heart failure by intracoronary Adriamycin injection: hemodynamic and energetic results. *J Cardiac Failure* 1999;5:255-264

Monnet E. Adynamic cardiomyoplasty: Effect on cardiac efficiency and contractile reserve in dogs with Adriamycin-induced cardiomyopathy. *J Card Surg* 2002;17:60-69

Monreal G, Gerhardt MA, Kambara A, et al. Selective microembolization of the circumflex coronary artery in an ovine model: Dilated, ischemic cardiomyopathy and left ventricular dysfunction. *J Card Fail* 2004;10:174-183

Mott BD, Oh JH, Misawa Y, et al. Mechanisms of cardiomyoplasty: comparative effects of adynamic versus dynamic cardiomyoplasty. *Ann Thorac Surg* 1998;65:1039-1045

Muders F, Elsner D. Animal models of chronic heart failure. *Pharmacol Res* 2000;41:605-612

Nakajima H, Niinami H, Hooper TL, et al. Cardiomyoplasty: probable mechanism of effectiveness using the pressure-volume relationship. *Ann Thorac Surg* 1994;57:407-415

Oh JH, Badhwar V, Mott BD, et al. The effects of prosthetic cardiac binding and adynamic cardiomyoplasty. *J Thorac Cardiovasc Surg* 1998;116:148-153

Ootaki Y, Tsukube T, Okita Y. Girdling effect of adynamic cardiomyoplasty in a model of dilated cardiomyopathy. *Jap J Thorac Cardiovasc Surg* 2002;50:104-108

Olson RD, Mushlin PS. Doxorubicin cardiotoxicity: analysis of prevailing hypotheses. *FASEB J* 1990;4:3076-3086

Oz MC, Konertz WF, Kleber FX, et al. Global surgical experience with the Acorn cardiac support device. *J Thorac Cardiovasc Surg* 2003;126:983-991

Ozols RF, Cunnion RE, Klecker RW, et al. Verapamil and Adriamycin in the treatment of drug-resistant ovarian cancer patients. *J Clin Oncol* 1987;5:641-647

Pak PH, Kass DA. Assessment of ventricular function in dilated cardiomyopathies. *Curr Opin Cardiol* 1995;10:339-344.

Patel HJ, Pilla JJ, Polidori DJ, et al. Ten weeks of rapid ventricular pacing creates a long-term model of left ventricular dysfunction. *J Thorac Cardiovasc Surg* 2002;119:834-841

Pfeffer MA. Cardiac remodeling and its prevention. In Colucci WS (ed.): Atlas of Heart Failure. Cardiac Function and Dysfunction. Current Medicine inc., Philadelphia, 2002, pp 87-101

Pilla JJ, Blow AS, Brockman DJ, et al. Passive ventricular constraint to improve left ventricular function and mechanics in an ovine model of heart failure secondary to acute myocardial infarction. *J Thorac Cardiovasc Surg* 2003;126:1467-1476

Power JM, Tonkin AM. Large animal models of heart failure. *Aust N Z J Med* 1999;29:395-402

Power JM, Raman J, Dornom A, et al. Passive ventricular constraint amends the course of heart failure: a study in an ovine model of dilated cardiomyopathy. *Cardiovasc Res* 1999;44:549-555

Rabkin SW, Godin DV. Adriamycin cardiotoxicity and calcium entry blockers: the need for caution in the combination. *Can J Cardiol* 1985;1:IV-VII

Rabkin SW, Otten M, Polimeni PI. Increased mortality with cardiotoxic doses of Adriamycin after verapamil pretreatment despite prevention of myocardial calcium accumulation. *Can J Physiol Pharmacol* 1983;61:1050-1056

Raman JS, Hata M, Storer M, et al. The mid-term results of ventricular containment (ACORN WRAP) for end-stage ischemic cardiomyopathy. *Ann Thorac Cardiovasc Surg* 2001;7:278-281

Rigatelli G, Barbiero M, Rigatelli G, et al. Maintained benefits and improved survival of dynamic cardiomyoplasty by activity-rest stimulation: 5-year results on the Italian trial on "demand" dynamic cardiomyoplasty. *Eur J Cardiothorac Surg* 2003;23:81-85

Sagawa K, Suga H, Shoukas AA, et al. End-systolic pressure/volume ratio: a new index of ventricular contractility. *Am J Cardiol* 1977;40:748-753.

Schenk S, Reichenspurner H, Groezner JG, et al. Myosplint implantation and ventricular shape change in patients with dilative cardiomyopathy – first clinical experience. *J Heart Lung Transplant* 2001;20:217

Schenk S, Reichenspurner H. Ventricular reshaping with devices. *Heart Surg Forum* 2003;6:237-243

Schoenfeld MG, Supple EW, Dec GW, et al Restrictive cardiomyopathy versus constrictive pericarditis: Role of endomyocardial biopsy in avoiding unnecessary thoracotomy. *Circulation* 1987;75:1012-1017

- Schreuder JJ, van der Veen FH, van der Velde ET, et al: Beat-to-beat analysis of left ventricular pressure-volume relation and stroke volume by conductance catheter and aortic Modelflow in cardiomyoplasty patients. *Circulation* 1995;91:2010-2017
- Shah HR, Vaynblat M, Saliccioli L, et al. Composite cardiac binding in experiment heart failure. *Ann Thorac Surg* 2000;9:429-434
- Shirota K, Kawaguchi O, Huang Y, et al. Ventricular remodeling after cardiomyoplasty in heart failure sheep: passive and dynamic effects. *Ann Thorac Surg* 2000;70:2102-2106
- Shirota K, Huang Y, Kawaguchi O, et al. Functional recovery of the native heart after cardiomyoplasty in sheep with heart failure: passive and dynamic effects of volume loading. *Ann Thorac Surg* 2002;73:849-854
- Silvestry SC, Lilly E, Atkins Z, et al. Ventricular and myocardial efficiencies during acute aortic regurgitation in conscious dogs. *Circulation* 1997;96[suppl II]:II-108-II-114.
- Starling RC. The heart failure pandemic: changing patterns, costs, and treatment strategies. *Cleve Clin J Med* 1998;65:351-358
- Starling RC, McCarthy PM, Buda T, et al. Results of partial left ventriculectomy for dilated cardiomyopathy: hemodynamic, clinical and echocardiographic observations. *J Am Coll Cardiol* 2000;36:2098-2103
- Stoddard MF, Seeger J, Liddell NE, et al. Prolongation of isovolumetric relaxation time as assessed by Doppler echocardiography predicts doxorubicin-induced systolic dysfunction in humans. *J Am Coll Cardiol* 1992;20:62-69
- Stolf NA, Moreira LF, Bocchi EA, et al. Determinants of midterm outcome of partial left ventriculectomy in dilated cardiomyopathy. *Ann Thorac Surg* 1998;66:1585-1591
- Suga H, Goto Y, Kawaguchi O, et al. Ventricular perspective on efficiency. *Basic Res Cardiol* 1993;88 Suppl 2:43-65.
- Takagaki M, McCarthy PM, Dessoffy R, et al. Device based left ventricular shape change: validation of conductance technology in shape changed hearts. *ASAIO J* 2002;48:268-271
- Takagaki M, McCarthy PM, Tabata T, et al. Induction and maintenance of an experimental model of severe cardiomyopathy with a novel protocol of rapid ventricular pacing. *J Thorac Cardiovasc Surg* 2002;123:544-549
- Thompson DS, Waldron CB, Juul SM, et al. Analysis of left ventricular pressure during isovolumic relaxation in coronary artery disease. *Circulation* 1982;65:690-697

- Todaka K, Leibowitz D, Homma S, et al. Characterizing ventricular mechanics and energetics following repeated coronary microembolization. *Am J Physiol* 1997;272:H186-194
- Toyoda Y, Okada M, Kashem MA. A canine model of dilated cardiomyopathy induced by repetitive intracoronary doxorubicin administration. *J Thorac Cardiovasc Surg* 1998;115:1367-1373
- Tsuruo T, Iida H, Nojiri M, et al. Circumvention of vincristine and Adriamycin resistance in vitro and in vivo by calcium influx blockers. *Cancer Research* 1983;43:2905-2910
- Tyberg TI, Goodyer AVN, Hursst VW, et al. Left ventricular filling in differentiating restrictive amyloid cardiomyopathy and constrictive pericarditis. *Am J Cardiol* 1981;47:791-796
- Van Oosterhout MFM, Prinzen FW, Sakurada S, et al. Fluorescent microspheres are superior to radioactive microspheres in chronic blood flow measurements. *Am J Physiol* 1998;275:H110-H115
- Vaynblat M, Chiavarelli M, Shah HR et al. Cardiac binding in experimental heart failure. *Ann Thorac Surg* 1997;64:81-85
- Weiss JL, Frederiksen JW, Weisfeldt ML. Hemodynamic determinants of the time-course of fall in canine left ventricular pressure. *J Clin Invest* 1976;58:751-756
- Westaby S. Surgical restoration of the failing left ventricle. *Med Clin North Am* 2003;87:523-552
- Zhou S, Starkov A, Froberg MK, et al. Cumulative and irreversible cardiac mitochondrial dysfunction induced by doxorubicin. *Cancer Res* 2001;61:771-777

## CHAPTER 1

Effect of sevoflurane on hemodynamic and cardiac energetic parameters in ferrets

Catriona M. MacPhail, DVM, Eric Monnet, DVM, PhD, James S. Gaynor, DVM, MS,  
Alberto Perini, DVM

From the Department of Clinical Sciences, College of Veterinary Medicine and  
Biomedical Sciences, Colorado State University, Fort Collins, CO 80523-1620

Published in the American Journal of Veterinary Research 2004;65:653-658.

**Objective** – To determine the effect of sevoflurane on cardiac energetic and hemodynamic parameters in ferrets.

**Animals** – 7 healthy domesticated ferrets.

**Procedure** – Sevoflurane was used as the sole anesthetic agent for general anesthesia in ferrets. Standard midline laparotomy and median sternotomy were performed to permit instrumentation. Myocardial blood flow was determined by use of colored microsphere technology. Measurements and blood samples were obtained at 1.25%, 2.5%, and 3.75% expired concentration of sevoflurane.

**Results** – A dose-dependent decrease in arterial blood pressure, left ventricular pressure, systemic vascular resistance, aortic flow, and  $dp/dt$  (an index of contractility) was detected as expired concentration of sevoflurane increased. Heart rate, central venous pressure, coronary vascular resistance, myocardial oxygen extraction ratio, and  $\tau$  (the time constant of relaxation) were unchanged. Cardiac external work decreased, as did myocardial oxygen consumption, causing increased cardiac efficiency at higher concentrations of sevoflurane.

**Conclusions and Clinical Relevance** – Sevoflurane caused minimal and predictable cardiovascular effects in ferrets without increasing myocardial metabolic demands. Data obtained from this study have not been previously reported for a species that is being commonly used in cardiovascular research. These findings also support use of sevoflurane as a safe inhalant anesthetic in ferrets for clinical and research settings.

The ferret (*Mustela putorius furo*) is a popular companion animal and, because of its specific anatomic features, it is an excellent cardiovascular animal model.<sup>1-2</sup> Volatile inhalant agents are commonly used to anesthetize ferrets in clinical and research settings. Use of sevoflurane<sup>a</sup> as an inhalant anesthetic is becoming more common because induction and recovery are quicker and smoother because of a lower blood-to-gas solubility coefficient and minimal respiratory irritation,<sup>3-5</sup> compared with isoflurane. The effect of sevoflurane on the heart in ferrets has only been assessed during in vitro studies of calcium transport and myocardial contractility.<sup>6-7</sup> Sevoflurane has been evaluated in Siberian polecats, which is a close relative of the domestic ferret.<sup>8</sup> That study found that sevoflurane permitted a more rapid induction and recovery, compared with isoflurane, and had less effect on heart rate and blood pressure. However, the cardiovascular effects of sevoflurane on the domestic ferret remain widely undetermined. Establishing the effect of sevoflurane on cardiac function may provide information to further validate the use of ferrets as models for cardiovascular research, as well as justifying use of sevoflurane for clinical anesthesia in ferrets. The purpose of the study reported here was to determine the effect of sevoflurane on cardiac energetic and hemodynamic parameters in ferrets.

## **Materials and Methods**

This study was approved by the Animal Care and Use Committee of Colorado State University. The 7 adult domesticated ferrets used in this study were determined to be of good general health from complete physical examination. Ferrets were anesthetized with sevoflurane in an induction chamber. After the righting reflex was lost, ferrets were

removed from the chamber and sevoflurane was administered through an anesthetic mask until intubation could be performed. Ferrets were mechanically ventilated with intermittent positive pressure ventilation of 10 to 12 breaths/min and 8 to 12 cm H<sub>2</sub>O of peak inspiratory pressure. A 22-gauge over-the-needle IV catheter was placed in a cephalic vein for administration of crystalloid fluids (10 mL/kg/h). Baseline heart rate and respiratory rate were recorded. During instrumentation, systolic blood pressure was monitored by a Doppler ultrasonic flow detector. The crystal was placed over the coccygeal artery with an occlusive cuff placed proximal to the crystal; mechanical ventilation and sevoflurane concentration were adjusted as needed to maintain end-tidal carbon dioxide at 40 mm Hg.

A standard midline laparotomy and median sternotomy were performed. The pericardial sac was opened, and the edges of the sac were sutured to either side of the sternotomy incision to support the heart in the field. A 22-gauge, over-the-needle catheter was placed in the abdominal aorta for direct measurement of arterial blood pressure and to collect arterial blood samples. A 22-gauge, over-the-needle catheter was placed in the cranial vena cava for direct measurement of central venous pressure (CVP). A 4-F microtip pressure transducer catheter was placed through a stab incision into the left ventricle for measurement of left ventricular pressure (LVP) and secured with an interrupted horizontal mattress suture of 4-0 polypropylene with pledgets.<sup>b</sup> A 2-mm transonic flow probe<sup>c</sup> was placed around the ascending aorta. A 22-gauge, over-the-needle catheter was placed in the left atrium for injection of colored microspheres. A 24-gauge, over-the-needle catheter was placed into the coronary sinus for collection of blood samples. The flow probe and pressure transducers were connected to a data acquisition

system, and calibration was performed. Blood samples were analyzed by use of a hemoximeter to determine oxygen saturation and oxygen content from the aorta and coronary sinus. The minimum alveolar concentration (MAC) for sevoflurane in the ferret is unknown. However, extrapolating from rats, measurements and samples were obtained at 0.5, 1.0, and 1.5 MAC, which corresponded to 1.25, 2.5, and 3.75% end-expiratory concentrations of sevoflurane. The MAC values selected for this study represent a range of clinically useful anesthetic concentrations; similar MAC values have been used in comparable studies evaluating sevoflurane in other species.<sup>9-11</sup> Ferrets were stabilized at each sevoflurane concentration for an arbitrarily chosen period of 10 minutes before data and samples were collected.

At each data point, colored microspheres were used to determine myocardial blood flow. Determination of tissue perfusion with microspheres requires injection into the left atrium and simultaneous withdrawal from the descending aorta. To prevent agglomeration of microspheres, ferrets were pretreated with an IV injection of 0.02 mL of 0.05% Tween 80. To assure uniform dispersion, each vial of colored microspheres was vortexed for 1 minute before administration. Microspheres were then immediately drawn from the vial into a syringe and administered to the ferret. At 1.25% expired concentration of sevoflurane, 0.35 mL of violet microspheres were injected into the left atrium. At 2.5% and 3.75% expired concentrations of sevoflurane, 0.15 mL yellow microspheres and 0.20 mL white microspheres were injected, respectively. Microspheres were injected as a bolus followed by a 1 mL bolus of saline (0.9% NaCl) solution. The number of injected microspheres varied to account for the different absorbance characteristics of each color. Blood samples during each injection were collected from

the descending aorta at a rate of 0.6 mL/min starting 10 seconds before injection and continuing for 100 seconds after injection for a total collected blood volume of 0.8 mL. After the last data and sample collection, ferrets were humanely euthanized with an overdose of pentobarbital sodium and the left ventricle was harvested.

The entire left ventricle was separated, weighed, and digested with 4M potassium hydroxide (KOH) solution. After tissue digestion, the solution was filtered with a 10- $\mu$ m filter to retain the microspheres. Filters were placed in microcentrifuge tubes and 100  $\mu$ L of dimethylformamide was added to extract the dye bonded to the microspheres. Blood samples were treated similarly except that digestion was performed with 8M KOH solution. Microcentrifuge tubes were centrifuged at 3,000 X g for 5 minutes. The supernatant of each sample was transferred to a microcuvet and placed in a spectrophotometer. Wavelengths of 594 nm for the violet dye, 448 nm for the yellow dye, and 370 nm for the white dye were used to measure the absorption of each sample. A reference sample of  $10^6$  microspheres of each color was used to establish a reference for the absorption of  $10^3$  microspheres. Calculation of myocardial blood flow was determined by comparing the number of microspheres in each tissue sample to the number of microspheres in the blood sample with the following equation:

$$\text{Myocardial blood flow (mL/min/g)} = \frac{\text{Total tissue spheres/tissue weight (g)} \times \text{1/total reference spheres (mL/min)}}{1}$$

Collected data included heart rate; systolic (SAP), diastolic (DAP) and mean (MAP) arterial blood pressure; CVP; aortic flow; LVP; arterial oxygen saturation and oxygen content, and coronary sinus oxygen saturation and oxygen content. Computer determined data included left ventricular end-diastolic pressure (LVEDP), +dp/dt (an

index of contractility),  $-dp/dt$  (an index of relaxation), and  $\tau$  (the time constant of relaxation).  $\tau$  Was determined from linear regression analysis of  $dp/dt$  versus LVP with  $\tau$  being equal to the slope of the regression plot during diastole.<sup>12</sup> Calculated data included systemic vascular resistance (SVR), coronary vascular resistance (CVR), myocardial oxygen extraction ratio (OER), myocardial oxygen consumption (MVO<sub>2</sub>), external cardiac work, and cardiac efficiency:

$$\text{SVR (mmHg} \times \text{mL/min)} = (\text{MAP [mm Hg]} - \text{CVP [mm Hg]}) / \text{aortic flow (mL/min)}$$

$$\text{CVR (mm Hg} \times \text{mL/min)} = (\text{DAP [mm Hg]} - \text{LVEDP [mm Hg]}) / \text{mean left ventricular coronary blood flow (mL/min)}$$

$$\text{Myocardial OER} = (\text{arterial O}_2 \text{ content} - \text{coronary sinus O}_2 \text{ content}) / \text{arterial O}_2 \text{ content} \times 100$$

$$\text{MVO}_2 \text{ (J)} = (\text{arterial O}_2 \text{ content} - \text{coronary sinus O}_2 \text{ content}) \times (\text{LVBF} / 100) \cdot 20$$

$$\text{Cardiac external work (J)} = (\text{MAP} - \text{LVEDP}) \times \text{aortic flow (mL/min)} \times 0.133$$

$$\text{Cardiac efficiency (\%)} = \text{cardiac external work (J)} / \text{MVO}_2 \text{ (J)} \times 100$$

### Statistical analyses.

Analyses were performed with a computer software package<sup>d</sup> by use of ANOVA for repeated measures with the *P* value set at < 0.05. Results are presented as mean  $\pm$  SD. Because of the small sample size of this experiment, statistical power was calculated for nonsignificant variables to determine the likelihood of Type II error. This was performed by use of a separate computer

software program.<sup>e</sup>

## Results

No adverse reactions to sevoflurane were observed in any ferret during the entire experiment. Ferrets were placed into the induction chamber at time zero; the righting reflex was lost in  $1.83 \pm 0.3$  minutes. All ferrets were breathing spontaneously ( $40.5 \pm 8.6$  breaths/min) following removal from the chamber and an anesthetic mask was used to continue sevoflurane administration. Intubation was performed  $11.83 \pm 4.2$  minutes from time zero. Respiratory rate at that time was  $38.8 \pm 7.2$  breaths/min. Baseline heart rate and systolic pressure were  $247.4 \pm 27.3$  beats/min and  $99.7 \pm 25.3$  mm Hg, respectively. Rectal temperature at the time of intubation was  $38.4^\circ\text{C}$  ( $101.1^\circ\text{F}$ ).

From 1.25% to 3.75% expired concentration of sevoflurane there was a significant dose-dependent decrease in arterial pressure ( $P < 0.001$ ), aortic flow ( $P = 0.014$ ), and LVP ( $P < 0.001$ ; Table 1). However, heart rate ( $P = 0.43$ ), CVP ( $P = 0.59$ ), and LVEDP ( $P > 0.99$ ) remained stable. Heart rate did not differ from baseline values obtained at intubation. Systemic vascular resistance ( $P < 0.001$ ),  $+dp/dt$  ( $P < 0.001$ ), and the magnitude of  $-dp/dt$  ( $P < 0.001$ ) significantly decreased and  $\tau$  was unaffected ( $P = 0.664$ ) as expired concentration of sevoflurane increased (Table 2). Rectal temperature decreased significantly from baseline to when measurements were taken at 1.25% expired sevoflurane concentration ( $38.4 \pm 1.0$  to  $35.0 \pm 1.1^\circ\text{C}$ ;  $P < 0.001$ ), but did not decrease further for the remainder of the experiment, which was approximately 1 to 1.5 hours.

Both arterial ( $P = 0.003$ ) and coronary sinus ( $P = 0.005$ ) oxygen content significantly decreased with increasing concentration of sevoflurane (Table 3). This was most likely caused by the corresponding significant ( $P = 0.002$ ) decrease in hemoglobin

concentration. A mild increase in myocardial oxygen extraction ratio was observed during this same time frame, but it was not significant ( $P = 0.29$ ). Myocardial blood flow could be correctly collected in 5 ferrets at 1.25% sevoflurane; microspheres could not be retrieved at this data point for 2 ferrets. Therefore, there were insufficient data points for myocardial blood flow at 1.25% sevoflurane to statistically compare with other concentrations. Consequently, data was also deficient for CVR,  $MVO_2$ , and cardiac efficiency at 1.25% sevoflurane, because myocardial blood flow was a determinant in those calculations. However, myocardial blood flow did significantly decrease from 2.5% to 3.75% expired concentrations of sevoflurane ( $4.6 \pm 4.1$  to  $1.9 \pm 1.8$  mL/min/g;  $P = 0.04$ ) as did  $MVO_2$  ( $11.5 \pm 12.4$  to  $2.6 \pm 1.7$  J/g;  $P = 0.17$ ; Fig 1). Coronary vascular resistance was unaffected as sevoflurane concentration increased from 2.5% to 3.75% ( $P = 0.19$ ; Table 1). Cardiac external work also decreased significantly ( $P = 0.002$ ) from 1.25% to 3.75% concentrations of sevoflurane ( $0.96 \pm 0.2$  to  $0.46 \pm 0.11$  J). Cardiac efficiency significantly ( $P = 0.02$ ) increased from 2.5% to 3.75% expired concentrations of sevoflurane ( $4.3 \pm 3.1$  to  $7.0 \pm 2.7\%$ ).

## Discussion

In the study reported here, myocardial blood flow and  $MVO_2$  decreased as expired sevoflurane concentration increased from 2.75% to 3.5% resulting in a more efficient transfer of energy in the myocardium. Use of sevoflurane in ferrets caused a dose-dependent decrease in arterial blood pressure, aortic flow, LVP, SVR, dp/dt, and cardiac external work as previously described in other species.<sup>11,13-19</sup>

Cardiac efficiency is the ratio of cardiac work to the  $MVO_2$  and is influenced by

heart rate, preload, afterload, and contractility. In this study, increasing the concentration of sevoflurane did not affect preload because CVP and LVEDP remained unchanged. However, SVR and dp/dt decreased with increasing concentrations of sevoflurane. Myocardial oxygen consumption was reduced by 65%, whereas the external work was reduced by 33%. The reduction of MVO<sub>2</sub> represents a true myocardial sparing effect because the myocardial OER did not change significantly. If the reduction in MVO<sub>2</sub> was caused by a reduction in contractility, as suggested by dp/dt, myocardial oxygen extraction would be expected to decrease resulting from a myocardial oxygen wasting effect. Therefore, afterload reduction, as suggested by the decrease in SVR, was the most important parameter to improve cardiac efficiency.

Volatile inhalant anesthetics cause a certain degree of hypotension, as well as a reduction in myocardial contractility. Sevoflurane is similar to isoflurane in that it induces a stable heart rate and rhythm, has a high arrhythmogenic dose of epinephrine, and has less effect on myocardial contractility than halothane and enflurane.<sup>9,20-21</sup>

Decreases in arterial blood pressure induced by sevoflurane are known to develop as a result of a reduction in afterload and reduction of contractility.<sup>22</sup> Sevoflurane is a less potent coronary vasodilator than isoflurane, which better preserves coronary blood flow reserve.<sup>3</sup> Conzem et al<sup>14</sup> found similar findings in rats anesthetized with varying concentrations of sevoflurane when compared with the ferrets in our study. In that study, they observed dose-dependent decreases in heart rate, cardiac output, aortic impedance, coronary blood flow, and CVR.

One particular concern about the use of sevoflurane to anesthetize patients with heart disease is that it may contribute to coronary steal (coronary vasodilation causing

redistribution of collateral blood flow away from ischemic regions). Regulation of coronary circulation is known to be dependent on myocardial oxygen demand.<sup>13,23</sup> Bernard et al<sup>13</sup> found sevoflurane to be a potent coronary vasodilator in chronically instrumented dogs; however, myocardial oxygen demand was not evaluated in that study. However, it was speculated that sevoflurane may interfere with coronary autoregulation.<sup>13</sup> This concern was supported by results of a study by Hirano et al<sup>23</sup> who found that in dogs, although sevoflurane was a less potent coronary vasodilator than isoflurane, myocardial oxygen extraction decreased, suggesting luxury perfusion of the myocardium and decrease in efficiency. In contrast, Crawford et al<sup>15</sup> found no effect of sevoflurane on coronary blood flow or any other organ blood flow in rats. Kersten et al<sup>21</sup> studied chronically instrumented dogs with steal-prone coronary artery anatomy undergoing sevoflurane anesthesia and found that no redistribution of blood flow away from the ischemic regions occurred. In our study, CVR was unaffected from 2.5% to 3.75% expired concentration of sevoflurane, as was myocardial OER. The minimal influence of sevoflurane on CVR and myocardial OER in our study suggests that in ferrets, sevoflurane has a myocardial sparing effect, maintains coronary vascular autoregulation, and does not potentiate coronary steal. These properties may make sevoflurane a preferential choice over other inhalants for patients with heart disease undergoing anesthesia by optimizing myocardial oxygen balance and protecting ischemic myocardium.

The effect of sevoflurane on myocardial relaxation in normal and diseased hearts has only been partially examined. In 1994, Harkin et al<sup>24</sup> suggested that sevoflurane may

have a greater lusitropic effect than other volatile anesthetics. This was determined by results from a study of dogs anesthetized with sevoflurane, which found a dose-related increase in  $\tau$  and a dose-related decrease in the magnitude of  $-dp/dt$ , which implies a delay in the isovolumic relaxation phase of diastole that is worsened with increasing concentrations of sevoflurane. The concern is that delay in left ventricular relaxation may impair coronary blood flow. This was found in dogs undergoing halothane anesthesia, which had a reduction in coronary blood flow during isovolumic relaxation and a strong inverse correlation of coronary blood flow with  $\tau$ .<sup>25</sup> Although the magnitude of  $-dp/dt$  also significantly decreased in our study,  $\tau$  was unaffected.  $\tau$ , the time constant of relaxation, is believed to be a more accurate assessment of isovolumic relaxation when compared to  $-dp/dt$ . The  $-dp/dt$  has limited reliability when evaluating left ventricular relaxation because it is dependent on LVP induced during systole, specifically the LVP at the time of aortic valve closure.<sup>26</sup>  $\tau$  Most closely reflects the rate of LVP decay even though it is heavily influenced by heart rate, ventricular loading conditions, and contractility.<sup>27</sup> Therefore, it is possible the lusitropic effect of sevoflurane and other volatile anesthetics in ferrets is not as significant as it is in dogs. Isoflurane, halothane, and enflurane have already been found to modestly enhance isotonic relaxation of isolated ferret myocardium in vitro.<sup>28</sup> Results of a study<sup>29</sup> in humans anesthetized with sevoflurane also found no change in myocardial relaxation before and after cardiopulmonary bypass. Therefore, because volatile anesthetics may have similar lusitropic effects on ferrets and humans, the ferret may be the preferable animal model for comparative cardiovascular research.

One limitation of the study reported here was that hemodynamic parameters

may have been affected by the duration each ferret was anesthetized. Ferrets were normothermic at the time of intubation, but rectal temperature decreased rapidly during instrumentation, most likely due to loss of heat from open body cavities. Hypothermia can adversely affect hemodynamic parameters and anesthetic requirements.

Reportedly, in anesthetized ferrets, rectal temperature can decrease as much as 10°C in 15 to 20 minutes.<sup>30</sup> Also, in the study reported here, data was obtained in an order of increasing expired concentrations of sevoflurane rather than randomization of the concentration and expired sevoflurane concentration was not returned to a baseline of 1.25% between data collections. This may be more of a concern if other volatile anesthetics were being evaluated. Because of the low blood-to-gas partition coefficient of sevoflurane, accumulation in body tissues is less of an issue than with halothane or isoflurane.

The ferret is believed to be an excellent model for cardiovascular research for the following reasons. Because of its small size, the ferret permits for economic drug use, and it is simple and inexpensive to house and care for them, especially with the increasing cost and decreasing availability of larger species.<sup>31</sup> The ferret has been validated as an animal model in an acute in vivo model for evaluation of the inotropic effects of cardiovascular drugs, and for study of in vivo model for myocardial ischemic injury and salvage assessments.<sup>31-32</sup> The favorable characteristics of the ferret heart include a well-differentiated conduction system, a dominant left coronary artery, good mechanical and electrical stability, large energy reserve, slower basal heart rate and higher arterial pressure than rats, and lack of an extensive coronary circulation.<sup>1,33-35</sup>

Although the rat heart shares many of the anatomic and physiologic characteristics of

the ferret heart, it has been suggested that the rat may be an inappropriate model for myocardial infarction research.<sup>36</sup> The ferret is particularly suited to nonterminal surgery as the heart has good mechanical and electrical stability in the recovery phase following injury.<sup>2,31,34</sup> Results of our study indicated that sevoflurane did not increase myocardial metabolic demands and did not interfere with isovolumic relaxation. There was also evidence of a myocardial sparing effect because coronary flow was maintained, oxygen extraction did not increase, and energy transfer was more efficient as concentration of sevoflurane increased. The sparing effect of sevoflurane observed in our study may also be beneficial to humans with heart failure or coronary disease undergoing anesthesia.

- <sup>a</sup> Sevoflurane, SevoFlo, Abbott Laboratories, North Chicago, Ill.
- <sup>b</sup> TFE polymer pledgets, Ethicon, Piscataway, NJ.
- <sup>c</sup> S-series flow probes, Transonic Systems, Ithaca, NY.
- <sup>d</sup> StatView, Abacus Concepts Inc, Berkely Calif.
- <sup>e</sup> Solo power analysis, BMDP Statistical Software, Los Angeles, Calif.

## References

1. Truex RC, Belej R, Ginsberg LM, et al. Anatomy of the ferret heart: an animal model for cardiac research. *Anat Rec* 1974;179:411-422.
2. Gomoll AW. Cardioprotection associated with preconditioning in the anesthetized ferret. *Basic Res Cardiol* 1996;91:433-443.
3. Larach DR, Schuler HG. Direct vasodilation by sevoflurane, isoflurane, and halothane alters coronary flow reserve in the isolated rat heart. *Anesthesiology* 1991;75:268-278.
4. Yasuda N, Targ AG, Eger EI II. Solubility of I-653, sevoflurane, isoflurane, and halothane in human tissues. *Anesth Analg* 1985;64:640-643.
5. Doi M, Ikeda K. Airway irritation produced by volatile anesthetics during brief inhalation: comparison of halothane, enflurane, isoflurane, and sevoflurane. *Can J Anaesth* 1993;40:122-126.
6. Bartunek AE, Claes VA, Housmans PR. Effects of volatile anesthetics on elastic stiffness in isometrically contracting ferret ventricular myocardium. *J Appl Physiol* 2002;92:2491-2500.
7. Bartunek AE, Claes VA, Housmans PR. Effects of volatile anesthetics on stiffness of mammalian ventricular muscle. *J Appl Physiol* 2001;91:1563-1573.
8. Gaynor JS, Wimsatt J, Mallinckrodt C, et al. A comparison of sevoflurane and isoflurane for short-term anesthesia in polecats (*Mustela eversmanni*). *J Zoo Wildlife Med* 1997;28:274-279.
9. Hikasa Y, Okabe C, Takase K, et al. Ventricular arrhythmogenic dose of adrenaline during sevoflurane, isoflurane, and halothane anaesthesia either with or without ketamine and thiopentone in cats. *Res Vet Sci* 1996;60:134-137.
10. Johnson RA, Striler E, Sawyer DC, et al. Comparison of isoflurane with sevoflurane for anesthesia induction and recovery in adult dogs. *Am J Vet Res* 1998;59:478-481.
11. Manohar M, Parks CM. Porcine systemic and regional organ blood flow during 1.0 and 1.5 minimum alveolar concentrations of sevoflurane anesthesia without and with 50% nitrous oxide. *J Pharmacol Exp Ther* 1984;231:640-648.
12. Kass DA. Assessment of diastolic dysfunction. Invasive modalities. *Cardiol Clin* 2000;18:571-586.
13. Bernard JM, Wouters PF, Doursout MF, et al. Effects of sevoflurane and isoflurane on cardiac and coronary dynamics in chronically instrumented dogs. *Anesthesiology* 1990;72:659-662.

14. Conzen PF, Vollmar B, Habazettl H, et al. Systemic and regional hemodynamics of isoflurane and sevoflurane in rats. *Anesth Analg* 1992;74:79-88.
15. Crawford MW, Lerman J, Saldivia V, et al. Hemodynamic and organ blood flow responses to halothane and sevoflurane anesthesia during spontaneous ventilation. *Anesth Analg* 1992;75:1000-1006
16. Ebert TJ, Harkin CP, Muzi M. Cardiovascular responses to sevoflurane: a review. *Anesth Analg* 1995;81:S11-22.
17. Hikasa Y, Ohe N, Takase K, et al. Cardiopulmonary effects of sevoflurane in cats: comparison with isoflurane, halothane, and enflurane. *Res Vet Sci* 1997;63:205-210.
18. Hikasa Y, Okuyama K, Kakuta T, et al. Anesthetic potency and cardiopulmonary effects of sevoflurane in goats: comparison with isoflurane and halothane. *Can J Vet Res* 1998;62:299-306.
19. Mutoh T, Nishimura R, Kim H, et al. Cardiopulmonary effects of sevoflurane, compared with halothane, enflurane, and isoflurane, in dogs. *Am J Vet Res* 1997;58:885-890.
20. Hayashi Y, Sumikawa K, Tashiro C, et al. Arrhythmogenic threshold of epinephrine during sevoflurane, enflurane, and isoflurane anesthesia in dogs. *Anesthesiology* 1988;69:145-147.
21. Kersten JR, Brayer AP, Pagel PS, et al. Perfusion of ischemic myocardium during anesthesia with sevoflurane. *Anesthesiology* 1994;81:995-1004.
22. Pagel PS, Farber NE, Warltier DC. Volatile anesthetics and cardiovascular function. In: Miller RD, ed. *Anesthesia*. 5th ed. Philadelphia: Churchill Livingstone Inc, 2000;96-124.
23. Hirano M, Fujigaki T, Shibata O, et al. A comparison of coronary hemodynamics during isoflurane and sevoflurane in anesthesia in dogs. *Anesth Analg* 1995;80:651-656.
24. Harkin CP, Pagel PS, Kersten JR, et al. Direct negative inotropic and lusitropic effects of sevoflurane. *Anesthesiology* 1994;81:156-167.
25. Doyle RL, Foëx P, Ryder WA, et al. Effects of halothane on left ventricular relaxation and early diastolic coronary blood flow in the dog. *Anesthesiology* 1989;70:660-666.
26. Courtois M, Ludbrook PA, Kovacs SJ. Unsolved problems in diastole. *Cardiol Clin* 2000;18:653-657.

27. Little WC. Assessment of normal and abnormal cardiac function. In: Braunwald E, Zipes DP, Libby P, eds. *Heart disease: a textbook of cardiovascular medicine*. 6th ed. Philadelphia: WB Saunders Co, 2001;479-502.
28. Housmans PR, Murat I. Comparative effects of halothane, enflurane, and isoflurane at equipotent anesthetic concentrations on isolated ventricular myocardium of the ferret. II: Relaxation. *Anesthesiology* 1988;69:464-471.
29. De Hert SG, ten Broecke PW, Mertens E, et al. Sevoflurane but not propofol preserves myocardial function in coronary surgery patients. *Anesthesiology* 2002;97:42-49.
30. Flecknell PA. Anesthesia of small mammals. *Vet Clin North Am Exotic Anim Pract* 2001;4:47-56.
31. Gomoll AW, Lekich RF. Use of the ferret for a myocardial ischemia/salvage model. *J Pharm Meth* 1990;23:213-223.
32. Baryla UM, Fleming JS, Stanton HC. The anesthetized ferret, an in vivo model for evaluating inotropic activity: effects of milrinone and anagrelide. *J Pharmacol Methods* 1988;20:299-306.
33. Flores NA, Davies RL, Penny WJ, et al. Coronary microangiography in the guinea pig, rabbit and ferret. *Int J Cardiol* 1984;6:459-471.
34. Neubauer S, Ingwall JS. The isolated, buffer-perfused ferret heart: a new model for the study of cardiac physiology and metabolism. *Lab Anim* 1991;25:348-353.
35. Maxwell MP, Hearse DJ, Yellon DM. Species variation in the coronary collateral circulation during regional myocardial ischemia: a critical determinant of the rate of evolution and extent of myocardial infarction. *Cardiovasc Res* 1987;21:737-740.
36. Hearse DJ. Species variation in the coronary collateral circulation during regional myocardial ischaemia: a critical determinant of the rate of evolution and extent of myocardial infarction. *Cardiovasc Res* 2000;45:213-219.

**Table 1-1.** Mean  $\pm$ SD values for hemodynamic parameters at various expired concentrations of sevoflurane in 7 ferrets.

Variable	Expired concentration of sevoflurane			p-value	power
	1.25%	2.50%	3.75%		
Heart rate (bpm)	222.4 $\pm$ 35.3	229.1 $\pm$ 42.1	218 $\pm$ 36.6	0.432	0.46
SAP (mmHg)	100.7 $\pm$ 14.3	83.4 $\pm$ 15.4	66.7 $\pm$ 8.9	< 0.0001	NA
MAP (mmHg)	91.2 $\pm$ 14.7	72.4 $\pm$ 15.9	54.0 $\pm$ 8.3	< 0.0001	NA
DAP (mmHg)	81.1 $\pm$ 15.1	45 $\pm$ 8.1	31.2 $\pm$ 4.8	< 0.0001	NA
CVP (mmHg)	2.4 $\pm$ 1.0	2.3 $\pm$ 1.1	2.7 $\pm$ 1.1	0.593	0.62
Aortic flow (mL/min)	83.7 $\pm$ 11.5	76.7 $\pm$ 19.0	72.4 $\pm$ 10.9	0.014	NA
LVP (mmHg)	124.6 $\pm$ 7.7	98.4 $\pm$ 17.4	81.1 $\pm$ 6.8	< 0.0001	NA

SAP = Systolic arterial pressure. MAP = Mean arterial pressure. DAP = Diastolic arterial pressure. CVP = Central venous pressure. LVP = Left ventricular pressure. NA = Not applicable.

**Table 1-2.** Mean  $\pm$  SD values for calculated hemodynamic and energetic parameters at varying levels of sevoflurane concentration.

Variable	Expired concentration of sevoflurane			p-value	power
	1.25%	2.5%	3.75%		
LVEDP (mmHg)	5.6 $\pm$ 2.74	5.6 $\pm$ 1.9	5.6 $\pm$ 2.73	> 0.999	1.0
+dp/dt	2771.4 $\pm$	2071.4 $\pm$	1500.0 $\pm$	< 0.0001	NA
-dp/dt	407.1	515.5	216.0	< 0.0001	NA
$\tau$ (sec)	-1942.9 $\pm$	-1371.4 $\pm$	-1014.3 $\pm$	0.664	0.68
SVR (mmHg X mL/min)	386.7	508.9	186.4	< 0.0001	NA
CVR (mmHg X mL/min)	0.022 $\pm$	0.025 $\pm$	0.023 $\pm$		
Myocardial blood flow (mL/min/gm)	0.006	0.008	0.006		
MVO <sub>2</sub> (J/g)	1.07 $\pm$ 0.2	0.9 $\pm$ 0.2	0.7 $\pm$ 0.1	< 0.0001	NA
Cardiac work (J)	NA	14.3 $\pm$ 10.0	18.7 $\pm$ 2.8	0.192	0.21
Cardiac efficiency (%)	NA	2.7 $\pm$ 1.1	1.1 $\pm$ 0.3	0.035	NA
	NA	4.5 $\pm$ 3.1	1.6 $\pm$ 0.3	0.023	NA
	0.96 $\pm$ 0.2	0.71 $\pm$ 0.3	0.47 $\pm$ 0.1	0.0002	NA
	NA	4.0 $\pm$ 3.1	7.3 $\pm$ 2.5	0.017	NA

LVEDP = left ventricular end-diastolic pressure;  $\tau$  = time constant of relaxation; SVR = systemic vascular resistance; CVR = coronary vascular resistance; MVO<sub>2</sub> = myocardial oxygen consumption; NA = not applicable.

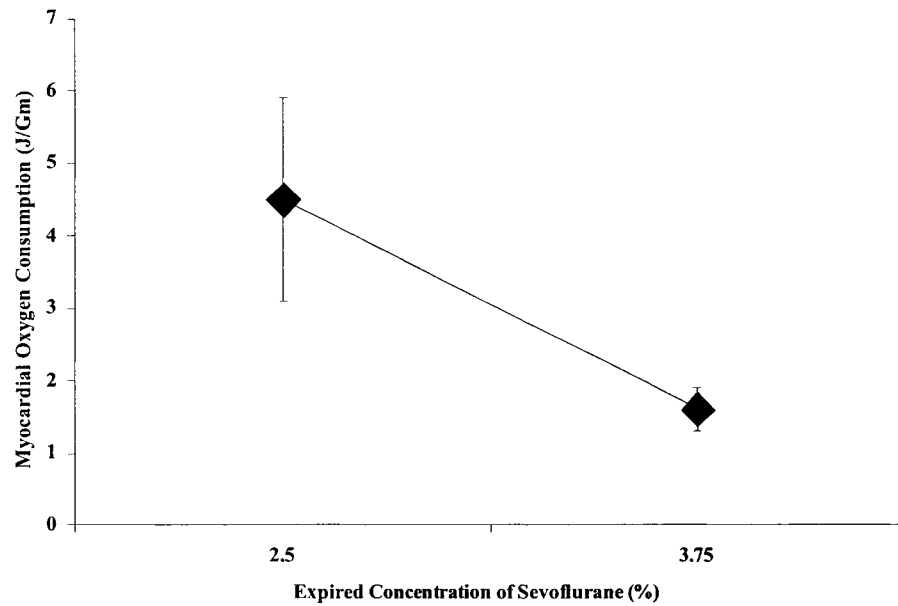
**Table 1-3.** Mean  $\pm$  SD values for blood gas parameters at various expired concentrations of sevoflurane in 7 ferrets.

Variable	Expired concentration of sevoflurane			p-value	power
	1.25%	2.50%	3.75%		
Arterial O <sub>2</sub> content	14.5 $\pm$ 2.6	13.7 $\pm$ 2.8	11.8 $\pm$ 3.5	0.003	NA
Coronary Sinus O <sub>2</sub> content	6.3 $\pm$ 1.7	5.6 $\pm$ 1.5	4.8 $\pm$ 2.2	0.005	NA
Myocardial Oxygen Extraction Ratio (%)	56.3 $\pm$ 7.0	59.5 $\pm$ 4.2	60.3 $\pm$ 7.4	0.286	0.31

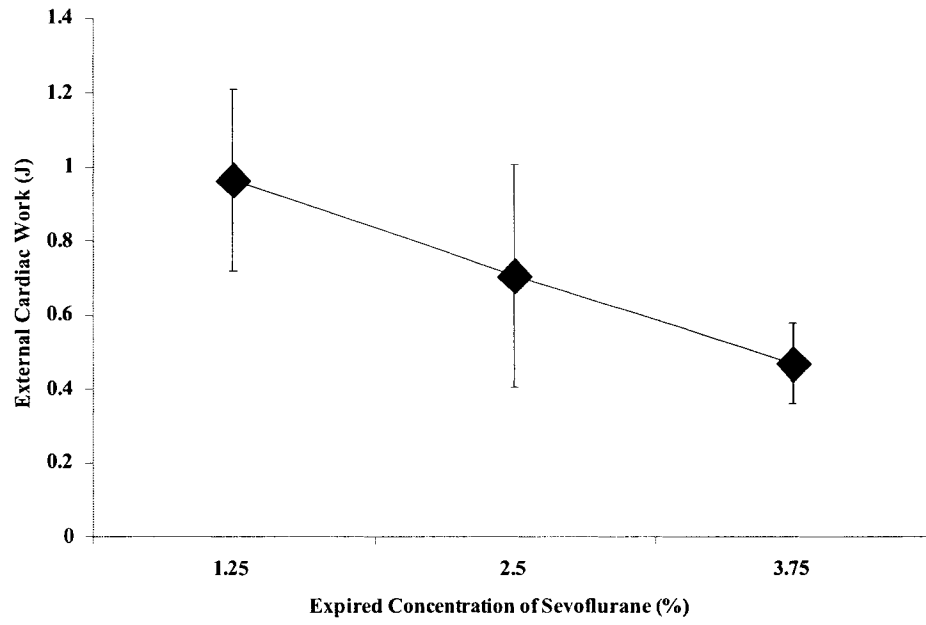
NA = Not applicable.

**Figure 1-1.** Effect of increasing expired concentration of sevoflurane on cardiac energetic parameters: A) myocardial oxygen consumption ( $p = 0.04$ ), B) cardiac external work ( $p = 0.0002$ ), and C) cardiac efficiency ( $p = 0.02$ ).

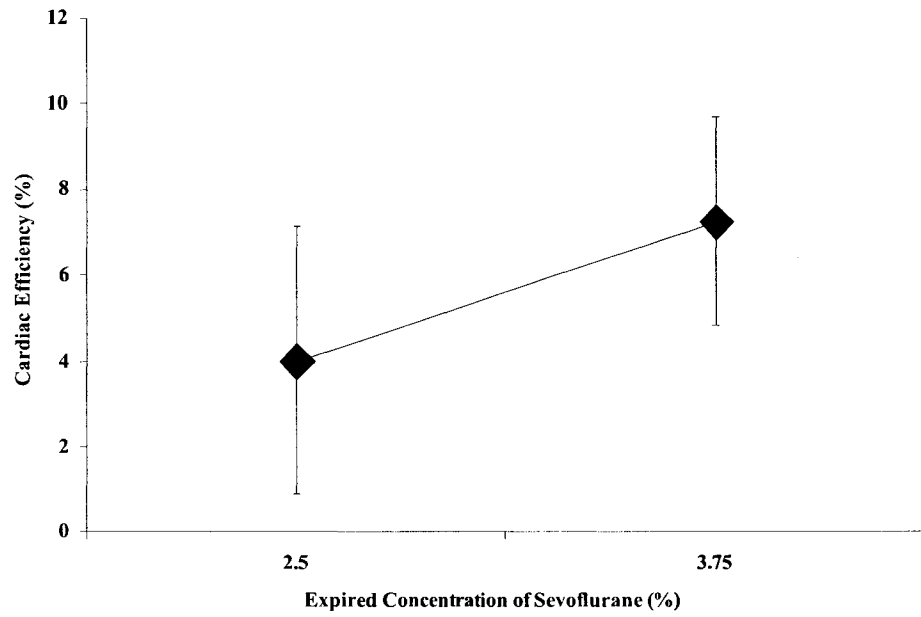
**A**



**B**



**C**



## CHAPTER 2

Evaluation of cardiac performance of the dog after induction of portal hypertension and gastric ischemia

Catriona M. MacPhail, DVM, Diplomate ACVS, Eric Monnet, DVM, PhD, Diplomate ACVS, ECVS, Davyd H. Pelsue, DVM, Diplomate ACVS, James S. Gaynor, DVM, MS, Diplomate ACVA

From the Department of Clinical Sciences, College of Veterinary Medicine and Biomedical Sciences, Colorado State University, Fort Collins, CO

Presented as an abstract at the 12<sup>th</sup> Annual Veterinary Symposium of the American College of Veterinary Surgeons, San Diego, CA, 2002.

Published in the Journal of Veterinary Emergency and Critical Care 2006;16(3): 192-196

**Objective:** To determine the changes in hemodynamic and cardiac energetic parameters in dogs after induction of portal hypertension and gastric ischemia. These blood flow alterations are similar to changes seen in splanchnic blood flow in dogs with gastric dilatation volvulus syndrome (GDV).

**Design:** Original experimental study.

**Setting:** Veterinary teaching hospital.

**Animals:** Seven purpose-bred, intact male dogs.

**Interventions:** Standard midline laparotomy and median sternotomy were performed under general anesthesia. Dogs were instrumented to obtain arterial blood pressure, aortic flow, cardiac chamber pressures, central venous pressure, portal flow, and portal pressure. Colored microsphere technology was used for determination of myocardial blood flow. Measurements and samples were obtained at baseline, following induction of portal hypertension, and after induction of portal hypertension and gastric ischemia.

**Measurements and main results:** Left ventricular myocardial blood flow was increased from  $81.8 \pm 20.1$  mL/100g/min at baseline to  $127.7 \pm 57.2$  mL/100g/min ( $P = 0.02$ ) after induction of portal hypertension and gastric ischemia. Myocardial oxygen consumption increased from  $142.2 \pm 27.4$  J/min/100gm at baseline to  $219.1 \pm 33.4$  J/min/100gm ( $P = 0.003$ ) after induction portal hypertension and gastric ischemia, but cardiac external work remained unchanged ( $13.67 \pm 6.2$  to  $13.27 \pm 9.6$  J/min;  $P = 0.78$ ; power = 0.79). Cardiac efficiency decreased from  $11.6 \pm 6.1\%$  at baseline to  $7.6 \pm 5.1\%$  ( $P = 0.017$ ) after induction of portal hypertension and gastric ischemia.

**Conclusions:** Transfer of energy within the myocardium was less efficient after induction of portal hypertension and ischemia of the stomach wall. On the basis of these results, alterations in cardiac function associated with GDV may result from deterioration of cardiac efficiency.

## Introduction

There are multiple causes of death for dogs with gastric dilatation-volvulus syndrome (GDV) including shock, disseminated intravascular coagulation, sepsis, and cardiac dysfunction. Cardiac dysfunction is typically manifested as ventricular arrhythmias in the postoperative period which occurs in 40 to 70% of dogs with GDV, although general electrocardiographic abnormalities have been identified in up to 80% of dogs.<sup>1-4</sup> Overall mortality for dogs with GDV is approximately 12-18%, but the occurrence of preoperative cardiac arrhythmias carries a mortality rate of 25-38%.<sup>3,a</sup> Evidence of cardiac damage has been found in 62-100% of GDV dogs examined at necropsy.<sup>4-5</sup> These abnormalities were primarily found in the myocardium and included degeneration, necrosis, edema, hemorrhage, infarction, inflammation, and fibrosis; necropsy findings were not necessarily associated with the presence or severity of antemortem arrhythmias. The exact cause of arrhythmias and cardiac damage in dogs with GDV is unknown. Speculated mechanisms include reperfusion injury, acid-base abnormalities, electrolyte abnormalities, release of myocardial depressant factors, and obstruction of venous return resulting in poor coronary perfusion.<sup>1-2,5-9</sup>

There have been multiple previous studies evaluating cardiac function in experimental and naturally-acquired GDV which have produced largely conflicting results.<sup>1-5,7,10-16</sup> Several early studies documented decreases in cardiac output, myocardial oxygen consumption, and coronary sinus blood flow in dogs with experimentally induced and naturally acquired GDV.<sup>7,14-15</sup> However, more recent studies have documented an increase in cardiac performance in experimental and clinical GDV cases.<sup>11,13,16</sup>

A model was developed for this study to examine the direct cardiovascular effects of two pathophysiological events that occur during GDV (gastric ischemia and portal hypertension) independent of the effect of other events that overtly influence hemodynamics (caudal vena cava occlusion and thoracic impingement). Gastric ischemia leads to gastric mucosal necrosis that allows absorption of bacteria and endotoxins. Partial occlusion of the portal vein causes a backward increase in venous pressure which causes interstitial edema and increased tissue hydrostatic pressure which further affects perfusion of abdominal organs. Portal hypertension can also negatively affect the function of the hepatic reticuloendothelial system causing decreased clearance of bacteria and endotoxins.<sup>17</sup> In response to increased bacterial and endotoxin absorption, multiple endogenous compounds or mediators are activated that cause vasodilation, increased capillary permeability, cell damage, and decreased cardiac contractility.<sup>18</sup> The hypothesis of this study is that these alterations in splanchnic blood flow that occur early in the course of GDV cause early intrinsic cardiac damage due to interference with myocardial energy transfer. This damage may make the heart more susceptible to injury from further insults.

Cardiac energetics is a field that evaluates mechanical efficiency, which is simply the ratio of the energy delivered by a system to the energy supplied to it. Determination of cardiac efficiency provides a more global evaluation of cardiac function and is considered one of the most important parameters of left ventricular pump performance.<sup>19,20</sup> Furthermore, decreased cardiac efficiency because of increased myocardial oxygen consumption or increased cardiac work may be responsible for decreased tolerance to ischemia.<sup>21</sup> Efficiency is an extremely valuable parameter for

assessing the effect of treatment on a failing heart and has been found to be a powerful predictor of mortality in patients with moderate heart failure because of dilated cardiomyopathy.<sup>22</sup> Improvement in the efficiency of energy transfer is thought to be an important factor in the improvement of a patient's clinical signs, particularly when other hemodynamic parameters are relatively unaffected.<sup>23</sup> The objective of this study is to determine the changes in hemodynamic and cardiac energetic parameters in dogs with induced portal hypertension and gastric ischemia.

## **MATERIALS AND METHODS**

This study was approved by the Animal Care and Use Committee of Colorado State University. Seven purpose-bred, intact male Walker Hounds involved in a concurrent research project were used in this study. The concurrent research project investigated LASER Doppler flowmetry as a tool to measure gastric capillary blood flow in this experimental model. Physical exams, complete blood counts, biochemical profiles, and heartworm tests were performed on each dog to evaluate their overall general health. Each dog served as its own control. Anesthesia and instrumentation protocols were identical for all dogs.

### *Anesthesia*

Dogs were premedicated with subcutaneous injections of atropine sulfate<sup>b</sup> (0.04 mg/kg), acepromazine<sup>c</sup> (0.1 mg/kg), and morphine<sup>d</sup> (0.5 mg/kg). An 18-gauge, over-the-needle catheter was placed in a cephalic vein. Anesthesia was induced by intravenous administration of propofol<sup>e</sup> (3 to 6 mg/kg). Isoflurane<sup>f</sup> in oxygen was used for anesthetic

maintenance following intubation. An 18-gauge, over-the-needle catheter was placed in the dorsal pedal artery to allow continuous arterial pressure monitoring. Additional anesthetic monitoring included electrocardiography, pulse oximetry, and capnography. Intermittent mechanical positive pressure ventilation was performed with a peak inspired pressure equal to 15-20 cm H<sub>2</sub>O at 8-10 breaths / min. An inhalant agent analyzer was used to ensure a stable anesthetic plane during the procedure.

### *Instrumentation*

Standard midline laparotomy and median sternotomy were performed. An 18-gauge, over-the-needle catheter was placed into a jejunal vein and secured with 3-0 polypropylene.<sup>g</sup> The abdominal aorta was exposed distal to the aortic hiatus. An 18-gauge, over-the-needle catheter was placed in the abdominal aorta and secured with 3-0 polypropylene mattress suture and polytetrafluoroethylene pledgets.<sup>h</sup> A flow-directed, balloon-tipped, pulmonary artery catheter was placed through an 8 Fr introducer into the right jugular vein and advanced to the level of the pulmonary artery. Pressure transducers, zeroed to the level of the right atrium, were connected to the jejunal vein, abdominal aorta, and pulmonary artery catheters with fluid-filled extension sets. The portal vein was dissected at the level of the epiploic foramen and a #1 silk Rummel tourniquet was placed around the portal vein just caudal to the porta hepatis. An 8mm ultrasonic flow probe<sup>i</sup> was placed around the portal vein caudal to the tourniquet. The pericardial sac was opened and the edges of the sac were sutured to either side of the sternotomy incision with 3-0 nylon. A 16 mm ultrasonic flow probe was placed around the ascending aorta. Both flow probes were connected to an ultrasonic flow analyzer.<sup>j</sup> A 20-gauge, over-the-needle catheter was introduced into the left atrium and secured with

3-0 polypropylene mattress suture with pledgets. A microtip pressure transducer catheter was placed directly into the apex of the left ventricle through a small stab incision and secured with a 3-0 polypropylene mattress suture and polytetrafluoroethylene pledgets. Data were collected and stored using a computerized data acquisition system.<sup>k</sup>

### *Procedure*

Following instrumentation, measurements and blood samples were obtained at baseline (time = 0). Blood samples were obtained from the descending aorta and right atrium through catheters already in place. Blood from the coronary sinus was sampled directly using a 1 mL syringe and 25-gauge needle. Oxygen content, hemoglobin, and oxygen saturation for both arterial and coronary sinus blood samples were determined by a hemoximeter.<sup>l</sup> Baseline measurements included heart rate, systolic arterial blood pressure (SAP), mean arterial blood pressure (MAP), diastolic arterial blood pressure (DAP), central venous pressure (CVP), aortic flow, left ventricular pressure (LVP), arterial oxygen saturation and oxygen content, and coronary sinus oxygen saturation and oxygen content. Portal hypertension was then created by gradual occlusion of the portal vein until a portal vein pressure of 18 cm H<sub>2</sub>O was obtained. This pressure was chosen arbitrarily to obtain a level of portal hypertension, but so as not to cause gross gastrointestinal congestion or pancreatic cyanosis. The pressure was maintained for 30 minutes and then measurements were repeated and samples were taken (t = 30 minutes). Gastric ischemia was created as described in a study by Berardi et al.<sup>24</sup> that used nuclear imaging to detect necrosis. Gastric ischemia was produced by ligating the short gastric arteries, the left gastroepiploic artery, the distal part of the right gastroepiploic artery at the level of the fundus, the left gastric artery, and the distal part of the right gastric artery.

Portal hypertension of 18 cm H<sub>2</sub>O was maintained during this time. Conditions were maintained for 30 minutes before measurements and blood sampling were repeated (t = 60 minutes).

Determination of tissue perfusion with colored microspheres<sup>m</sup> requires injection into the left atrium and simultaneous blood withdrawal from the descending aorta. To prevent agglomeration of microspheres, dogs were pretreated with 1 mL of 0.05% Tween 80 administered intravenously. One million yellow microspheres were injected into the left atrium to measure blood flow at baseline. Two million blue microspheres were injected into the left atrium following induction of portal hypertension, and 3 million red microspheres were injected into the left atrium following induction of ischemia. Different volumes of microspheres were injected to account for the different absorbance characteristics of the individual colors. Microspheres were injected as a bolus followed by a 6 mL flush of saline. Blood samples during each injection were collected from the descending aorta at a rate of 6 mL/min. Sampling began 10 seconds prior to microsphere injection and continued for 100 seconds following injection.

Following data collection, the animals were humanely euthanized with an overdose of pentobarbital sodium and full-thickness tissue samples from the mid-wall of the left ventricle were harvested. Samples were weighed and then digested with 4 M KOH solution. After tissue digestion, the solution was filtered with 10-micron filter to retain the microspheres. Filters were placed in microcentrifuge tube and 100µL of dimethylformamide was added to extract the dye bonded to the microspheres. Each blood sample was treated similarly except for digestion with 8 M KOH solution. Microcentrifuge tubes were spun at 3000 × g for 5 minutes. The supernatant of each

sample was transferred to a microcuvet and placed in a spectrophotometer. Wavelengths of 448 nm for the yellow dye, 672nm for the blue dye, and 535nm for the red dye were used to measure the absorption of each sample. A reference sample of one million microspheres of each color was used to establish a reference for the absorption of 1000 microspheres. Calculation of the number of microspheres in each sample could be performed by comparing the number of microsphere in each tissue sample to the blood sample to calculate the blood flow in each tissue region:

$$\begin{aligned} & \text{Left myocardial blood flow (LMBF) (mL/g/min)} \\ & = \text{Total tissue spheres / tissue weight (g)} \\ & \quad \times 1 / \text{total reference spheres (mL/min)} \end{aligned}$$

Systemic vascular resistance (SVR), coronary vascular resistance (CVR), oxygen extraction ratio, myocardial oxygen consumption (MVO<sub>2</sub>), external cardiac work, and cardiac efficiency were calculated using the following formulas:

$$\begin{aligned} & \text{SVR (mmHg} \times \text{min/mL)} \\ & = [\text{MAP(mmHg)} - \text{CVP(mmHg)}] / \\ & \quad \text{mean aortic flow (mL/min)} \end{aligned}$$

$$\begin{aligned} & \text{CVR (mmHg} \times \text{min/mL)} \\ & = [\text{DAP(mmHg)} - \text{LVEDP(mmHg)}] / \\ & \quad \text{LMBF (mL/min)} \end{aligned}$$

$$\begin{aligned} & \text{Myocardial oxygen extraction ratio (\%)} \\ & = (\text{arterial O}_2 \text{ content} - \text{coronary sinus O}_2 \text{ content}) / \\ & \quad \text{arterial O}_2 \text{ content} \times 100 \end{aligned}$$

$$\begin{aligned} & \text{MVO}_2 \text{ (J/min)} \\ & = (\text{arterial O}_2 \text{ content} - \text{mixed venous O}_2 \text{ content}) \times \\ & \quad (\text{LMBF (mL/g/min)} / 100) \times 20 \end{aligned}$$

$$\begin{aligned} & \text{Cardiac external work (J/min)} \\ &= [\text{MAP(mmHg)} - \text{LVEDP(mmHg)}] \times \\ & \quad \text{mean aortic flow (L/min)} \times 0.133 \end{aligned}$$

$$\text{Cardiac efficiency (\%)} = \text{Cardiac external work (J/min)} / \text{MVO}_2 \text{ (J/min)}$$

### *Statistical analysis*

Results are reported as mean  $\pm$  standard error. Statistical analyses were performed with a computer software package<sup>n</sup> using an analysis of variance for repeated measure to evaluate the effect of treatment on hemodynamic parameters and cardiac efficiency. Values of  $P < 0.05$  were considered statistically significant.

## **RESULTS**

Hemodynamic data are reported in Table 1. No arrhythmias were identified in any dog during the experiment. There was no gross evidence of myocardial ischemia or infarction at necropsy. Left ventricular myocardial blood flow increased significantly from  $81.8 \pm 20.1$  mL/100g/min at baseline to  $98.7$  mL/100g/min after induction of portal hypertension to  $127.7 \pm 57.2$  mL/100g/min ( $P = 0.02$ ) after induction of portal hypertension and gastric ischemia. Arterial oxygen content decreased from  $14.5 \pm 1.3$  mL O<sub>2</sub>/dL at baseline to  $13.0 \pm 2.1$  mL O<sub>2</sub>/dL after induction of portal hypertension to  $12.2 \pm 3.2$  mL O<sub>2</sub>/dL ( $P = 0.19$ ) after induction of portal hypertension and gastric ischemia, but this change was not statistically significant. Coronary sinus oxygen content decreased significantly from  $6.8 \pm 1.9$  mL O<sub>2</sub>/dL at baseline to  $3.8 \pm 1.5$  mL O<sub>2</sub>/dL ( $P = 0.006$ ) after induction of portal hypertension and gastric ischemia. Coronary sinus oxygen content after induction of portal hypertension was  $4.7 \pm 1.4$  mL O<sub>2</sub>/dL and was

significantly different from baseline ( $P = 0.041$ ), but not after induction of portal hypertension and gastric ischemia ( $P = 0.35$ ). The myocardial oxygen extraction ratio increased significantly from  $52.7 \pm 14.6\%$  at baseline to  $63.5 \pm 9.3\%$  ( $P = 0.04$ ) after induction of portal hypertension and gastric ischemia.

After induction of portal hypertension and gastric ischemia,  $MVO_2$  ( $219.1 \pm 33.4$  J/min/100g) was significantly increased from baseline ( $142.2 \pm 27.4$  J/min/100g;  $P = 0.003$ ) and induction of portal hypertension ( $168.60 \pm 58.70$  J/min/100g;  $P = 0.024$ ; Figure 1). Cardiac external work remained unchanged from  $13.67 \pm 6.2$  J/min at baseline,  $12.6 \pm 8.3$  J/min after induction of portal hypertension, and  $13.27 \pm 9.6$  J/min ( $P = 0.78$ ) after induction of portal hypertension and gastric ischemia. Cardiac efficiency after induction of portal hypertension ( $10.9 \pm 6.4\%$ ) was not significantly different from baseline ( $11.6 \pm 6.1\%$ ;  $P = 0.63$ ). Cardiac efficiency after induction of portal hypertension and ischemia ( $7.6 \pm 5.1\%$ ) was significantly different from baseline ( $P = 0.017$ ) and portal hypertension ( $P = 0.038$ ; Figure 2).

## **DISCUSSION**

Portal hypertension and gastric ischemia caused an increase in  $MVO_2$ , while cardiac external work was maintained. Therefore, a less efficient transfer of energy occurred in the myocardium following alteration of splanchnic blood flow. We speculate that reduction of cardiac efficiency could be an early event that occurs in GDV that may predispose these dogs to further cardiac dysfunction.

Cardiac efficiency, which is the ratio of external work to  $MVO_2$ , is affected by heart rate, systolic wall stress, and contractility.<sup>25</sup> Increases in heart rate and systolic wall stress increase the amount of work produced by the heart. As cardiac work is an important component of  $MVO_2$ , augmentation of cardiac work, especially due to increases in systolic wall stress (afterload), will result in a significant reduction of cardiac efficiency.<sup>23</sup> When contractility is enhanced by catecholamines, calcium, or other positive inotropic drugs, there is also reduction in cardiac efficiency as more myocardial oxygen is required for the same level of mechanical work. This reduction in cardiac efficiency results in oxygen wasting.<sup>23</sup> Heart rate, CVP, and SVR remained unchanged throughout the experiment as did cardiac external work. SVR is a somewhat weak index of afterload.<sup>26</sup> Determination of systolic wall stress or arterial impedance would have allowed better evaluation of afterload, but these indices were not performed in this study. However, the deterioration of cardiac efficiency in this study is most likely due to an oxygen wasting effect. The increase in myocardial oxygen extraction ratio without an increase in external work supports this statement. Inotropic support was not used during this experiment; therefore, the positive inotropic influence causing the oxygen wasting effect is likely a result of endogenous mediators, such as catecholamines. Unfortunately, concentrations of endogenous mediators were not measured in this study. The effect of splanchnic blood alterations on contractility cannot be described as this requires measurement of left ventricular volume to determine maximum elastance ( $E_{max}$ ), which was not performed in this study.

The oxygen wasting effect and the compensatory response lead to an increase in coronary blood flow until coronary reserve is exhausted.<sup>19</sup> Once this occurs, the

myocardium is at risk for injury, and possibly failure. Myocardial injury occurs when additional demands are placed on the already inefficient myocardium.<sup>23</sup> The absence of arrhythmias in this experimental model was most likely due to the relatively short duration of our experiment and, therefore, coronary reserve was not exhausted. This reserve is demonstrated by the significant decrease in CVR from induction of portal hypertension to creation of portal hypertension and gastric ischemia with LMBF increasing during the same time frame.

Release of intrinsic catecholamines and myocardial depressant factor (MDF) has been demonstrated in experimental studies on GDV.<sup>15</sup> Measurement of these factors may have provided valuable information to allow further conclusions to be drawn regarding to the origin of cardiac dysfunction in GDV. Intrinsic catecholamines and MDF could cause changes in cardiac metabolism and myocardial oxygen consumption by affecting coronary blood flow, myocardial oxygen extraction ratio, and/or cardiac work. The effect of intrinsic catecholamines or MDF could be sufficient to modify myocardial metabolism without affecting cardiac contractility.

A previous study by Horne et al.<sup>7</sup> demonstrated an increase in myocardial oxygen extraction and an overall decrease in  $MVO_2$  in an experimental GDV model. The decrease in  $MVO_2$  was due to the decrease in coronary sinus blood flow. They reported a 50% reduction of myocardial oxygen consumption associated with an 89% reduction of cardiac output. Cardiac work was not calculated in Horne's study, but with such a dramatic reduction of cardiac output and a 49% reduction in MAP, a reduction in cardiac work of more than 50% can be anticipated. Therefore, cardiac efficiency would have likely been reduced, as demonstrated in this study. Another reason for reduced cardiac

output and cardiac work in the Horne<sup>7</sup> study was the use of pentobarbital anesthesia. By itself, pentobarbital is a potent myocardial depressant which could have influenced the effect of experimentally-induced GDV on cardiac performance.<sup>27</sup> Constant-dose anesthesia was maintained by monitoring the expired concentration of isoflurane.

Preload greatly influences cardiac output and cardiac work. In the study presented here, indicators of preload remained constant during the experiment. In the study from Horne et al.<sup>7</sup>, preload was not reported. However, experimental gastric dilatation is known to cause a dramatic reduction in preload and cardiac output, which by definition, would negatively affect efficiency.<sup>20</sup> Therefore, in naturally-acquired cases of GDV, cardiac efficiency is likely negatively affected by both alterations in splanchnic blood flow and impairment of venous return because of gastric distension.

An additional concern with this model is the effect of time over the effect of treatment. In all dogs, portal hypertension was always created first and then maintained through the rest of the study. The data recorded after induction of gastric ischemia may also be influenced by the long-standing portal hypertension. Dogs were not allowed to hemodynamically recover between stages of the experiment and there was no randomization of the study design. However, this model accurately reflects the splanchnic hemodynamic alterations that occur in a clinical situation of GDV. As hemodynamic parameters were largely unchanged over time, the alterations seen in myocardial blood flow, oxygen consumption, and efficiency can be attributed to the interference in splanchnic perfusion and not a consequence of general anesthesia and surgical procedures.

To summarize, alterations of splanchnic blood flow, similar to events that occur early in GDV, induce a reduction of cardiac efficiency with augmentation of myocardial oxygen consumption. Although the true etiology of cardiac dysfunction in dogs with GDV still remains to be determined, the results of this study demonstrate that the combination of portal hypertension and gastric ischemia has an affect on myocardial energy transfer, which may make the heart more susceptible to further injury.

## Footnotes

- <sup>a</sup> Unpublished data, Colorado State University, 2005.
- <sup>b</sup> Atropine sulfate, Vedco, St. Joseph, MO
- <sup>c</sup> Acepromazine maleate, Vedco.
- <sup>d</sup> Morphine sulfate, Dosette®, Elkins-Sinn Inc., Cherry Hill, NJ
- <sup>e</sup> Propofol. Diprivan®, Abbott Laboratories, North Chicago, IL
- <sup>f</sup> Isoflurane, Aerrane®, Anaquest, Madison, WI
- <sup>g</sup> Polypropylene, Surgilene®, Davis0Geck, Danbury, CT
- <sup>h</sup> TFE polymer pledgets, Ethicon, Piscataway, NJ
- <sup>i</sup> S-series flow probes, Transonic Systems, Ithaca, NY
- <sup>j</sup> T206 Flowmeter, Transonic Systems.
- <sup>k</sup> Superscope II, GW Instruments, East Cambridge, MA
- <sup>l</sup> OSM 3 Hemoximeter™, Radiometer America Inc., Westlake, OH
- <sup>m</sup> Dye-Trak®, Triton Technologies, San Diego, CA
- <sup>n</sup> Statview, Abacus Concepts Inc., Berkeley CA

## References

1. Muir WW, Lipowitz AJ: Cardiac dysrhythmias associated with gastric dilatation-volvulus in the dogs. *J Am Vet Med Assoc* 1978;172:682-689.
2. Muir WW: Gastric dilatation volvulus in the dogs, with emphasis on cardiac arrhythmias. *J Am Vet Med Assoc* 1982;180:739-742.
3. Brouman JD, Schertel ER, Allen DA: Factors associated with perioperative mortality in dogs with surgically managed gastric dilatation-volvulus: 137 cases (1988-1993). *J Am Vet Med Assoc* 1996;11:1855-1858.
4. Schober KE, Cornand C, Kirbach B, et al: Serum cardiac troponin I and cardiac troponin T concentrations in dogs with gastric dilatation-volvulus. *J Am Vet Med Assoc* 2002;221:381-388.
5. Muir WW, Weisbrode SE: Myocardial ischemia in dogs with gastric dilatation-volvulus. *J Am Vet Med Assoc* 1982;181:363-366.
6. Muir WW: Acid-base and electrolyte disturbance in dogs with gastric-dilatation-volvulus. *J Am Vet Med Assoc* 1982;181:229-231.
7. Horne WA, Gilmore DR, Dietze AE, et al: Effects of gastric distention-volvulus on coronary blood flow and myocardial oxygen consumption in the dog. *Am J Vet Res* 1985;46:98-104.
8. Wingfield WE, Betts CS, Rawlings CA: Pathophysiology associated with gastric dilatation-volvulus in the dog. *J Am Anim Hosp Assoc* 1976;12:136-142.
9. Lantz GC, Badylak SF, Hiles MC, et al: Treatment of reperfusion injury in dogs with experimentally induced gastric dilatation-volvulus. *Am J Vet Res* 1992;53:1594-1598
10. Engler HS, Kennedy TE, Ellison LT, et al: Hemodynamics of experimental acute gastric dilatation. *Am J Surg* 1967;113:194-198.
11. Hodgson DS, Dunlop CI, Chapman PL, et al: Cardiopulmonary responses to experimentally induced gastric dilatation in isoflurane-anesthetized dogs. *Am J Vet Res* 1992;53:938-943.
12. Merkeley DF, Howard DR, Eyster GE, et al: Experimentally induced acute gastric dilatation in the dogs: cardiopulmonary effect. *J Am Anim Hosp Assoc* 1976;12:143-148.
13. Miller TL, Schwartz DS, Nakayama T, et al: Effects of acute gastric distension and recovery on tendency for ventricular arrhythmia in dogs. *J Vet Intern Med* 2000;14:436-444.

14. Orton EC, Muir WW: Hemodynamics during experimental gastric dilatation-volvulus in dogs. *Am J Vet Res* 1983;44:1512-1515.
15. Orton EC, Muir WW: Isovolumetric indices and humoral cardioactive substance bioassay during clinical and experimentally induced gastric dilatation-volvulus in dogs. *Am J Vet Res* 1983;44:1516-1520.
16. Wagner AE, Dunlop CI, Chapman PL: Cardiopulmonary measurements in dogs undergoing gastropexy without gastrectomy for corrections of gastric dilatation-volvulus. *J Am Vet Med Assoc* 1999;215:484-488.
17. Wingfield WE: The stomach, in Bojrab MJ (ed.): *Pathophysiology in Small Animal Surgery*. Philadelphia, PA, Lea & Febiger, 1981, pp. 101-111.
18. Matthiesen DT: Pathophysiology of gastric dilatation-volvulus, in Bojrab MJ (ed.): *Disease Mechanisms in Small Animal Surgery*. Philadelphia, PA, Lea & Febiger, 1993, pp. 220-231.
19. Silvestry SC, Lilly E, Atkins Z, et al: Ventricular and myocardial efficiencies during acute aortic regurgitation in conscious dogs. *Circulation* 1997;96[suppl II]:II-108-II-114.
20. Kameyama T, Asanoi H, Ishizaka S, et al. Energy conversion efficiency in human left ventricle. *Circulation* 1992;85:988-996.
21. Izzi G, Zile MR, Gaasch WH: Myocardial oxygen consumption and the left ventricular pressure-volume area in normal and hypertrophic canine hearts. *Circulation* 1991;84:1384-1392.
22. Kim IS, Izawa H, Sobue T, Et al. Prognostic value of mechanical efficiency in ambulatory patients with idiopathic dilated cardiomyopathy in sinus rhythm. *Am Coll Cardiol* 2002;39:1264-1268.
23. Suga H, Goto Y, Kawaguchi O, et al: Ventricular perspective on efficiency. *Basic Res Cardiol* 1993;88 Suppl 2:43-65.
24. Berardi C, Wheaton LG, Twardock AR, et al: Use of a nuclear imaging technique to detect gastric wall ischemia. *Am J Vet Res* 1991;52:1089-1096
25. Schipke JD: Cardiac efficiency. *Bas Res Cardio* 1994;89:207-240.
26. Little WC: Assessment of normal and abnormal cardiac function, in Braunwald E, Zipes DP, Libby P (eds): *Heart Disease: A Textbook of Cardiovascular Medicine* (ed 6), Philadelphia, PA, Saunders, 2001, pp. 479-502.

27. Roesch C, Haselby KA, Paradise RR, et al: Comparisons of cardiovascular effects of thiopental and pentobarbital at equivalent levels of CNS depression. *Anesth Analg* 1983;62:749-753.

**Table 2-1.** Hemodynamic parameters at baseline, following induction of portal hypertension, and following creation of portal hypertension and gastric ischemia. LV, left ventricle; SVR, systemic vascular resistance; CVR, coronary vascular resistance.

	<b>Baseline</b>	<b>Portal Hypertension</b>	<b>Portal Hypertension and Gastric Ischemia</b>	<b>p-value</b>
<b>Heart Rate (bpm)</b>	123.7 ± 12.1	126.5 ± 18.4	122.5 ± 24.4	0.73
<b>Systolic arterial pressure (mmHg)</b>	97.34 ± 18.25	87.86 ± 10.90	95.00 ± 19.98	0.37
<b>Mean arterial pressure (mmHg)</b>	58.71 ± 11.5	57.95 ± 18.46	59.43 ± 19.92	0.94
<b>Diastolic arterial pressure (mmHg)</b>	39.36 ± 25.17	43.00 ± 26.94	41.64 ± 28.+0	0.73
<b>Central venous pressure (mmHg)</b>	7.83 ± 3.09	11.62 ± 4.63	12.22 ± 2.31	0.10
<b>LV pressure (mmHg)</b>	96.14 ± 41.21	96.86 ± 15.3	102.21 ± 21.3	0.89
<b>LV end-diastolic pressure (mmHg)</b>	12.06 ± 14.78	10.28 ± 16.58	12.06 ± 15.74	0.36
<b>Aortic flow (L/min)</b>	2.16 ± 0.55	1.79 ± 0.60	2.92 ± 0.81	0.12
<b>SVR (mmHg × min/mL)</b>	25.31 ± 6.97	28.33 ± 7.72	27.36 ± 5.20	0.45
<b>CVR (mmHg × min/mL)</b>	0.33 ± 0.29	0.37 ± 0.31	0.20 ± 0.18	0.04
<b>Arterial O<sub>2</sub> saturation (%)</b>	97.9 ± 2.7	99.5 ± 0.7	99.9 ± 0.2	0.11
<b>Coronary sinus O<sub>2</sub> saturation (%)</b>	45.7 ± 14.3	36.0 ± 10.5	31.6 ± 11.3	0.006

**Figure 2-1.** Comparison of myocardial oxygen consumption (mean  $\pm$  standard deviation; n=5) obtained at baseline, 30 minutes after induction of portal hypertension (p=0.003), and 30 minutes after creation of gastric ischemia (p=0.024).

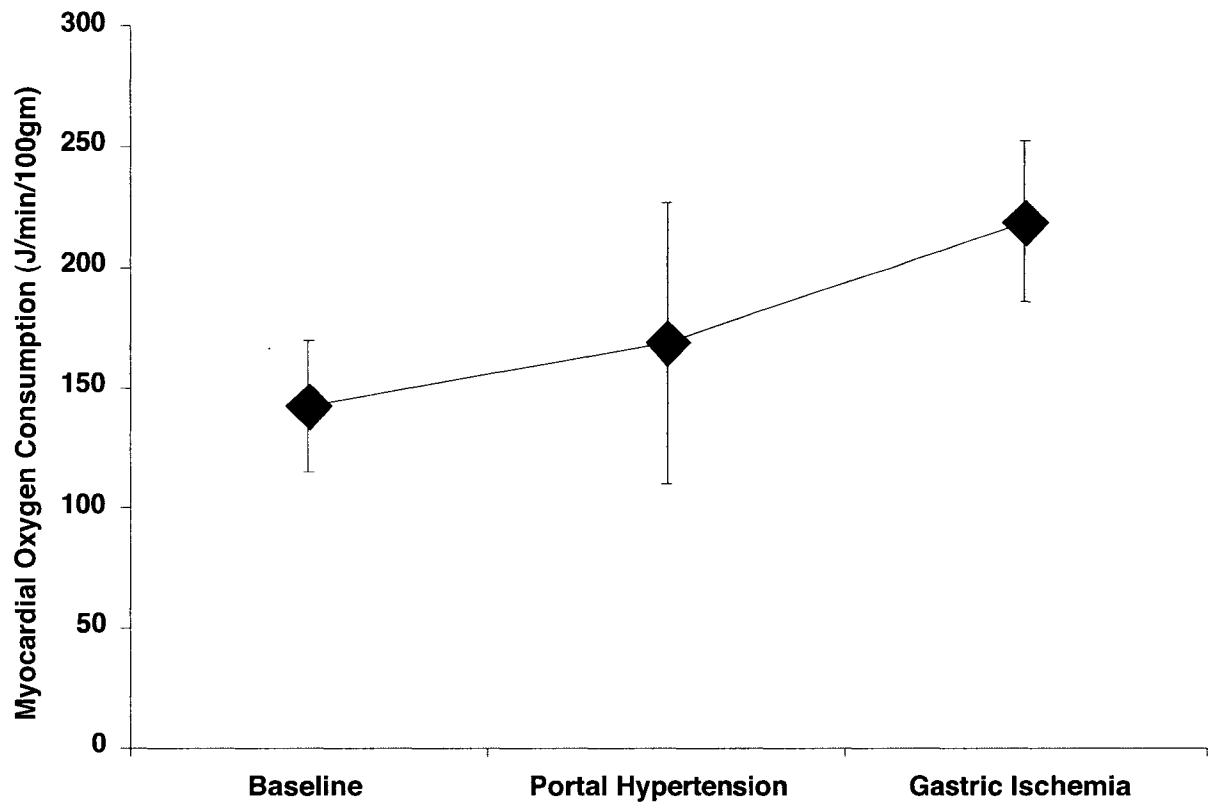
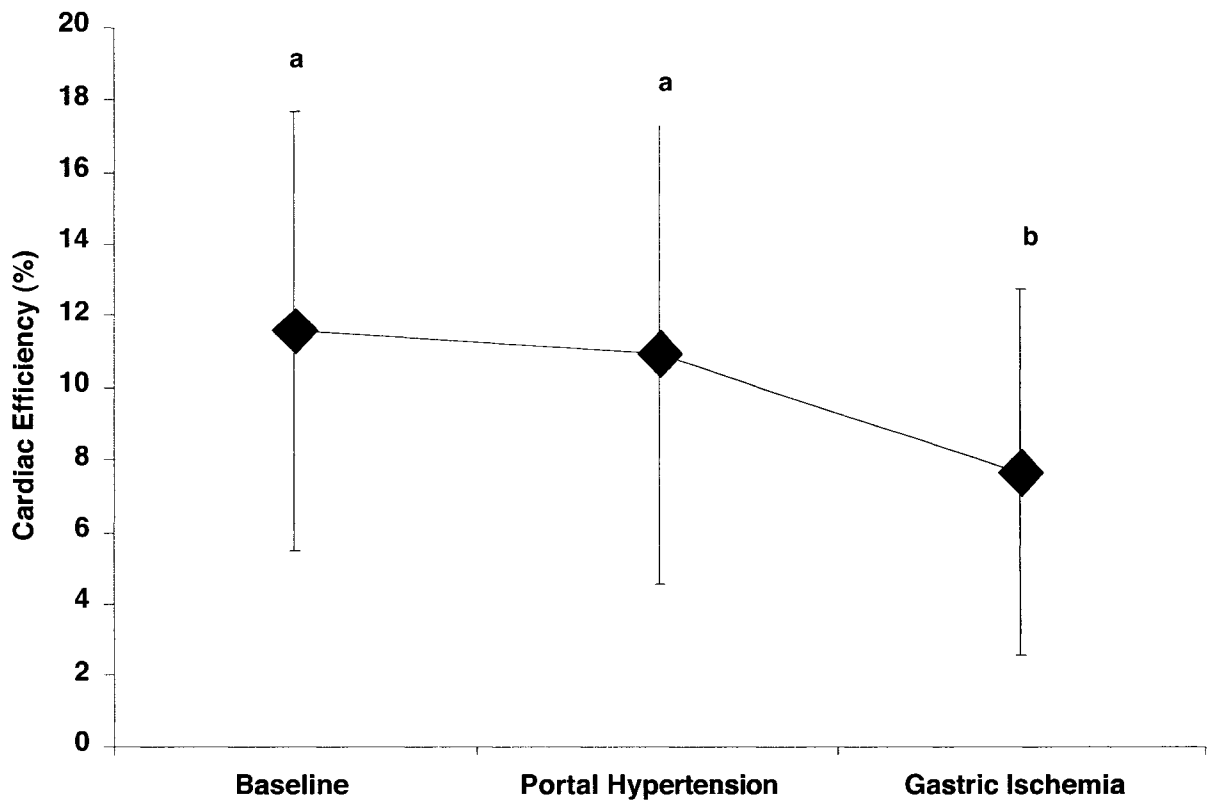


**Figure 2-2.** Comparison of cardiac efficiency (mean  $\pm$  standard deviation; n=5) obtained at baseline, 30 minutes after induction of portal hypertension, and 30 minutes after creation of gastric ischemia. Different letters indicate significant statistical difference (a: P = 0.017, b: P = 0.038).



## CHAPTER 3

Adjustments in protocol for induction of canine heart failure by intracoronary

Adriamycin injection decreases untimely mortality

Catriona M. MacPhail, DVM, Diplomate ACVS, David Getzy, DVM, Diplomate ACVP,

E. Christopher Orton, DVM, PhD, Diplomate ACVS, Eric Monnet, DVM, PhD,

Diplomate ACVS, ECVS

## **Abstract**

Numerous heart failure models in a variety of species have been developed, all with their unique advantages and disadvantages. However, none of the models are the ideal reproduction of the human cardiac failure. Anthracycline-induced cardiac injury is most commonly performed using Adriamycin. This model not only replicates the clinical occurrence of doxorubicin-induced cardiotoxicity observed in cancer patients, but also causes severe dilated cardiomyopathy and heart failure that is seen in clinical dilated cardiomyopathy of various etiologies. The objective of this study was to alter a previously established protocol for Adriamycin-induced cardiomyopathy in an effort to create a more consistent and less lethal model of heart failure. Adjustments that were enacted included a decrease in the cumulative dose of Adriamycin, reduction in number of intracoronary injections, and distribution of Adriamycin injection between the descending branch and the circumflex branch of the left coronary artery. The protocol of 22.5mg Adriamycin in 60mL saline administered intracoronary weekly for 2 weeks with concurrent administration of verapamil resulted in a predictable and severe model of dilated cardiomyopathy with reduced overall mortality compared to a previously published protocol. This protocol for induction of heart failure described here is relatively fast, technically simple, well tolerated by the animal, and has an acceptable mortality rate.

**Keywords:** doxorubicin, animal model, cardiomyopathy

## **Introduction**

Small laboratory animals appear to be unsuitable for research involving surgical treatment of heart failure due to size limitations and differences in myocardial metabolism and hemodynamic variables.<sup>1,2</sup> However, due to the substantial costs associated with care and housing of larger animals, sample sizes in experimental studies are often quite small. To advance the development of surgical techniques for congestive heart failure, extensive experimentation needs to continue on appropriate animal models, specifically a large animal model that produces a predictable and repeatable course of chronic heart failure with low unexpected mortality. The ideal animal model of CHF does not exist, as there are difficulties with species differences and creation of heart disease that accurately simulates the clinical course in humans.<sup>3</sup> The most common models include chronic rapid ventricular pacing, coronary microembolization, and Adriamycin-induced cardiomyopathy. Intracoronary Adriamycin administration creates a predictable, progressive, and irreversible model of dilated cardiomyopathy.<sup>4,5</sup> However, the main problems with this model are the necessity for multiple interventions, variable degrees of left ventricular dysfunction achieved, occurrence of systemic signs of Adriamycin toxicity, premature onset of clinical signs of heart failure, and ill-timed death.<sup>6</sup> In this study, adjustments to a previously published protocol were performed.<sup>4</sup> Our hypothesis is that modifications to the protocol for intracoronary administration of Adriamycin will result in a predictable model of dilated cardiomyopathy with minimal systemic side effects and reduced overall mortality rate.

## Materials and Methods

### *Summary*

Twelve adult male Walker hounds were used in this study. This study was approved by *The Animal Care and Use Committee* of Colorado State University as dogs were treated according to *The Guide for the Care and Use of Laboratory Animals* (NIH publication, No. 85-23, revised 1996). The dogs were assessed to be normal on physical examination, complete blood count, diagnostic biochemical profile, and echocardiogram and were negative for *Dirofilaria immitis* antigen in serum. Cardiomyopathy was induced through two intracoronary injections of Adriamycin performed two weeks apart (t = 0 and 2 weeks). The first evaluation was performed at 5 weeks when echocardiography was repeated and complete cardiac catheterization was performed. Following those procedures, dogs were randomized into control (n=6) and treatment (n=6) groups. Dogs in the treatment group were eliminated from the study at this point as an interventional procedure was performed for a separate study. Echocardiography and complete cardiac catheterization was repeated at 12 weeks on the remaining 6 dogs. Following data collection, dogs were humanely euthanized with an overdose of pentobarbital while still under general anesthesia. Dogs were necropsied and the hearts were harvested for gross and histopathological examination.

### *Anesthesia*

Dogs were premedicated with subcutaneous injections of atropine sulfate (0.04 mg/kg), acepromazine (0.1 mg/kg), and morphine (0.5 mg/kg). An 18-gauge, over-the-needle catheter was placed in a cephalic vein. Anesthesia was induced by intravenous

administration of propofol (3 to 6 mg/kg); isoflurane in oxygen was used for anesthetic maintenance following intubation. Additional anesthetic monitoring included direct or indirect blood pressure measurement, electrocardiography, pulse oximetry, and capnography. Intermittent mechanical positive pressure ventilation was performed with positive inspiratory pressure equal to 15 to 20 cmH<sub>2</sub>O at 8 to 10 breaths per minute. An inhalant agent analyzer was used to ensure a stable anesthetic plane during each procedure.

### *Echocardiography*

Echocardiographic examination was on the dogs without sedation in right and left lateral recumbency. The heart was examined using 2-D long-axis and short-axis views. Dimensions of the left and right ventricular walls and chambers during systole and diastole were obtained from 2-D guided M-mode.

### *Cardiomyopathy induction*

Dogs were started on verapamil (160mg, PO, bid, 3 weeks) and aspirin (80mg, PO, eod, 18 weeks) three days prior to first Adriamycin administration. Under general anesthesia, a 5-fr introducer was placed in the right femoral artery. A left, 5-fr, 3.0-3.5cm Judkins catheter was inserted through the introducer over a guidewire and advanced to the level of the left coronary ostia. Placement was confirmed by fluoroscopy using 3 to 5mL iodinated contrast material. Over a 20-minute period, 22.5mg of Adriamycin in 60mL saline was administered into either the anterior descending or circumflex branch of the left coronary artery at a rate of 3mL/min. This event was

repeated 2 weeks later. Atenolol (1mg/kg, PO, q24hr) was started 2 days following the second injection of Adriamycin and continued until the end of the study. To prevent interference with results of cardiac catheterization, the atenolol was temporarily discontinued for 48 hours prior to each catheterization procedure.

### *Cardiac Catheterization*

Dogs were placed under general anesthesia and 30 U/kg heparin and 22 mg/kg cefazolin were administered intravenously. Two 8-fr introducers were placed percutaneously into the left jugular vein. Right heart catheterization was performed using a 7-fr Swan-Ganz thermodilution catheter placed through one introducer and positioned in the pulmonary artery. Pulmonary arterial pressure, right atrial and ventricular pressure, central venous pressure, and pulmonary artery wedge pressure were measured with fluid-filled pressure transducers by advancing the catheter to those locations under fluoroscopic guidance. Cardiac output (CO) was determined using a thermodilution technique. Iced saline (10 cc) was injected into the Swan-Ganz catheter as a rapid bolus with mechanical ventilation temporarily discontinued. Thermodilution curves were evaluated for exponential decline and CO was calculated from the area underneath the thermodilution curve by a thermodilution computer system. The results of 3 to 5 curves were averaged to determine cardiac output.

A 7-fr dual-thermistor thermodilution catheter (Baim Coronary Sinus Flow Catheter, Wilton Webster Labs Inc., Altadena, CA) was placed through the second introducer and positioned in the coronary sinus. Coronary sinus blood flow was determined by continuous thermodilution technique. Iced saline solution was injected at

a constant rate (60 mL/min) at the distal port of the dual-thermistor catheter. Blood temperature, saline temperature, and mixture of blood and saline temperature were measured continuously during injection. Coronary sinus blood flow (CSBF) was continuously calculated by a Baim coronary sinus flow analyzer (CF 300A Flowmeter; Webster Labs Inc.) according to the following equation:

$$CSBF = C \times F_i(T_m - T_i) / (T_b - T_m)$$

where  $C = 1.19$  (ratio of specific heats of blood and saline),  $F_i = 60\text{mL/min}$  (saline flow),  $T_m =$  temperature of mixed blood and saline,  $T_i =$  saline temperature, and  $T_b =$  blood temperature.

An 8-fr introducer was placed in the right femoral artery to allow measurement of systemic arterial pressures and to facilitate placement of a micromanometer multi-segment pressure catheter (Mikro-tip pressure transducer catheter SPC-550, Millar Instruments, Dallas TX) in the left ventricle to measure left ventricular pressure. Measurements were recorded using a software-based data acquisition system (Superscope II, GW Instruments, East Cambridge, MA). Left ventricular  $\pm dP/dt$  was digitally derived using the computer software. Arterial ( $CaO_2$ ), venous, and coronary sinus ( $CcsO_2$ ) blood samples were collected at the time of data collection to determine oxygen content and allow calculation of systemic and myocardial oxygen extraction ratios. Other calculated data included stroke volume index (SVI), left ventricular stroke work index (LVSWI), myocardial oxygen consumption ( $MVO_2$ ), external work (EW), and cardiac efficiency (CE) based on the following equations:

$$SVI = CO / HR / BSA$$

$$LVSWI = SVI \times (MAP - PCWP) \times 0.0136$$

$$\text{MVO}_2 = (\text{CaO}_2 - \text{CcsO}_2) \times \text{CSBF (mL O}_2 / \text{min)}$$

$$\text{EW} = (\text{MAP} - \text{PCWP}) \times \text{CO}$$

$$\text{CE} = 0.133 \times \text{EW}/20 \times \text{MVO}_2$$

where CO = cardiac output, HR = heart rate, BSA = body surface area, MAP = mean arterial pressure, PCWP = pulmonary capillary wedge pressure, Ca O<sub>2</sub> = arterial oxygen content, and CcsO<sub>2</sub> = coronary sinus oxygen content.

### *Euthanasia / Necropsy*

Following the final cardiac catheterization, dogs were euthanized with an overdose of pentobarbital while still under general anesthesia. Hearts were harvested and representative sections of the left ventricle and right ventricle were evaluated using hematoxylin and eosin staining. Specimens were taken from the base, mid-ventricular wall, and apex regions. Each biopsy was scored for severity of histological changes, where 0 indicates no damage; 1, mild damage (vacuolar degeneration in < 10% of myocytes); 2, moderate damage (vacuolar degeneration in 10% to 50% of myocytes); 3, marked damage (vacuolar degeneration in > 50% of myocytes). A mean cardiomyopathy score was calculated for each dog.<sup>4</sup>

### *Statistical Analysis*

A computer software package (StatView, Abacus Concepts Inc, Berkeley CA) was used for statistical analysis. A Kaplan-Meier actuarial survival analysis was performed to determine mean survival, mortality rate, and the 75% probability of survival time point. Data was analyzed using ANOVA for repeated measures to evaluate the

effect of Adriamycin injection on hemodynamic and echocardiographic parameters. Histological grades of the ventricles were compared between dogs that survived the 12 weeks and those that did not using a Mann-Whitney U test. Comparison of the severity of histological lesions between the right and left ventricles was performed using a Wilcoxon's signed-rank test. Values of  $p < 0.05$  were considered significant. Values of  $P < 0.05$  were considered significant.

## Results

All 12 dogs survived until the 5-week evaluation. Of the 6 dogs that were evaluated out to 12 weeks for this study, four survived the entire study. Two dogs died suddenly from presumed ventricular arrhythmias at 6 and 11 weeks, respectively, resulting in a mortality rate of 33.3%. The 75% probability of survival was 12 weeks. The 5- and 10-week survival rates were 100% and 80% respectively (Figure 1a). No clinical signs of heart failure were apparent in any of the 12 dogs for the respective time periods that the dogs were evaluated.

All dogs had normal baseline echocardiographic parameters (Table 1). From baseline to the evaluation at 5 weeks, there was a significant decrease in ejection fraction (EF)  $64.2 \pm 9.8$  to  $54.0 \pm 13.4$  ( $P = 0.019$ ) and fractional shortening (FS) from  $64.2 \pm 9.8$  to  $27.8 \pm 8.0\%$  ( $P = 0.005$ ), but these parameters did not significantly worsen from 5 weeks to 12 weeks (EF,  $P = 0.298$ ; FS,  $P = 0.144$ ). Although left ventricular systolic and diastolic chamber dimensions increased from baseline to 5 weeks, this change was not significant. However, the left ventricular end-systolic and end-diastolic volume indices significantly increased from  $22.0 \pm 10.6$  to  $49.8 \pm 23.1$  ml/m<sup>2</sup> ( $P = 0.016$ ) and from  $71.1 \pm$

16.4 to  $99.4 \pm 23.4$  ml/m<sup>2</sup> (P = 0.004), respectively. Right ventricular dimensions also slightly increased during the same time frame, although the change was not statistically significant. Aortic velocity and isovolumetric relaxation time were only sporadically calculated during echocardiographic examination and therefore could not be evaluated.

Hemodynamic results are presented in Table 2. Left ventricular end-diastolic pressure (LVEDP) (P = 0.975), PCWP (P = 0.184), SVI (P = 0.826), and LVSWI (P = 0.721) did not significantly change from 5 to 12 weeks. Left ventricular end-systolic pressure (LVESP) was within normal limits at both 5 and 12 weeks. Myocardial oxygen consumption increased from  $72.4 \pm 27.6$  J at 5 weeks to  $181.2 \pm 56.8$  J at 12 weeks (P = 0.08) and cardiac efficiency decreased from  $26.9 \pm 3.8\%$  at 5 weeks to  $16.8 \pm 2.9\%$  at 12 weeks (P = 0.116) although these changes were not significant.

Histological specimens were characterized by varying degrees of cardiac myocyte degeneration (Figures 2 and 3). Degenerative regions were characterized by loss of myocyte cross striations, beginning in the perinuclear region, and progressing to the more peripheral portions of the myocyte. These areas also exhibited loss of normal cytoplasmic density (myocytolysis), which in more severe regions, progressed to marked cytoplasmic vacuolation (so called adria cells). In small focal areas, there was progression to hyaline type degeneration and myocyte necrosis, characterized by dense eosinophilic hyalinization and shrinking of the cytoplasm, and nuclear pyknosis. Mild to moderate interstitial edema was present in the most severely affected regions.

## Discussion

Administration of 45mg of Adriamycin divided in two intracoronary injections results in a predictable, stable, and nonreversible model of dilated cardiomyopathy in dogs. Survival rates were 100% at 5 weeks, 80% at 10 weeks, and 67% at 12 weeks. Verapamil, aspirin, and atenolol were administered to increase Adriamycin toxicity, prevent coronary artery thrombosis, and prevent ventricular fibrillation, respectively. None of the dogs demonstrated clinical signs of heart failure during the study period. Therefore, adjustments in the originally protocol<sup>4</sup> for dosing Adriamycin resulted in a model of severe dilated cardiomyopathy with improved survival.

The ideal animal model of heart failure should reflect a common human cardiac condition, mimic the clinical course of human heart failure, have consistent hemodynamic alterations, induce neurohumoral activation, and be practical, simple, and inexpensive to create.<sup>7-9</sup> The Adriamycin-induced cardiomyopathy model not only replicates the clinical occurrence of Adriamycin-induced cardiotoxicity seen in cancer patients, but also causes a severe dilated cardiomyopathy and heart failure that models dilated cardiomyopathy of various etiologies. Adriamycin (doxorubicin) is an anthracycline antibiotic that is isolated from cultures of *Streptomyces* species. Cardiotoxicity is a fairly unique property to this chemotherapeutic agent. Acute cardiotoxicity can occur, but cardiomyopathy most commonly occurs from chronic cumulative dosing. The exact mechanism of Adriamycin-induced cardiomyopathy is unclear, but proposed mechanisms include release of superoxides and hydroxyl radicals as well as mitochondrial calcium overload.<sup>10-11</sup> Classic histologic features include degeneration and atrophy of myocytes with loss of myofilaments.<sup>12</sup> There is also loss of

subcellular structural elements, mitochondrial degeneration, and cytoplasmic vacuolization.

Use of intracoronary Adriamycin administration to induce heart failure is not a new idea. Adriamycin-induced cardiomyopathy was first performed in a rabbit model by Jaenke et al<sup>11</sup> in 1976, who demonstrated that the cardiotoxic effects of Adriamycin are cumulative and nonreversible. The cardiotoxic properties of Adriamycin have since been well described, however the use of Adriamycin to create an animal model of heart failure to evaluate the effects of new therapies was first reported by Magovern et al in 1992.<sup>13</sup> It was shown that experimental administration of Adriamycin induces a repeatable, progressive, and irreversible pattern of left ventricular dysfunction.

There are several ways to administer Adriamycin to induce cardiomyopathy. The first and easiest method is intravenous administration. However, systemic doses of Adriamycin necessary to cause cardiac damage are associated with significant toxic effects on other organ systems, particularly the gastrointestinal tract and bone marrow.<sup>14-16</sup> Intracoronary administration allows application of a lower Adriamycin dose because it is not diluted in the systemic circulation. This allows the heart to be directly affected without secondary systemic adverse effects, such as myelosuppression. Access to the coronary vasculature can be achieved through surgical placement of an intracoronary catheter with a subcutaneous access port or through repeated cardiac catheterization through the femoral artery. The original description of surgical catheter placement was in 1992 by Magovern et al.<sup>13</sup> Following thoracotomy for catheter positioning in the left coronary artery, dogs were given 5 weekly infusions of 10mg doxorubicin. There were problems with catheter occlusion and overt heart failure occurred in only 1 of 6 dogs, yet

all dogs survived the 3-month study period. Repeated intracoronary injection through nonsurgical cardiac catheterization has also been described.<sup>4,5</sup> A Judkins catheter is used to selectively infuse the left main coronary artery. The obvious advantage to this method is the avoidance of a major surgical procedure. The disadvantage is the necessity for repeated femoral artery puncture under general anesthesia, which may become increasingly difficult with weekly injections.<sup>17</sup> However, surgically placed catheters still require the animal to be sedated during Adriamycin infusion. The implanted catheters are also prone to occlusion and may contribute to thrombosis of the coronary artery and major ventricular infarction. In an effort to decrease problems with repeated femoral artery puncture, the previously described protocol<sup>4</sup> was adjusted by increasing the overall dose and decreasing frequency of administration. As the protocol described here decreased the number of intracoronary injections to two, there was little difficulty in successfully catheterizing the same femoral artery two weeks in a row.

A variety of Adriamycin doses and dosing protocols for induction of cardiomyopathy have been described. The pilot protocol described by Magovern et al,<sup>13</sup> (10mg intracoronary infusions of Adriamycin weekly for 5 weeks) resulted in a significant decrease in left ventricular EF, cardiac output, and dP/dt with a significant increase in end-diastolic volume. Histological changes were consistent with previous descriptions of Adriamycin-induced cardiotoxicity. This same protocol was used recently by Christiansen et al,<sup>1,17</sup> in a project to further evaluate partial left ventriculectomy. An intracoronary catheter with a subcutaneous port was surgically placed in 6 large (30kg) dogs. An Adriamycin dose of 10mg was administered over a 1 hour period weekly for five weeks. Adriamycin administration resulted in a severe

dilated cardiomyopathy as determined by a significant increase in central venous pressure, mean pulmonary artery pressure, pulmonary wedge pressure, and ventricular dimensions with a significant drop in cardiac output and EF. Overall mortality was 17%, however the authors describe the management of the surgically placed catheters as delicate and tedious but necessary, to prevent thrombosis of the coronary artery or occlusion of the catheter.

Toyoda et al,<sup>5</sup> describes intracoronary administration of Adriamycin through repeated catheterization of the femoral artery using a protocol of 0.7mg/kg weekly for five weeks in six Beagles (8-12kg in body weight). A preliminary protocol of 1.0-1.5mg/kg within this study resulted in death before the completion of a 5-week study period, therefore the dosing regimen was altered. All dogs receiving the 0.7 mg/kg developed chronic dilated cardiomyopathy and survived a 12-week study period. Significant elevations in plasma norepinephrine and antinatriuretic peptide levels were also documented. However, by the end of the study period 3 dogs, or 50%, developed pericardial effusion and 1 dog also developed pleural effusion.

The protocol described in this study is an adjustment to the method described by Monnet et al,<sup>4</sup> using a dose of 15mg in 22 large breed dogs, administered intracoronary weekly for 4 weeks through serial cardiac catheterization. This resulted in an overall total dose of 60mg of Adriamycin per dog that produced a consistent dilated cardiomyopathy. Cardiac efficiency was documented to significantly decrease. However, the overall mortality rate for the study was 41%. Untimely deaths that could be attributed directly to Adriamycin toxicity and congestive heart failure occurred in 31% of dogs. The actuarial survival curve showed that 75% of the dogs died after the 48<sup>th</sup> day

following the first Adriamycin injection, while in the study presented here, 90% of the dogs were still alive on that day (Figure 1a and 1b). The weight of the animal was shown to be a risk factor in this previous study, as larger dogs had better survival than smaller dogs.<sup>4</sup> For the study presented here, the 30kg dogs received a total dose of only 45mg of Adriamycin using only two injections, and a marked dilated cardiomyopathy was still achieved.

Changes in echocardiographic variables were similar as left ventricular end-systolic and end-diastolic indices increased and ejection velocity decreased in both protocols. In the previous study,<sup>4</sup> aortic velocity significantly decreased while isovolumetric relaxation time significantly increased by 35%. Isovolumic relaxation time has been shown to be a sensitive and predictive indicator of Adriamycin cardiotoxicity.<sup>18</sup>

Significant alterations to hemodynamic variables were not observed in the study presented here compared to the previous protocol as likely the degree of cardiomyopathy achieved was less severe than that attained in the original study.<sup>4</sup> In that study, SVI and LVSWI decreased over the 10-week time period while these parameters were unchanged in the study described here. However, left ventricular end diastolic pressure was elevated when compared to normal, and in the presence of a normal LVESP, it is consistent with dilated cardiomyopathy.<sup>19</sup> Similar trends were seen in cardiac energetic parameters in both protocols as  $MVO_2$  increased and CE decreased. This change in CE was significant only in the original protocol as it was reduced by 50%.<sup>4</sup> Although not statistically significant in the study presented here, likely due to the reduced number of dogs, cardiac efficiency was decreased by close to 40%.

Unique to the study performed by Monnet et al,<sup>4</sup> was the use of verapamil to potentiate the cardiotoxic effects of Adriamycin and allow the use of a lower total overall dose. Using verapamil at a dose of 5 mg/kg q12h in combination with the 4-week protocol for intracoronary Adriamycin administration was found to give the most satisfactory reduction in EF. It has been shown that dogs receiving both doxorubicin and verapamil had a shorter survival time when compared to dogs receiving only doxorubicin.<sup>20</sup> Multiple other experimental studies have also demonstrated a more severe heart failure and reduction in survival with concurrent administration of Adriamycin and calcium channel blockers.<sup>21-22</sup> It is postulated that a heart injured by Adriamycin may need a higher calcium concentration to maintain function. Increased levels of myocardial cell calcium concentrations have been repeatedly shown to accompany Adriamycin cardiotoxicity.<sup>23</sup> Therefore, the presence of calcium channel blockers may contribute to further deterioration of cardiac function.<sup>24</sup> An additional mechanism that has been suggested is that both Adriamycin and calcium channel blockers may interfere with intracellular calmodulin-regulated calcium-dependent mechanisms.

Unexpected deaths due to intracoronary administration of Adriamycin are often a result of sudden fatal arrhythmias. Atenolol was utilized in this study to minimize the risk of sudden death. Atenolol is a  $\beta_1$ -adrenoreceptor blocker that is used preferentially in the dog due to few adverse reactions and simple once-a-day dosing. Beta-blockers are anti-arrhythmogenic due to inhibition of the effects of the sympathetic nervous system on the heart through limitation of spontaneous depolarization, reduction of sinus rate, and depression of atrio-ventricular conduction. The half-life of atenolol is 6 to 7 hours, so the washout period of 48 hours prior to cardiac catheterization is sufficient to prevent

interference with hemodynamic results.<sup>25</sup> Aspirin therapy was also instituted in this study as a method of platelet inhibition to minimize risk of thrombus formation secondary to repeated catheterization of large vessels for both intracoronary Adriamycin administration and for hemodynamic studies. Perhaps the use of both atenolol and aspirin in these dogs contributed to reduced morbidity and mortality.

Monnet et al,<sup>4</sup> also found that dogs that died prematurely had more severe lesions in the left ventricle when compared to the right. In the study presented here, the myocardial lesions were consistent between left and right ventricular tissues. A particular effort was made in this study to alternate injection sites between the anterior descending and circumflex branches of the left coronary artery for the individual dog. The circumflex branch travels in the coronary groove and then turns into the subsinusoidal interventricular branch (formerly called the caudal descending coronary artery), which has branches to the left ventricle, right ventricle, and interventricular septum.<sup>26</sup> The subsinusoidal interventricular branch also has normal anastomoses to the last branch of the right coronary artery. Although Adriamycin injection is primarily directed toward the left ventricle, by utilizing the circumflex branch of the left coronary artery and due to the extensive collateral circulation of the canine, there is likely more even distribution of Adriamycin throughout the entire left ventricle as well as distribution to the right ventricle. Perhaps this adjustment to the technique can also be linked to reduced mortality, as the impact to the left ventricle is not as concentrated.

There are two significant limitations to the study. First, we only had a small number of dogs to evaluate. Although we have early echocardiographic data on 12 dogs, hemodynamic data could only be collected on six dogs that did not go on to have

interventional treatment. Also, due to study design limitations, we did not obtain baseline hemodynamic data for the six dogs that completed the entire 12-week study interval. This prevents us from drawing significant conclusions from the data that we have available to us.

However, our protocol of 22.5mg in 60mL saline administered intracoronary weekly for 2 weeks with concurrent administration of verapamil resulted in a predictable and severe model of dilated cardiomyopathy. Survival at 5 and 10 weeks was highly acceptable at 100 and 80%, respectively. Therefore, the protocol for heart failure induction described in this study is relatively fast, technically simple, well tolerated by the animal, and has an acceptable mortality rate.

## References

1. Christiansen S, Stypmann J, Jahn UR, Redmann, K, Fobker M, Gruber AD, Scheld HH, Hammel D. Partial left ventriculectomy in modified Adriamycin-induced cardiomyopathy in the dog. *J Heart Lung Transplant* 2003;22:301-308.
2. Iannini JP, Spinale FG. The identification of contributory mechanisms for the development and progression of congestive heart failure in animal models. *J Heart Lung Transplant* 1996;15:1138-1150.
3. Monnet E, Chachques JC. Animal models of heart failure: what is new? *Ann Thorac Surg* 2005;79:1445-1453.
4. Monnet E, Orton EC. A canine model of heart failure by intracoronary Adriamycin injection: hemodynamic and energetic results. *J Cardiac Failure* 1999;5:255-264.
5. Toyoda Y, Okada M, Kashem MA. A canine model of dilated cardiomyopathy induced by repetitive intracoronary doxorubicin administration. *J Thorac Cardiovasc Surg* 1998;115:1367-1373.
6. Yarborough WM, Spinale FG. Large animal models of congestive heart failure: a critical step in translating basic observations into clinical applications. *J Nucl Cardiol* 2003;10:77-86.
7. Arnolda LF, Llewellyn-Smith IJ, Minson JB. Animal models of heart failure. *Aust N Z J Med* 1999;29:403-409.
8. Muders F, Elsner D. Animal models of chronic heart failure. *Pharmacol Res* 2000;41:605-612.
9. Power JM, Tonkin AM. Large animal models of heart failure. *Aust N Z J Med* 1999;29:395-402.
10. Doroshow JH. Effect of anthracycline antibiotics on oxygen radical formation in the rat heart. *Cancer Res* 1983;43:460-472.
11. Jaenke RS. Delayed and progressive myocardial lesions after Adriamycin administration in the rabbit. *Cancer Res* 1976;36:2958-2966.
12. Bristow MR, Mason JW, Billingham ME, et al. Doxorubicin cardiomyopathy: Evaluation by phonocardiography, endomyocardial biopsy, and cardiac catheterization. *Ann Intern Med* 1978;88:168-175.
13. Magovern JA, Christleb IY, Badylak SF, Lantz GC, Kao RL. A Model of left ventricular dysfunction caused by intracoronary Adriamycin. *Ann Thorac Surg* 1992;53:861-863.

14. Gralla EJ, Fleischman RW, Luthra YK, Stadnicki SW. The dosing schedule dependent toxicities of Adriamycin in beagle dogs and rhesus monkeys. *Toxicology* 1979;13:263-273.
15. Tomlinson CW, Godin DV, Rabkin SW. Adriamycin cardiomyopathy: pathological and membrane functional changes in a canine model with mild impairment of left ventricular function. *Can J Cardiol* 1986;2:368-374.
16. Van Vleet JF, Greenwood LA, Ferrans VJ. Pathologic features of Adriamycin toxicosis in young pigs: nonskeletal lesions. *Am J Vet Res* 1979;40:1537-1552.
17. Christiansen S, Redmann K, Scheld HH, Jahn UR, Stypmann J, Fobker M, Gruber AD, Hammel D. Adriamycin-induced cardiomyopathy in the dog – an appropriate model for research on partial left ventriculectomy? *J Heart Lung Transplant* 2002;21:783-790.
18. Stoddard MF, Seeger J, Liddell NE, et al. Prolongation of the isovolumetric relaxation time as assessed by Doppler echocardiography predicts doxorubicin-induced systolic dysfunction in humans. *J Am Coll Cardiol* 1992;20:62-69.
19. Thomas WP, Sisson D. Cardiac catheterization and angiography. In Fox PR, Sisson D, Moise NS (eds.): *Textbook of Canine and Feline Cardiology*. WB Saunders Co., Philadelphia, 1998, pp 173-192.
20. Bright JM, Buss DD. Effects of verapamil on chronic doxorubicin-induced cardiotoxicity. *J Nat Cancer Inst* 1990;82:963-964.
21. Klugmann S, Bartoli Klugmann F, Decroti G, et al. Adriamycin experimental cardiomyopathy in Swiss mice. Different effects of two calcium antagonistic drugs on ADM-induced cardiomyopathy. *Pharmacol Res Commun* 1981;13:769-776.
22. Rabkin SW, Otten M, Polimeni PI. Increased mortality with cardiotoxic doses of Adriamycin after verapamil pretreatment despite prevention of myocardial calcium accumulation. *Can J Physiol Pharmacol* 1983;61:1050-1056.
23. Kusuoka H, Futaki S, Koretsune Y, et al. Alterations of intracellular calcium homeostasis and myocardial energetics in acute Adriamycin-induced heart failure. *J Cardiovasc Pharmacol* 1991;18:437-444
24. Rabkin SW, Godin DV. Adriamycin cardiotoxicity and calcium entry blockers: the need for caution in the combination. *Can J Cardiol* 1985;1:IV-VII.
25. Opie LH, Yusuf S.  $\beta$ -blocking agents. In Opie LH (ed.): *Drugs for the heart*. 5<sup>th</sup> ed. Philadelphia: WB Saunders, 2001.
26. Evans HE. *Miller's Anatomy of the Dog*. 3<sup>rd</sup> ed. Philadelphia: WB Saunders, 1993.

**Table 3-1.** Echocardiographic data presented as mean  $\pm$  standard deviation.

Parameter (# of dogs)	Baseline (12)	5 weeks (12)	12 weeks (4)
Fractional Shortening (%)	34.6 $\pm$ 7.0 <sup>a</sup>	27.8 $\pm$ 8.0 <sup>b</sup>	24.68 $\pm$ 8.3 <sup>b</sup>
Ejection fraction (%)	64.2 $\pm$ 9.8 <sup>a</sup>	54.0 $\pm$ 13.4 <sup>b</sup>	51.2 $\pm$ 13.1 <sup>b</sup>
LV-EDT (mm)	10.3 $\pm$ 1.6 <sup>a</sup>	10.6 $\pm$ 1.5 <sup>a</sup>	9.3 $\pm$ 1.3 <sup>a</sup>
LV-EDD (mm)	39.8 $\pm$ 3.2 <sup>a</sup>	40.3 $\pm$ 4.6 <sup>a</sup>	44.8 $\pm$ 3.5 <sup>b</sup>
LV-EST (mm)	15.4 $\pm$ 2.1 <sup>a</sup>	14.4 $\pm$ 2.4 <sup>a</sup>	12.4 $\pm$ 2.8 <sup>a</sup>
LV-ESD (mm)	25.7 $\pm$ 4.6 <sup>a</sup>	28.5 $\pm$ 4.9 <sup>a</sup>	33.8 $\pm$ 6.1 <sup>b</sup>
LV-ESV (ml)	22.0 $\pm$ 10.6 <sup>a</sup>	30.6 $\pm$ 11.4 <sup>a</sup>	49.8 $\pm$ 23.1 <sup>b</sup>
LV-EDV (ml)	71.1 $\pm$ 16.4 <sup>a</sup>	74.0 $\pm$ 21.8 <sup>a</sup>	99.4 $\pm$ 23.4 <sup>b</sup>
RV-EDT (mm)	5.0 $\pm$ 1.0 <sup>a</sup>	5.6 $\pm$ 1.2 <sup>a</sup>	5.2 $\pm$ 1.4 <sup>a</sup>
RV-EDD (mm)	10.4 $\pm$ 1.2 <sup>a</sup>	14.0 $\pm$ 4.6 <sup>a</sup>	12.5 $\pm$ 4.4 <sup>a</sup>

LV = left ventricle; EDT = end-diastolic wall-thickness; EDD = end-diastolic chamber diameter; ESV = end-systolic volume; EDV = end-diastolic volume; RV = right ventricle; different letters (a vs. b) indicate statistical significance.

**Table 3-2.** Hemodynamic data presented as mean  $\pm$  standard deviation.

Parameter (# of dogs)	5 weeks (12)	12 weeks (4)
CVP (mmHg)	9.1 $\pm$ 4.7	5.1 $\pm$ 2.7
Mean PAP (mmHg)	16.86 $\pm$ 2.0	19.87 $\pm$ 4.6
PCWP (mmHg)	8.4 $\pm$ 2.5	11.6 $\pm$ 3.6
LVESP (mmHg)	120.6 $\pm$ 28.8	114.9 $\pm$ 17.1
LVEDP (mmHg)	21.75 $\pm$ 5.6	22.12 $\pm$ 17.6
dP/dt	1590 $\pm$ 456.2	1782 $\pm$ 701.3
SVI (ml/m <sup>2</sup> /beat)	25.57 $\pm$ 10.19	26.99 $\pm$ 6.67
LVSWI (g/m/m <sup>2</sup> /beat)	23.96 $\pm$ 7.70	26.53 $\pm$ 3.44
MVO <sub>2</sub> (J)	72.4 $\pm$ 27.6	181.2 $\pm$ 56.8
External Work (J)	0.27 $\pm$ 0.04	0.17 $\pm$ 0.03
Cardiac Efficiency (%)	26.9 $\pm$ 3.8	16.8 $\pm$ 2.9

CVP = central venous pressure; PAP = pulmonary artery pressure; PCWP = pulmonary capillary wedge pressure; LVESP = left ventricular end-systolic pressure; LVEDP = left ventricular end-diastolic pressure; MVO<sub>2</sub> = myocardial oxygen consumption

Figure 3-1a. Actuarial survival curve.

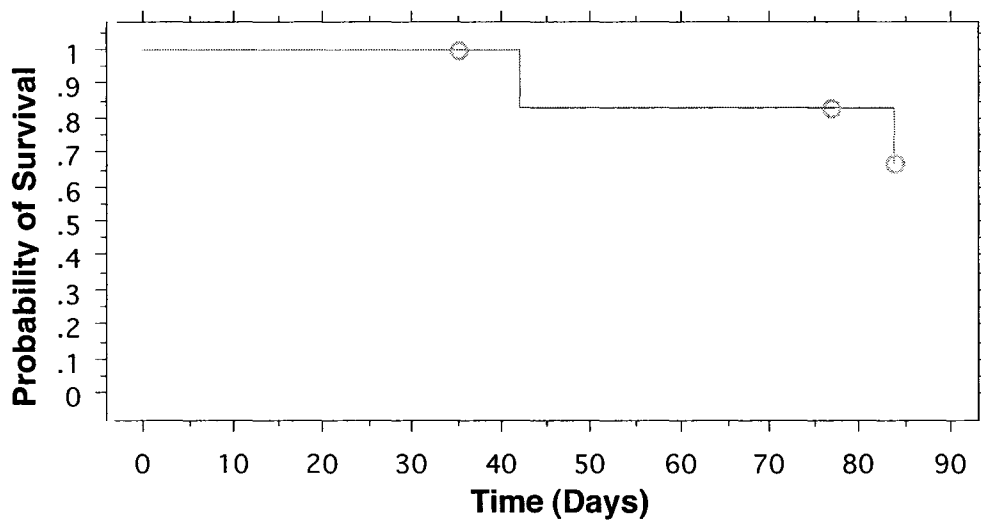
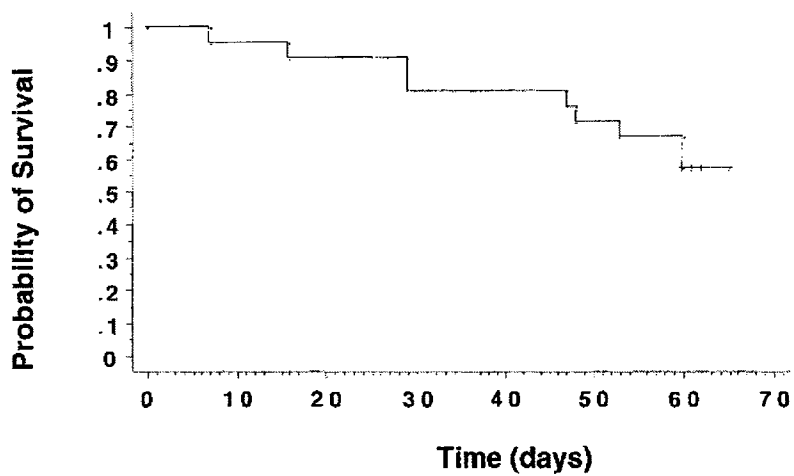
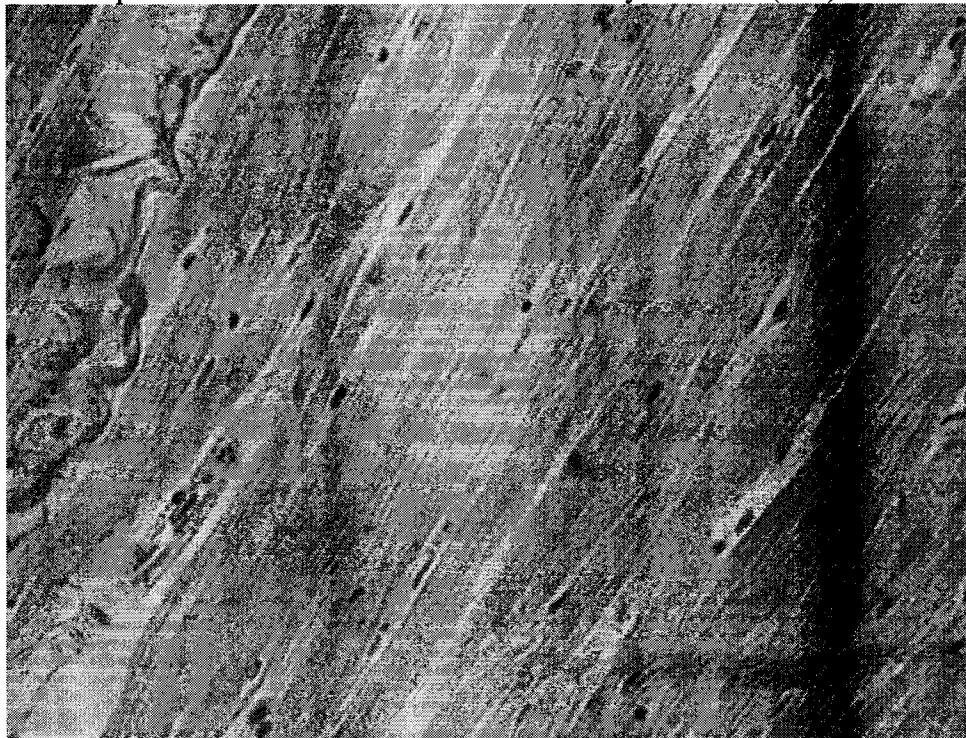


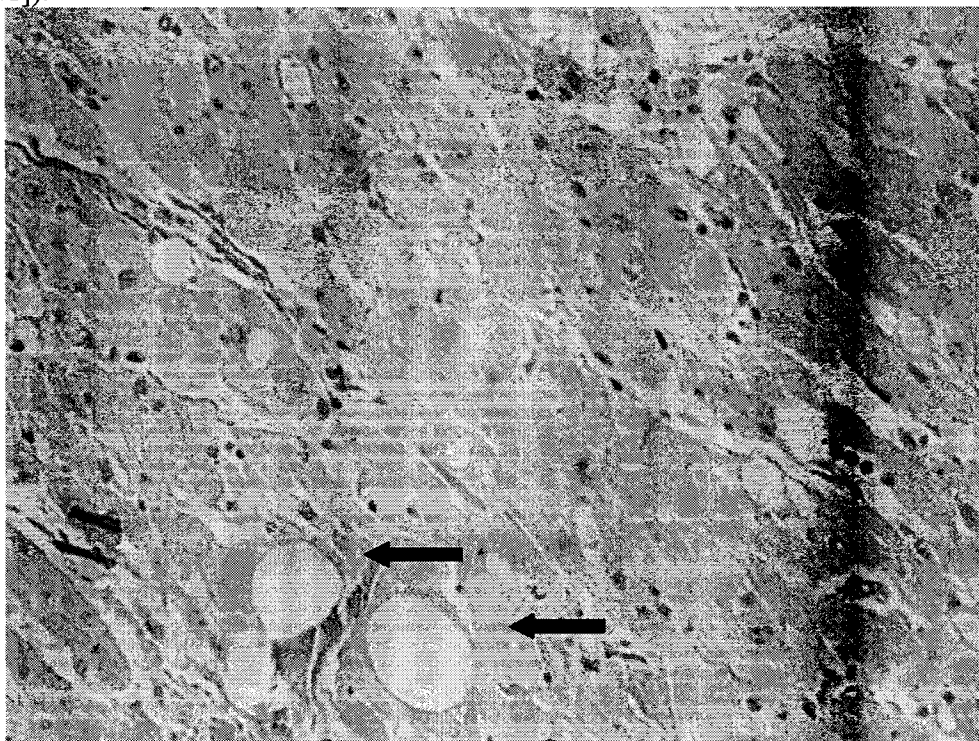
Figure 3-1b. Actuarial survival curve from Monnet et al.<sup>4</sup>



**Figure 3-2.** Representative section of normal canine myocardium (40x).



**Figure 3-3.** Representative section of canine myocardium (40x) following intracoronary administration of Adriamycin. This section demonstrates myocyte degeneration, interstitial edema, myocytolysis and marked cytoplasmic vacuolization (adria cells [arrows]).



## CHAPTER 4

Evaluation of prosthetic cardiac binding as an interventional treatment in a canine model  
of Adriamycin-induced dilated cardiomyopathy

Catriona M. MacPhail, DVM, Diplomate ACVS, Eric Monnet, DVM, PhD, Diplomate  
ACVS, ECVS, David Getzy, DVM, Diplomate ACVP

## Introduction

For surgical treatment of heart failure, there are several distinct approaches. The gold standard is heart transplantation, but due to the shortage of donor organs and often poor candidate eligibility, other procedures have been investigated. Use of trained skeletal muscle to assist the heart is one modality that has been explored in experimental and clinical settings. The most well known surgical technique is dynamic cardiomyoplasty. In this procedure latissimus dorsi muscle is harvested, transposed into the thoracic cavity, and wrapped around the heart. After a period of training, stimulation of the muscle wrap is synchronized with cardiac contraction, which is thought to augment systolic function.<sup>1-3</sup> However, the main benefit of dynamic cardiomyoplasty may be from the presence of the wrap itself. When the muscle is wrapped around the heart, it results in what is known as the “girdling effect” which prevents progressive ventricular dilatation and may lead to reverse ventricular remodeling.<sup>4</sup> Wrapping the heart with skeletal muscle without muscle stimulation is known as adynamic cardiomyoplasty. Unfortunately, both dynamic and adynamic cardiomyoplasty are associated with significant morbidity due to latissimus dorsi muscle harvest. Thus, recent research has focused on the use of nonbiological materials to accomplish the same goals as adynamic cardiomyoplasty. Prosthetic cardiac binding and device-based ventricular reshaping are currently under investigation for surgical treatment of heart failure.

Prosthetic cardiac binding is an experimental surgical procedure that is designed to mimic the girdling effect seen in dynamic cardiomyoplasty. The Corcap Cardiac Support Device (CSD) (Acorn Cardiovascular, Inc., St. Paul, MN) is an example of a ventricular reshaping method that is very similar to prosthetic cardiac binding. Multiple

studies have demonstrated that both prosthetic cardiac binding and ventricular reshaping limit progressive ventricular dilatation and may improve cardiac function by decreasing myocardial wall stress.<sup>5-11</sup>

Several studies have evaluated PCB in experimental settings; most studies have consistently found that PCB limits progressive ventricular dilatation and may contribute to improvement in cardiac function.<sup>8-10</sup> However, in those studies the surgical procedure was always performed first and heart failure induced later, which fails to mimic any clinical course of heart failure. We believe that to optimally evaluate PCB, cardiac failure should be induced first, followed by the interventional therapy. In the study described here, prosthetic cardiac binding was performed as an interventional treatment in a canine model of Adriamycin-induced cardiomyopathy. Therefore, the initial hypothesis was that cardiac binding would prevent further progression of left ventricular dilatation and improve overall cardiac function in an established model of heart failure.

An additional concern regarding cardiac binding is whether or not prosthetic ventricular containment constricts diastolic filling. This issue has been evaluated in the CSD, but not with other methods of cardiac binding.<sup>9,12</sup> Constrictive pathology can develop from either the presence of the wrap itself or from the reaction of the epicardium to the presence of the nonbiologic wrap. Histological evaluation of the CSD after chronic implantation revealed thin encapsulation of the CSD by connective tissue, with no evidence of active inflammation.<sup>9</sup> Also, there was a distinct demarcation between the epicardium and the CSD and no hemodynamic evidence of constrictive or restrictive physiology. The CSD is a knitted mesh jacket made of polyester fibers. However, the presence or interference of an epicardial reaction from prosthetic cardiac binding using

polypropylene has not been well investigated. This is of concern as constrictive pericarditis has been previously attributed to polypropylene mesh, which was used as a pericardial substitute in two human patients.<sup>13</sup>

In the study presented here, we additionally examined parameters that may be indicative of ventricular constraint as well as performing histological examination of the epicardial surface. Therefore, an additional hypothesis to this study was that cardiac binding would provide ventricular constraint and improve cardiac function without causing a constrictive pathology or significant epicardial reaction.

## **MATERIALS & METHODS**

### *Summary*

This study was approved by *The Animal Care and Use Committee* of Colorado State University as dogs were treated according to *The Guide for the Care and Use of Laboratory Animals* (NIH publication, No. 85-23, revised 1996). Twelve young adult male Walker hounds were used in this study. The dogs were assessed to be normal on physical examination, complete blood count, diagnostic biochemical profile, and echocardiogram and were negative for *Dirofilaria immitis* antigen in serum.

Cardiomyopathy was induced by administration of Adriamycin into the left coronary artery twice, two weeks apart (t = 0 and 2 weeks) with concurrent verapamil and atenolol administration. Echocardiography and complete cardiac catheterization were performed on week 5 of the study, 3 weeks after the last intracoronary injection. Following those procedures, dogs were randomized into control (n=6) and treatment (n=6) groups.

Individual treatment dogs were designated and referred to as Dogs #1 through 6. Dogs in

the treatment group underwent surgery one week following the baseline cardiac catheterization. The PCB procedure was performed through a median sternotomy under general anesthesia. Echocardiography and complete cardiac catheterization were repeated on all dogs at 12 weeks. Following data collection, dogs were humanely sacrificed with an overdose of pentobarbital while still under general anesthesia. Dogs were necropsied and the hearts were harvested for gross and histopathological examination.

### *Anesthesia*

Dogs were premedicated with subcutaneous injections of atropine sulfate (0.04 mg/kg), acepromazine (0.1 mg/kg), and morphine (0.5 mg/kg). Anesthesia was induced by intravenous administration of propofol (3 to 6 mg/kg); isoflurane in oxygen was used for anesthetic maintenance following intubation. For the 2 intracoronary injections of Adriamycin, systolic blood pressure was monitored using the noninvasive Doppler ultrasound method. During cardiac catheterization, systolic (SAP), diastolic (DAP), and mean (MAP) arterial blood pressures were monitored directly through an arterial catheter placed in the femoral or dorsal pedal artery. Additional anesthetic monitoring for all procedures included electrocardiography, pulse oximetry, and capnography. Intermittent mechanical positive pressure ventilation was performed with positive inspiratory pressure equal to 15 to 20 cmH<sub>2</sub>O at 8 to 10 breaths per minute. An inhalant agent analyzer was used to ensure a stable anesthetic plane during each procedure.

### *Echocardiography*

Echocardiographic examination was performed on the dogs using only gentle restraint without sedation in both right and left lateral recumbency. The heart was examined using 2-D long-axis and short-axis views. Dimensions of the left and right ventricular walls and chambers during systole and diastole were obtained from 2-D guided M-mode. Aortic, mitral, and tricuspid blood flow velocities were measured using Doppler and pulsed Doppler echocardiography.

### *Induction of Cardiomyopathy*

Dogs were administered verapamil (160 mg, PO, bid, 3 weeks) and aspirin (80 mg, PO, eod, 18 weeks) beginning three days prior to the first Adriamycin administration. Under general anesthesia, an 8-fr introducer was placed in the right femoral artery. Following introducer placement, heparin (30U/kg) was administered intravenously. A Judkins catheter was inserted through the introducer over a guidewire and advanced to the level of the coronary ostia. Placement was confirmed by fluoroscopy using 3 to 5 mL iodinated contrast material. Over a 20 minute period, 22.5 mg of Adriamycin in 60 mL saline was administered into either the anterior descending or circumflex branch of the left coronary artery at a rate of 3 mL/min. The injection was repeated 2 weeks later into the branch of the left coronary artery not previously injected. To minimize the risk of sudden death from ventricular arrhythmias, atenolol (1 mg/kg, PO, q24hr) was started 2 days following the second injection of Adriamycin and continued until the end of the study. To prevent interference with results of cardiac

catheterization, atenolol administration was temporarily discontinued for 48 hours prior to each catheterization procedure and resumed the following day.

### *Cardiac Catheterization*

Dogs were placed under general anesthesia as described and 30 U/kg heparin and 22 mg/kg cefazolin were administered intravenously. Two 8-fr introducers were placed percutaneously into the left jugular vein. Right heart catheterization was performed using a 7-fr Swan-Ganz thermodilution catheter placed through one introducer. Pulmonary arterial pressure, right atrial and ventricular pressure, central venous pressure, and pulmonary capillary wedge pressure (PCWP) were measured with fluid-filled pressure transducers by advancing the catheter to those locations under fluoroscopic guidance. Cardiac output was determined using a thermodilution technique. Iced saline (10 cc) was injected into the Swan-Ganz catheter as a rapid bolus with mechanical ventilation temporarily discontinued. Thermodilution curves were evaluated for exponential decline and CO was calculated from the area underneath the thermodilution curve by a thermodilution computer system. The results of 3 to 5 curves were averaged to determine cardiac output.

A 7-fr dual-thermistor thermodilution catheter (Baim Coronary Sinus Flow Catheter, Wilton Webster Labs Inc., Altadena, CA) was placed through the second introducer and positioned in the coronary sinus. Coronary sinus blood flow was determined by continuous thermodilution technique. Iced saline solution was injected at a constant rate (60 mL/min) at the distal port of the dual-thermistor catheter. Blood temperature, saline temperature, and mixture of blood and saline temperature were

measured continuously during injection. Coronary sinus blood flow (CSBF) was continuously calculated by a Baim coronary sinus flow analyzer (CF 300A Flowmeter; Webster Labs Inc.) according to the following equation:

$$\text{CSBF} = C \times F_i(T_m - T_i) / (T_b - T_m)$$

where  $C = 1.19$  (ratio of specific heats of blood and saline),  $F_i = 60\text{mL/min}$  (saline flow),  $T_m =$  temperature of mixed blood and saline,  $T_i =$  saline temperature, and  $T_b =$  blood temperature.

An 8-fr introducer was placed in the right femoral artery to allow measurement of systemic arterial pressures and to facilitate placement of a micromanometer multi-segment pressure-volume catheter (Mikro-tip multi-segment pressure-volume transducer catheter SPC-550, Millar Instruments, Dallas TX) in the left ventricle to measure left ventricular pressure and volume. Measurements were recorded using a software-based data acquisition system (Superscope II, GW Instruments, East Cambridge, MA). Left ventricular  $\pm dP/dt$ ,  $\pm dV/dt$ , and tau ( $\tau$ , the time constant of relaxation). Tau was determined from linear regression analysis of  $dp/dt$  versus LVP with  $\tau$  being equal to the slope of the regression plot during diastole. Pressure-volume loops were created from the accumulated data. Arterial ( $\text{CaO}_2$ ), venous, and coronary sinus ( $\text{CcsO}_2$ ) blood samples were collected at the time of data collection to determine oxygen content and allow calculation of systemic and myocardial oxygen extraction ratios. At the 12-week catheterization, the end-systolic pressure-volume relation (ESPVR; slope of the pressure-volume line at end-systole) and end-diastolic pressure-volume relation (EDPVR) were determined after creation of multiple pressure-volume loops by transient interruption of caudal vena cava inflow. This was accomplished by inflation of 20mL balloon catheter

placed through a 12fr introducer in the femoral vein to the level of the post-hepatic caudal vena cava. Calculated data included myocardial oxygen consumption ( $MVO_2$ ), external cardiac work (EW), and cardiac efficiency (CE).

$$MVO_2 = (Ca O_2 - CcsO_2) \times CSBF \text{ (mL } O_2 / \text{ min)}$$

$$EW = (MAP - PCWP) \times CO$$

$$CE = 0.133 \times EW/20 \times MVO_2$$

### *Surgery*

Under general anesthesia dogs were placed in dorsal recumbency. A triple-lumen jugular catheter was placed in the right jugular vein. The thoracic cavity was accessed through a median sternotomy. A subtotal pericardiectomy was performed to the level atrioventricular groove so as to preserve the phrenic nerves bilaterally. A 20 x 20cm sheet of polypropylene (Marlex®) mesh was fitted around the heart and sutured to the remaining pericardium using 3-0 polypropylene suture (Surgilene®) and 3/8" x 3/16" x 1/16" polytetrafluoroethylene pledgets in an interrupted horizontal mattress pattern. The mesh was then sutured to itself completing the wrap around the ventricles. The mesh was placed such that it was in complete contact with the epicardium without causing an increase in central venous pressure (Figure 1). Heavy polybutester suture was placed from the apex of the mesh to the xiphoid to replace the sternopericardial ligament. A thoracostomy tube was placed and closure was routine.

Dogs were recovered in an intensive care unit for 3 days and continuously monitored with electrocardiography and arterial pressure determination. Dogs were maintained on continuous infusion of intravenous fentanyl (1-6 mcg/kg/hr) and crystalloid fluids (30 mg/kg/day Normosol with 40 to 60 mEq/L KCl) for at least 48

hours. Oral carprofen (2 mg/kg, BID, 10 days; Rimadyl®, Pfizer Animal Health, Exton, PA) was started as soon as the dogs were willing to eat. Lidocaine (1-2 mg/kg) and bupivacaine (1-2 mg/kg) were infused into the thoracostomy tube every 6 hours for local anesthetic effects. Thoracostomy tubes were evacuated every hour for four hours, and then once every four hours until drainage abated and the tube was removed. Dogs were then moved to routine housing and evaluated daily for evidence of surgical complications or clinical signs consistent with progressive cardiomyopathy.

#### *Euthanasia / Necropsy*

Following the final cardiac catheterization, dogs were sacrificed with an overdose of pentobarbital while still under general anesthesia. Representative sections of the left ventricular free wall and right ventricular free wall with in situ synthetic cardiac wrap mesh were evaluated, using routine hematoxylin and eosin staining. Samples were taken from the base, mid-ventricular wall, and apex regions. Polarization microscopy was also utilized to evaluate the synthetic material as well as to assess early fibrosis.

#### *Statistical Analysis*

A computer software package (StatView, Abacus Concepts Inc, Berkeley CA) was used for statistical analysis. Data were analyzed using analysis of variance for repeated measures to evaluate the effect of PCB on hemodynamic and echocardiographic parameters. Values of  $P < 0.05$  were considered significant

## Results

Three of six treatment dogs and four of six control dogs completed the entire study. One treatment dog (Dog #6) developed clinical signs of congestive biventricular heart failure four weeks after surgery ( $t = 10$  weeks) and died during the final catheterization procedure ( $t = 12$  weeks). The other two treatment dogs died one ( $t = 7$  weeks) and two ( $t = 8$  weeks) weeks after surgery from pulmonary thromboembolism (Dog #2) and presumed ventricular arrhythmias (Dog #5), respectively. Two control dogs died suddenly at  $t = 6$  and 11 weeks presumably from ventricular arrhythmias. Due to the small number of dogs surviving the study, statistical comparison of several parameters was not possible.

### *Descriptive Statistics for Individual Treatment Dogs*

#### DOG #1

Baseline echocardiographic parameters were within normal limits. Echocardiographic evaluation at 5 weeks revealed decreased ejection fraction from 74 to 61% and fractional shortening from 42 to 32%, however ventricular dimensions were unaltered. Following surgery, ejection fraction and fractional shortening continued to deteriorate. Ejection fraction decreased from 61 to 51% at 9 weeks (3 weeks after surgery) to 46% at 12 weeks (6 weeks after surgery). Fractional shortening decreased from 32 to 26 to 23% during the same time frame. However, no change in the size of the left and right ventricles was noted.

From the initial hemodynamic study to six weeks postoperatively, heart rate, arterial blood pressure, left ventricular end-diastolic pressure, and  $dp/dt$  were unchanged. However, several parameters did decrease during this time frame including pulmonary

capillary wedge pressure (17.1 to 12.9 mmHg) central venous pressure (11.8 to 5.3 mmHg) and cardiac index (4.5 to 2.3 L/min/m<sup>2</sup>). Oxygen extraction ratio increased from 10.7 to 22.3% with external cardiac work decreasing from 33.5 to 15.6J. Due to technical error, MVO<sub>2</sub> was not measured during the initial cardiac catheterization, therefore cardiac efficiency could not be determined. However, at 12 weeks MVO<sub>2</sub> was 33.9 J and cardiac efficiency was calculated to be 46%.

### DOG #3

From baseline to the end of the study, ejection fraction decreased from 54 to 44% and fractional shortening decreased from 27.5 to 21.4%. Left ventricular chamber diameter during diastole was 42.6 mm at baseline, 45.5 mm at 5 weeks, and 47.1 mm at 12 weeks with left ventricular free wall thickness decreasing from 9.5 to 9.2 to 8.5 mm and left ventricular diastolic volume index increasing from 83.3 to 96.6 to 118.8 mm/m<sup>2</sup> during the same time frame.

Basic hemodynamic parameters (heart rate, blood pressure, central venous pressure) were unchanged over the course of this study, as was pulmonary capillary wedge pressure. However, left ventricular end-diastolic pressure increased from 24.4 to 34.4 mmHg and left ventricular end-diastolic volume increased from 151.6 to 190.3 mL from 5 weeks to 12 weeks. Dp/dt decreased from 2228.0 to 985.0, cardiac index decreased from 5.27 to 2.63 L/min/m<sup>2</sup>, and oxygen extraction ratio increased from 16.1 to 31.6% during the same time frame. Myocardial oxygen consumption decreased from 77.0 to 65.8 J as did cardiac external work (20.2 to 6.1 J) with a resulting dramatic decrease in cardiac efficiency from 26.2 to 9.3%. Single and multiple pressure-volume

loops were created for this dog at the 6 and 12-week catheterization, respectively (Figures 2 and 3).

#### DOG #4

For this dog, left ventricular dimensions were increased following induction of heart failure and then remained unchanged for the remainder of the study. Fractional shortening decreased from 27.5% at 5 weeks to 20.6% at 12 weeks while ejection fraction decreased from 53% to 42%. Left ventricular diastolic volume index increased from 78.5 mm/m<sup>2</sup> at baseline to 96.0 mm/m<sup>2</sup> at 5 weeks, but then returned to normal value (78.3 mm/m<sup>2</sup>) at 12 weeks.

Heart rate and arterial blood pressure remained normal, however central venous pressure (7.5 to 10 mmHg), pulmonary capillary wedge pressure (11.6 to 17.5 mmHg), and left ventricular end-diastolic pressure (18.75 to 36.6 mmHg) increased from 5 to 12 weeks. Dp/dt decreased from 1623.0 to 847.0, cardiac index decreased from 3.1 to 1.96 L/min/m<sup>2</sup>, and oxygen extraction ratio increased from 18.6 to 22.7% during the same time frame. Due to technical errors measuring coronary sinus blood flow, myocardial oxygen consumption was not determined at either cardiac catheterization event. Consequently, cardiac efficiency could not be calculated. However, cardiac external work did decrease from 25.2 to 7.9 J.

#### DOG #6

This dog developed clinical signs of biventricular heart failure (ascites, pulmonary edema) at 10 weeks (4 weeks postoperatively). As attitude and appetite remained normal, the dog was started on furosemide (2.2 mg/kg PO q12hr) and digoxin (0.25 mg PO bid). Echocardiographic data was collected at each time point, however the

dog arrested shortly after induction of general anesthesia for the final cardiac catheterization procedure. Resuscitation was not attempted.

Ejection fraction and fractional shortening were still within normal limits at 5 weeks. However, these parameters rapidly deteriorated over the next 7 weeks. At the 12 week echocardiographic evaluation, ejection fraction had decreased from 57% to 21% and fractional shortening had decreased from 29.5% to 9.8%. Left ventricular diastolic volume index increased from 43.4 at baseline to 57.6 at 5 weeks to 81.5 mm/m<sup>2</sup> at 12 weeks. Left ventricular chamber diameter during diastole increased from 34.6 mm at baseline to 43 mm at the end of the study with left ventricular wall thickness decreasing from 9.8 mm at baseline to 6.3 mm at 12 weeks.

#### *Control vs. Treatment Dogs*

All dogs had normal baseline echocardiographic parameters (Table 1). From baseline to the evaluation at 5 weeks, there was a significant decrease in ejection fraction ( $P = 0.02$ ) and fractional shortening ( $P = 0.005$ ) in all dogs (Figures 4 and 5). Ejection fraction (EF) and fractional shortening (FS) deteriorated in both groups over the course of the study. Values at 12 weeks were not significantly different between control and treatment dogs (EF,  $P = 0.5$ ; FS,  $P = 0.67$ ) (Figure 6 and 7), but were significantly different from baseline (EF,  $P = 0.006$ ; FS,  $P = 0.002$ ).

Left ventricular dimensions increased in all dogs from baseline to 5 weeks. However, measurements of chamber volume were unchanged in the treatment dogs from 5 weeks to 12 weeks and were significantly different from the control dogs, which continued to enlarge over time ( $P = 0.04$ ; Figure 8).

There were some trends to suggest a negative influence on diastolic function when comparing data from 5 weeks to 12 weeks, yet due to small numbers the following results were not statistically significant. For example, left ventricular end diastolic pressure (LVEDP) tended to increase in treatment dogs while remaining unchanged in control dogs (Figure 9 and 10). Isovolumic relaxation time (IVRT) tended to increase in all dogs after induction of cardiomyopathy and either stayed the same or increased in the control dogs at the end of the study. However, in treatment dogs, IVRT tended to decrease from 5 weeks to 12 weeks ( $95 \pm 14.1$  to  $54.5 \pm 0.71$ ;  $P=0.086$ ). Tau slightly decreased in the one control dog in which it was successfully measured ( $37.18$  to  $35.34$ ), while it increased in treatment dogs over the same time frame ( $55.53 \pm 62.76$  to  $66.76 \pm 84.72$ ;  $P = 0.76$ ). However, there was no difference in  $-dP/dt$  between the control and treatment groups at 12 weeks ( $-1491.0 \pm 517.7$  vs.  $-1047.7 \pm 101.2$ ;  $P = 0.277$ ). There were technical errors that prevented assessment of  $dV/dt$  of the control group. However, there was no statistical difference in  $dV/dt$  of the treatment group from 5 to 12 weeks ( $251.7 \pm 12.4$  to  $262.3 \pm 106.36$ ;  $p = 0.867$ ). In addition, left and right pressure tracings of the treatment dogs did not have any characteristics indicative of constrictive pathology (“square root” sign during ventricular filling and elevation and equilibrium of diastolic pressures in all four cardiac chambers).

Histological examination (Figures 11 and 12) found that the synthetic polypropylene mesh around the ventricles was evident as clear spaces, where the material had dropped out during histologic processing, or as refractile and birefringent fragments in these clear zones. Some of the fragments were ovoid in profile, and likely represent whole fiber cross sections, whereas other fragments were irregular to acicular in profile,

likely indicating fragmentation of fibers or biodegradation. These clear spaces, whole fiber cross sections, or fiber fragments were surrounded by a mild to moderate accumulation of reactive macrophages, multinucleate foreign body giant cells, and lesser numbers of plasma cells, and rare neutrophils. These inflammatory foci were most severe immediately surrounding the fiber fragments and became less severe, centrifugally. In some regions, early dystrophic mineralization or mineralized debris was encountered, and appeared as dark blue-black irregular foci. Mild numbers of siderophages (mononuclear phagocytes containing hemosiderin) were found in these regions. In the background of the inflammatory response, was a mild to moderate fibroblastic proliferation. The density of the fibrosis was least nearest the fibers, where presumably, there was on-going inflammation and stimulation for active fibrosis, and became more dense or mature towards the periphery of the inflammatory foci, and ultimately, blended with surrounding connective tissue elements of the epicardium. Polarization microscopy was used to confirm and accentuate the reactive fibrosis. Polarization revealed the presence of moderately dense orange birefringent fibers in the epicardial region, surrounding the polypropylene mesh and extending into surrounding connective tissues. These birefringent fibers were seen in the areas of pleural/pulmonary adhesions as well. In many sections, early fibrous adhesions of the lungs to the fibrous connection tissue and inflammation surrounding the cardiac mesh wrap were observed. The associated pulmonary parenchyma appeared normal, but a mild degree of pleural/subpleural atelectasis was present. These inflammatory lesions remained predominantly on the epicardial surface. Rarely, small tendrils of reactive fibroblasts extended to a minimal degree, mostly along preexisting vascular tissue along the epicardial surface. It should be

noted that in several animals, the myocardial degenerative changes appeared to be quantitatively more severe in the region immediately below the epicardial inflammatory process. Also, severity of epicardial and myocardial changes correlated with the length of survival. Dogs that completed the study had more significant epicardial inflammation and more severe evidence of myocardial degeneration than dogs that died early in the study.

## **Discussion**

We believe that the results of this study demonstrate that PCB can limit progressive ventricular dilatation when used as an interventional treatment in an Adriamycin-induced model of heart failure. While PCB may limit progressive cardiac dilatation without overt interference in diastolic function, no overall improvement in cardiac function is attained with this procedure in dogs with Adriamycin-induced cardiomyopathy. Cardiac function continued to deteriorate despite this surgical treatment.

Vaynblat et al,<sup>7</sup> were the first to describe prosthetic cardiac binding. In that study, a polytetrafluoroethylene mesh was used in a canine model of Adriamycin-induced heart failure. Cardiac binding prevented biventricular dilatation and significantly attenuated the anticipated increase in LVEDP. However no improvement in systolic function was achieved when compared to an untreated group. Yet it was concluded that if no significant advantage of muscle stimulation in cardiomyoplasty can be proven, then an equivalent girdling effect may be achieved through artificial means rather than through muscle harvest. Oh et al,<sup>5</sup> directly compared the effects of adynamic cardiomyoplasty

versus cardiac binding in a canine model of rapid-pacing induced heart failure. This study found that both adynamic cardiomyoplasty and cardiac binding reduce cardiac enlargement and functional deterioration although adynamic cardiomyoplasty appeared to be more effective. The ability of the muscle to both yield to and support the ventricle is an advantage over prosthetic materials as ventricular dilatation is limited but diastolic filling is not compromised. It was concluded that the passive restraint from prosthetic cardiac binding was not sufficient to reverse ventricular remodeling, but proposed that it could be used as an adjunct to other procedures. The results of our study also support this statement as ventricular dilatation was attenuated in 3 of 4 dogs, yet cardiac function continued to deteriorate.

There are significant limitations to this study. In our design, we assumed a minimum of six dogs would be required to detect statistically significant differences. However, we had an untimely mortality rate of 50%, which precludes statistical assessment. This could be due to the model of heart failure that was utilized, as Adriamycin-induced cardiomyopathy is associated with small incidence of fatal arrhythmias. However, thromboembolic disease and sudden death are common in patients undergoing cardiac surgery for heart failure and may actually represent an expected complication. These findings should be considered when calculating the number of subjects to be assessed in future studies. There were also numerous technical difficulties in data accumulation for multiple dogs. This is likely due to inexperience of the primary investigator with some of the methodology as well as the inherent challenges associated with these techniques.

Even though all dogs in this study were administered the same Adriamycin protocol and had identical surgery, there were measurable differences between outcomes. For example, dog #6 deteriorated much more rapidly than the other 3 surviving dogs. This may have related to our failure to appropriately place the wrap. While we attempted to control for the tightness of the wrap between dogs, the placement was largely subjective and tightness could be objectively assessed only based on lack of alteration of CVP. As some positive benefits of PCB have been documented in other experiments, our model of canine heart failure may be too rapid and too severe to allow any improvements from placement of a binding wrap. Although we have improved our success with our model of heart failure, the protocol may need to be adapted to allow for a slower development of cardiomyopathy to further assess the influence of PCB. Further adjustment in the Adriamycin protocol might allow for improved post-surgical survival and more accurately reflect the naturally-occurring condition.

Of particular interest in this study was the potential restraining effect of PCB on diastolic function. While the isovolumetric relaxation phase of diastole can be evaluated by the time course in the fall of LVP, ventricular filling is best assessed from indices of passive left ventricular characteristics derived from the EDPVR. The position of the EDPVR suggests the distensibility of the left ventricle, with a left and upward shift of the curve indicating less ventricular compliance. Increasingly higher pressures are then required to distend the left ventricle enough to accommodate a normal left ventricular volume. There are practical problems in using pressure-volume loops for assessment of contractility and ventricular filling properties, which were experienced in this study. Because of the technical problems, in-depth analysis cannot be performed. However, an

isolated preparation for an individual dog suggests a profound decrease in contractility typically associated with dilated cardiomyopathy due to a decrease in the slope of the ESPVR (Figure 2). Also, the slope of EDPVR is slightly steeper at 12 weeks compared to the single loop at 6 weeks, which could reflect a decrease in compliance (Figure 3).

Another factor that should be considered in the evaluation of PCB is the type of material used to wrap the ventricles. An ideal restraining device would provide the delicate balance of myocardial support without any constrictive effect. The prosthetic wrap used in this study was composed of polypropylene. Recently, some experimental and clinical success has been documented with a custom-made ventricular reshaping device (Corcap Cardiac Support Device [CSD], Acorn Cardiovascular, Inc.), which is composed of polyester.<sup>11-14</sup> The orientation of the polyester material used in the CSD provides compliance in both the circumferential and longitudinal direction, but allows greater compliance in the longitudinal direction (apex to base) than circumferentially.<sup>15</sup> This feature of the CSD attempts to return the left ventricle to a more normal elliptical shape rather than restricting the heart to a contained spherical shape.<sup>15</sup> We speculate that polypropylene is more compliant than polyester, which would still allow for a degree of containment, but would not provide enough support for reverse ventricular remodeling.

Most studies evaluating cardiac binding or ventricular constraint have used either polytetrafluoroethylene (PTFE) or polyester for the wrap material.<sup>6-11</sup> Aside from the information presented here, only one other study has described using polypropylene for cardiac binding.<sup>5</sup> Polypropylene was thought to be a preferable material as it can stretch in both directions, thus providing an elasticity that may be similar to skeletal muscle in that it provides constraint without constriction. However, polypropylene is known to

induce more of a fibrotic response than PTFE.<sup>5</sup> Constrictive pericarditis has been documented in two human patients in which polypropylene mesh was used as a pericardial substitute following mitral valve repair.<sup>13</sup> Symptoms appeared 10 and 12 months after the initial surgery. Constrictive pericarditis was diagnosed by computed tomography and cardiac catheterization, and cardiac function improved following removal of the mesh. PTFE has been evaluated experimentally and used clinically as a pericardial substitute with mixed results.<sup>14-17</sup> In general, minimal adhesions form between the PTFE wrap and the epicardium, which is beneficial if reoperation becomes necessary. However, a significant epicardial reaction obscures coronary anatomy making further surgical procedures extremely difficult. This presence of such an epicardial reaction when PTFE has been used for cardiac binding has not been investigated.

Using polyester as a pericardial substitute had similar results to those seen with PTFE, as it prevents adhesions yet still induces a significant epicardial reaction.<sup>16</sup> This reaction has not been demonstrated with the CSD.<sup>9</sup> The CSD is a knitted polyester jacket which closely and evenly conforms to the surface of the heart, thus providing constraint of ventricular dilatation and diastolic support.<sup>15</sup> The CSD was designed to allow more compliance in a longitudinal direction than in a circumferential direction, which attempts to return the dilated spheroid-shaped left ventricle to a more normal ellipsoid shape. Not only has the CSD been shown to prevent progressive left ventricular dilatation, but it has also improved ejection fraction in experimental studies.<sup>12,18</sup> Long-term implantation of the CSD in a canine model of ischemic dilated cardiomyopathy resulted in a decrease in both left ventricular end-diastolic and end-systolic volume with a leftward shift of the end-systolic pressure-volume relation, indicative of reverse remodeling.<sup>12</sup> Similar results

were demonstrated in clinical cases followed out 12 months postoperatively where left ventricular dimensions, NYHA class, mitral regurgitation, and ejection fraction all improved.<sup>11</sup> At this time, no study evaluating CSD has found any evidence of a restrictive or constrictive cardiac pattern in experimental models or clinical patients.<sup>10,12,18-</sup>

19

Although we are suspicious of a detrimental effect of polypropylene cardiac binding, a longer study is needed. Our study demonstrated histological evidence of a substantial epicardial reaction that was most severe in dogs that completed the study. Unfortunately, due to untimely mortality, we are lacking supportive hemodynamic evidence of diastolic dysfunction. The patients described by Chen and Lai<sup>13</sup> that developed constrictive pericarditis secondary to polypropylene implantation did not develop clinical signs until 10 and 12 months postoperatively. However, the model of cardiomyopathy used in the current study is not ideal for such long-term studies.

Adriamycin-induced cardiomyopathy is severe, progressive, and irreversible. Shah et al,<sup>6</sup> is the only other study aside from ours that uses a canine model of Adriamycin-induced cardiomyopathy to evaluate passive prosthetic ventricular containment. All other studies used rapid-ventricular pacing or coronary microembolization models. The total dose used by Shah was 1 mg/kg of Adriamycin administered intracoronary over weekly doses for 4 weeks. We used a total dose of 1.5 mg/kg of Adriamycin split into two doses administered directly into the left coronary artery one week apart. Although this protocol results in a predictable model of cardiomyopathy and heart failure, perhaps it is too severe to be helped by passive ventricular containment.<sup>20-21</sup> Also of interest is that myocardial degenerative changes

were occasionally observed to be most severe immediately beneath the zone of epicardial inflammation. This could possibly be a result of the additive toxic effects of the polypropylene fibers, fiber degradation products, and inflammatory by-products. This has not been previously reported so we are unsure whether this is a unique finding when polypropylene cardiac binding is used in an Adriamycin-induced model of heart failure or if it is a common problem seen with all forms of ventricular containment that has just been overlooked.

Also of note is that we chose to perform prosthetic cardiac binding after cardiomyopathy had already been induced, which is not the study design typically performed in other experimental studies. This decision allowed us to evaluate prosthetic cardiac binding as an interventional treatment, which more accurately reflects the clinical course of heart failure treatment. Our lack of success may suggest that prosthetic cardiac binding using polypropylene is inadequate as a treatment in established heart failure.

In this study prosthetic cardiac binding using polypropylene mesh in a canine model of Adriamycin-induced cardiomyopathy limited progressive ventricular dilatation without overt interference of diastolic function, although epicardial reaction to the presence of the mesh was severe. No overall improvement in cardiac function was attained when this procedure was used after heart failure had been established.

We found the use of PCB as an interventional treatment for this model to be of no benefit.

## References

1. Carpentier A, Chachques JC, Acar C, et al: Dynamic cardiomyoplasty at seven years. *J Thorac Cardiovasc Surg* 1993;106:42-52
2. Jatene AD, Moreira LF, Stolf NA, et al: Left ventricular function changes after cardiomyoplasty in patients with dilated cardiomyopathy. *J Thorac Cardiovasc Surg* 1991;102:132-139
3. Schreuder JJ, van der Veen FH, van der Velde ET, et al: Beat-to-beat analysis of left ventricular pressure-volume relation and stroke volume by conductance catheter and aortic Modelflow in cardiomyoplasty patients. *Circulation* 1995;91:2010-2017
4. Kawaguchi O, Goto Y, Futaki S, et al: The effects of dynamic cardiac compression on ventricular mechanics and energetics. Role of ventricular size and contractility. *J Thorac Cardiovasc Surg* 1994;107:850-859
5. Oh JH, Badhwar V, Mott BD, et al. The effects of prosthetic cardiac binding and adynamic cardiomyoplasty. *J Thorac Cardiovasc Surg* 1998;116:148-153
6. Shah HR, Vaynblat M, Saliccioli L, et al. Composite cardiac binding in experiment heart failure. *Ann Thorac Surg* 2000;9:429-434
7. Vaynblat M, Chiavarelli M, Shah HR et al. Cardiac binding in experimental heart failure. *Ann Thorac Surg* 1997;64:81-85
8. Power JM, Raman J, Dornom A, et al. Passive ventricular constraint amends the course of heart failure: a study in an ovine model of dilated cardiomyopathy. *Cardiovasc Res* 1999;44:549-555
9. Chaudhry PA, Mishima T, Sharov VG, et al. Passive epicardial containment prevents ventricular remodeling in heart failure. *Ann Thorac Surg* 2000;70:1275-1280
10. Konertz WF, Shapland JE, Hotz H, et al. Passive containment and reverse remodeling by a novel textile cardiac support device. *Circulation* 2001;104[suppl 1]:I207-I275
11. Raman JS, Hata M, Storer M, et al. The mid-term results of ventricular containment (ACORN WRAP) for end-stage ischemic cardiomyopathy. *Ann Thorac Cardiovasc Surg* 2001;7:278-281
12. Saavedra WF, Tunin RS, Paolucci N, et al. Reverse remodeling and enhance adrenergic reserve from passive external support in experimental dilated heart failure. *J Am Coll Cardiol* 2002;19:2069-2076
13. Chen RF, Lai CP. Constrictive pericarditis associated with Marlex mesh. Two case reports. *Tex Heart Inst J* 2001;28:63-64

14. Heydorn WH, Daniel JS, Wade CE. A new look at pericardial substitutes. *J Thorac Cardiovasc Surg* 1987;94:291-296
15. Loebe M, Alexi-Meskhishvili V, Weng Y, et al. Use of polytetrafluoroethylene surgical membrane as a pericardial substitute in the correction of congenital heart defects. *Tex Heart Inst J* 1993;20:213-217
16. Meus PJ, Wernly JA, Campbell CD, et al. Long-term evaluation of pericardial substitutes. *J Thorac Cardiovasc Surg* 1983;85:54-58
17. Ozeren M, Han U, Mavioglu I, et al. Consequences of PTFE membrane used for prevention of re-entry injuries in rheumatic valve disease. *Cardiovasc Surg* 2002;10:489-493
18. Sabbah HN. The cardiac support device and the myosplint: treating heart failure by targeting left ventricular size and shape. *Ann Thorac Surg* 2003;75:S13-19
19. Raman JS, Byrne MJ, Power JM, et al. Ventricular constraint in severe heart failure halts decline in cardiovascular function associated with experimental dilated cardiomyopathy. *Ann Thorac Surg* 2003; 76:141-147
20. Monnet E, Orton EC. A Canine model of heart failure by intracoronary Adriamycin injection: hemodynamic and energetic results. *J Cardiac Failure* 1999;5:255-264
21. MacPhail CM, Monnet E, Getzy D. Adjustments in protocol for induction of canine heart failure by intracoronary Adriamycin injection decreases untimely mortality. Unpublished data.

**Table 4-1.** Selected echocardiographic and hemodynamic data from control and treatment dogs at 12 weeks presented as mean  $\pm$  standard deviation. P-values less than 0.05 were considered significant.

Parameter	Control	Treatment	p-Value
Fractional shortening(%)	24.7 $\pm$ 8.3	18.6 $\pm$ 5.9	0.231
Ejection fraction (%)	51.2 $\pm$ 5.9	38.4 $\pm$ 5.7	0.121
LV chamber diameter – systole (mm)	33.9 $\pm$ 2.8	34.2 $\pm$ 5.2	0.946
LV chamber diameter – diastole (mm)	44.8 $\pm$ 3.5	41.9 $\pm$ 5.1	0.356
LV wall thickness (mm)	9.26 $\pm$ 1.25	9.33 $\pm$ 2.55	0.961
LVDVI (mm/m <sup>2</sup> )	99.4 $\pm$ 23.4	80.1 $\pm$ 31.4	0.04
IVRT (msec)	80.7 $\pm$ 2.8	50.2 $\pm$ 10.2	0.112
Tau (msec)	N/A	66.8 $\pm$ 48.9	N/A
CVP (mmHg)	5.1 $\pm$ 2.4	7.6 $\pm$ 3.3	0.342
RVDP (mmHg)	8.0 $\pm$ 2.8	7.9 $\pm$ 5.1	0.619
PCWP (mmHg)	11.6 $\pm$ 3.3	12.6 $\pm$ 5.0	0.371
LVESP (mmHg)	114.9 $\pm$ 17.0	90.4 $\pm$ 8.3	0.896
LVEDP (mmHg)	22.1 $\pm$ 17.6	29.3 $\pm$ 10.6	0.530
dP/dt Max	1782.5 $\pm$ 701.3	950.7 $\pm$ 91.5	0.356
dP/dt Min	-1491 $\pm$ 517	-1047 $\pm$ 101	0.556
dV/dt	N/A	262.3 $\pm$ 106.36	NA

LVDVI = left ventricular diastolic volume index; IVRT = isovolumetric relaxation time; PCWP = pulmonary capillary wedge pressure; LVESP = left ventricular end-systolic pressure; LVEDP = left ventricular end-diastolic pressure

**Figure 4-1.** Intraoperative photographs following completion of prosthetic cardiac binding.

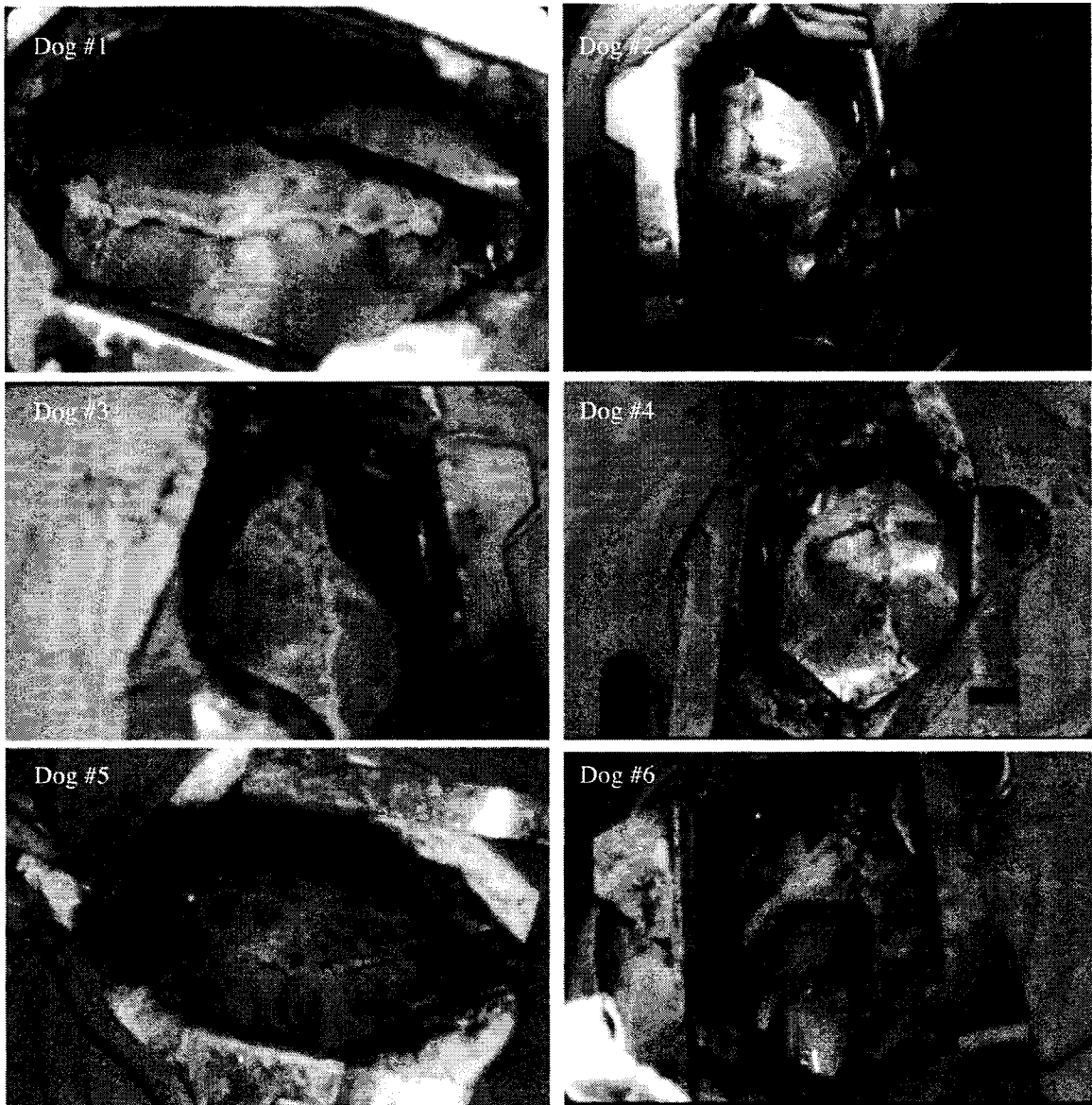


Figure 4-2. Variably loaded pressure-volume loops for Dog #3.

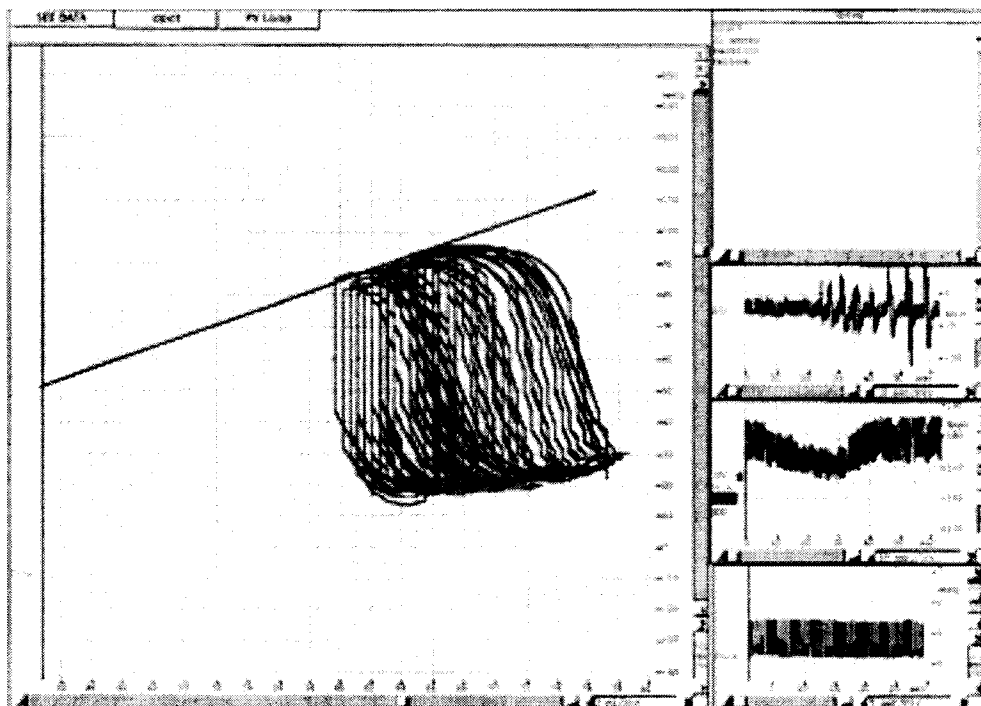
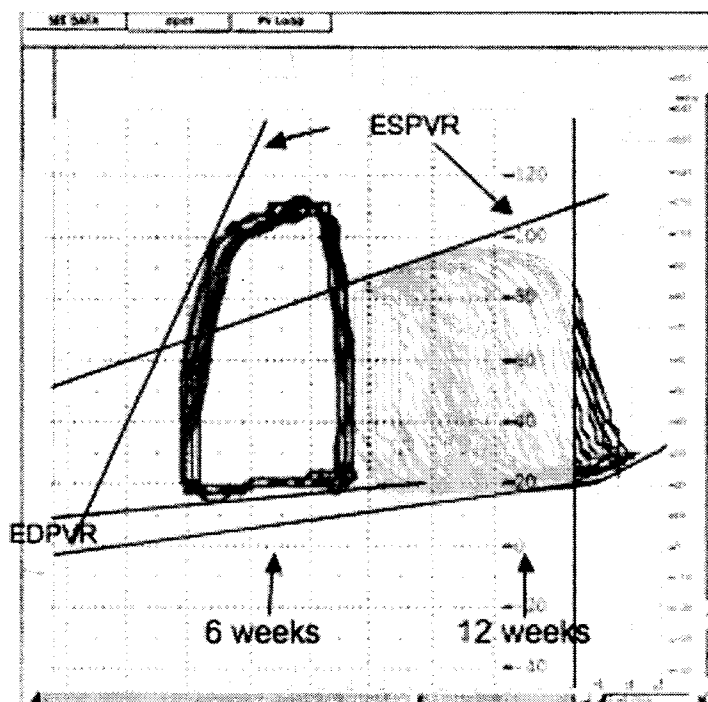
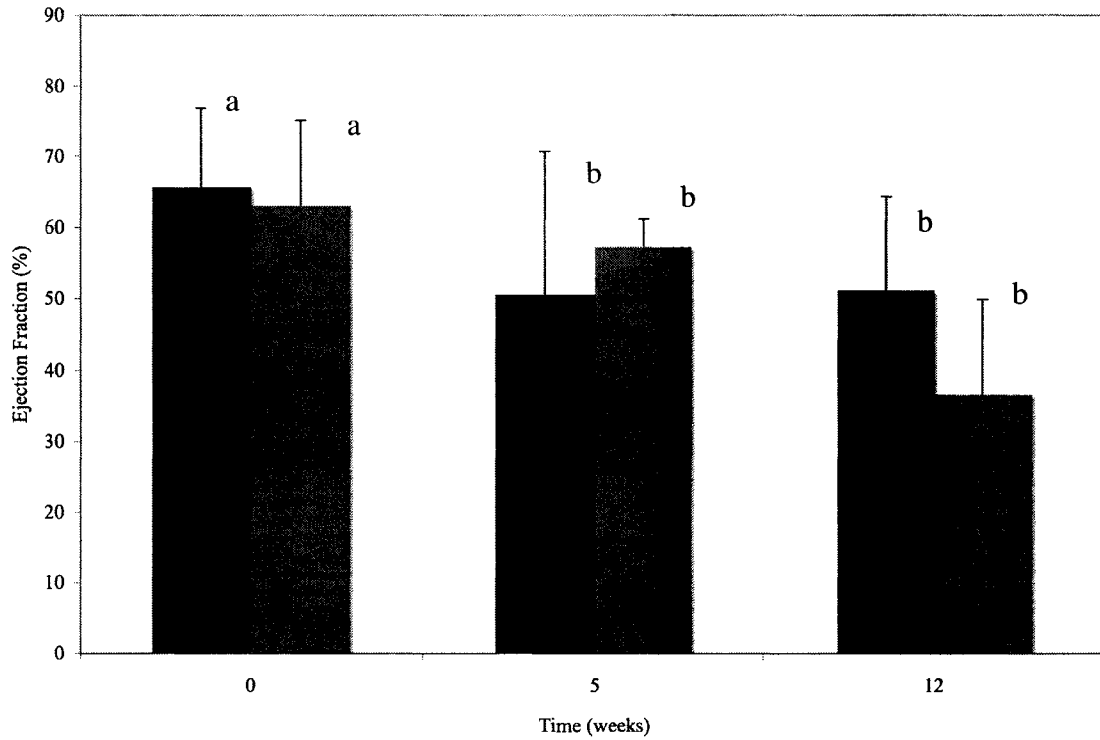


Figure 4-3. Comparison of ESPVR in Dog #3 at 6 weeks and 12 weeks.



**Figure 4-4.** Ejection fraction of the control group (■) and treatment group (▣) at baseline, 5 weeks, and 12 weeks. Values at 12 weeks were not significantly different between control and treatment dogs ( $P = 0.5$ ), but were significantly different from baseline ( $P = 0.006$ ).



**Figure 4-5.** Fractional shortening of the control group (■) and treatment group (■) at baseline, 5 weeks, and 12 weeks. Values at 12 weeks were not significantly different between control and treatment dogs ( $P = 0.43$ ), but were significantly different from baseline ( $P = 0.002$ ).

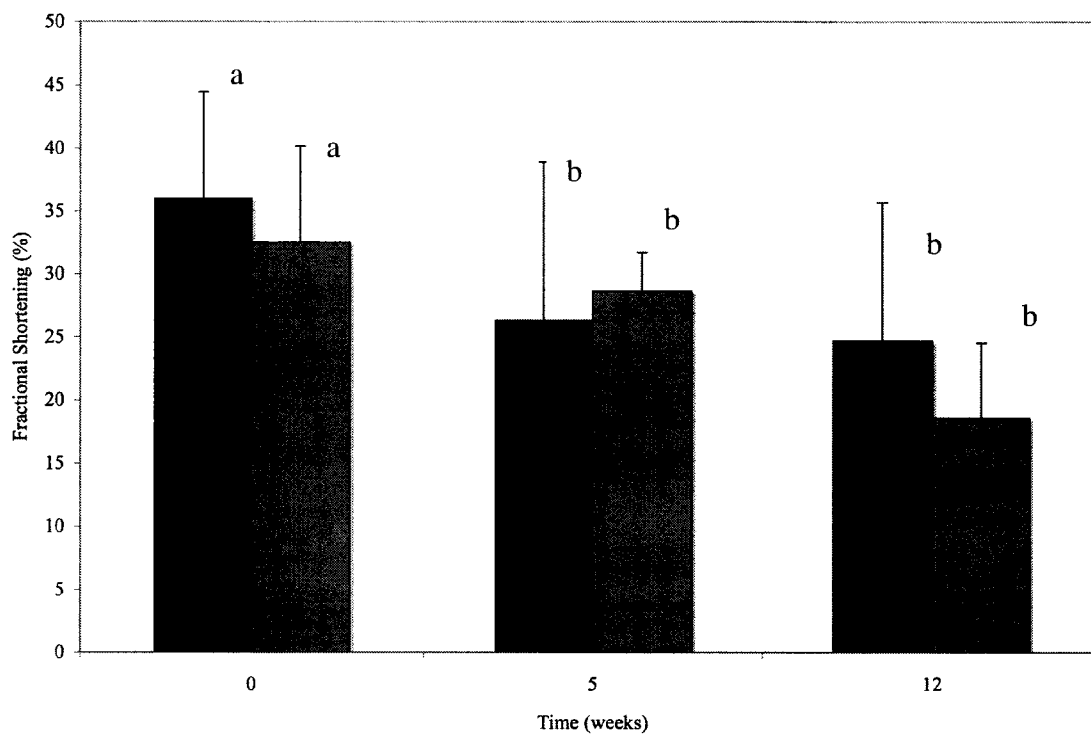


**Figure 4-6.** Comparison of ejection fraction of individual dogs; Control dogs = C# (--◇--); Treatment dogs = T# (—□—).

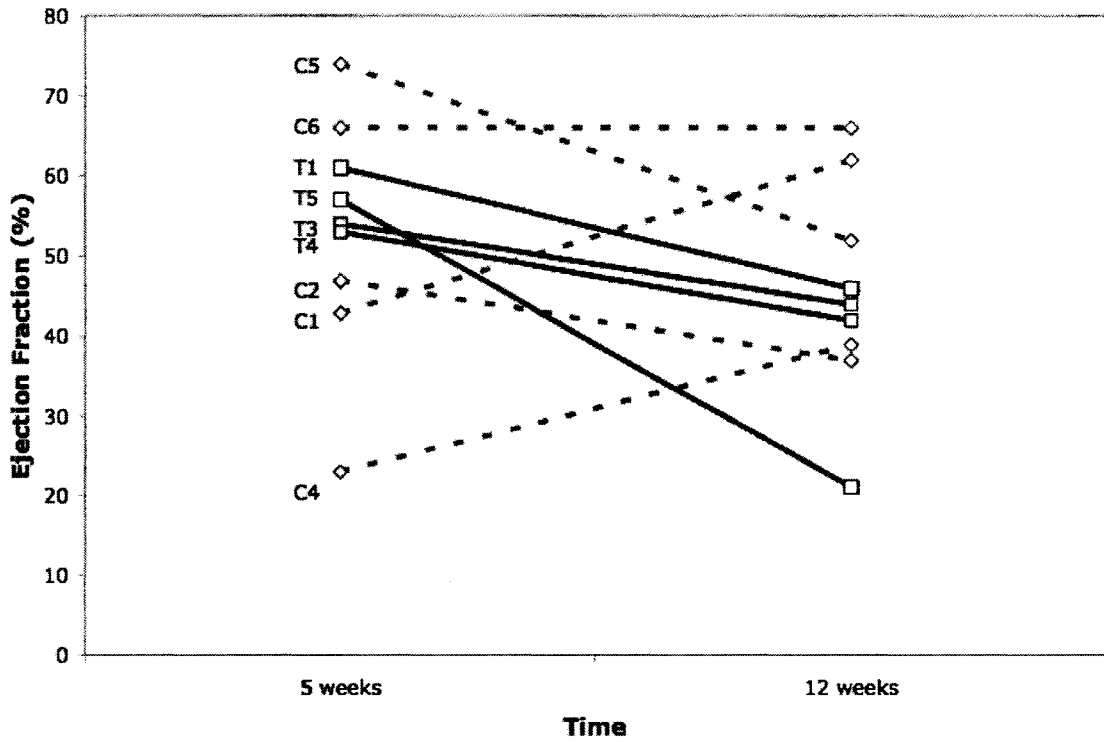


**Figure 4-7.** Comparison of fractional shortening of individual dogs; Control dogs = C# (--◇--); Treatment dogs = T# (—□—).

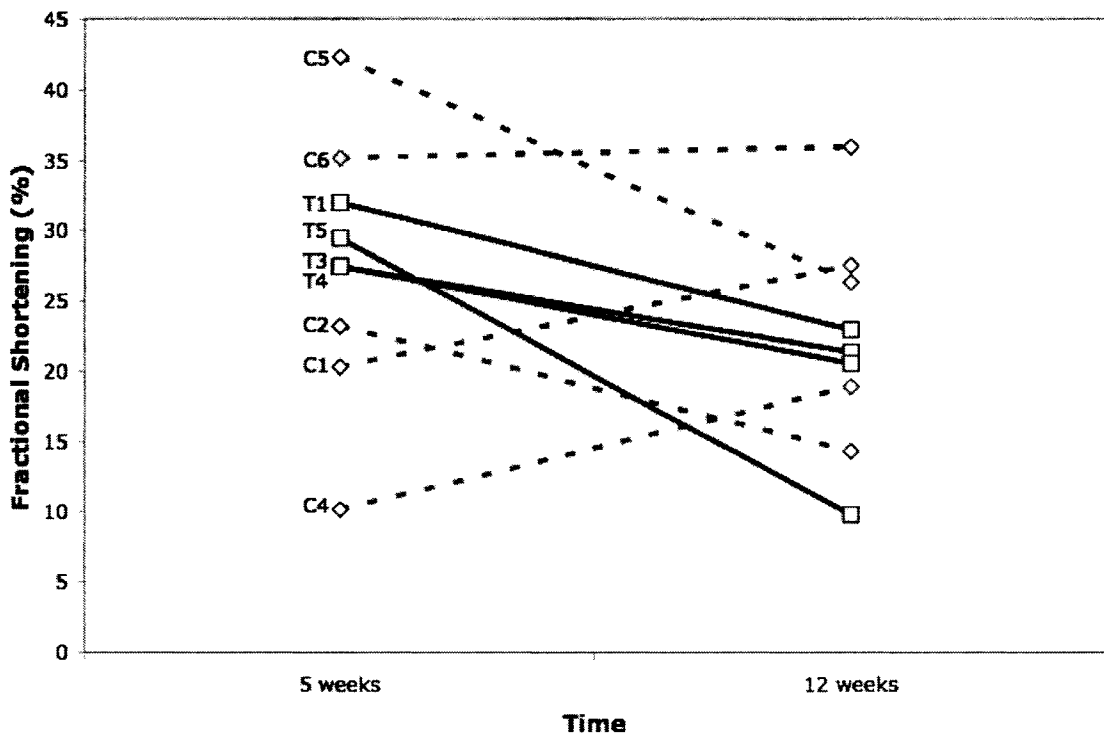


**Figure 4-8.** Left ventricular diastolic volume index (LVDVI) of the control group (■) and treatment group (▒) at baseline, 5 weeks, and 12 weeks. Control dogs were significantly different from treatment dogs at 12 weeks ( $P = 0.04$ ).

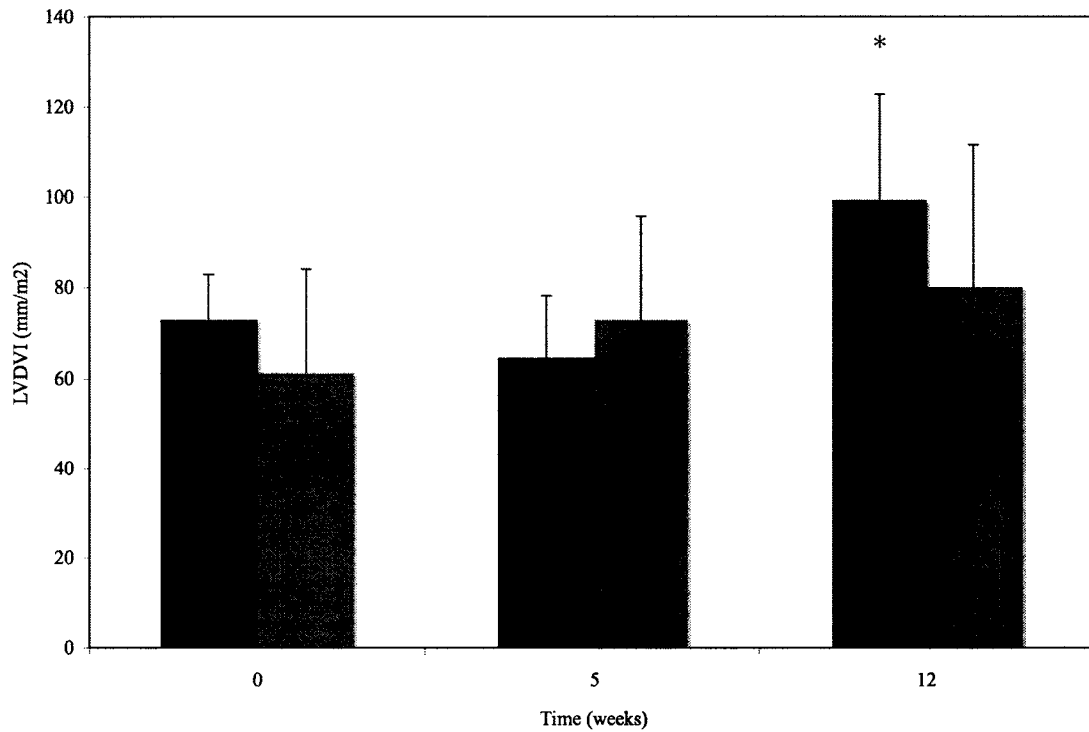


**Figure 4-9.** Left ventricular end-diastolic pressure of the control group (■) and treatment group (▒) at 5 weeks and 12 weeks (P-value = NA).

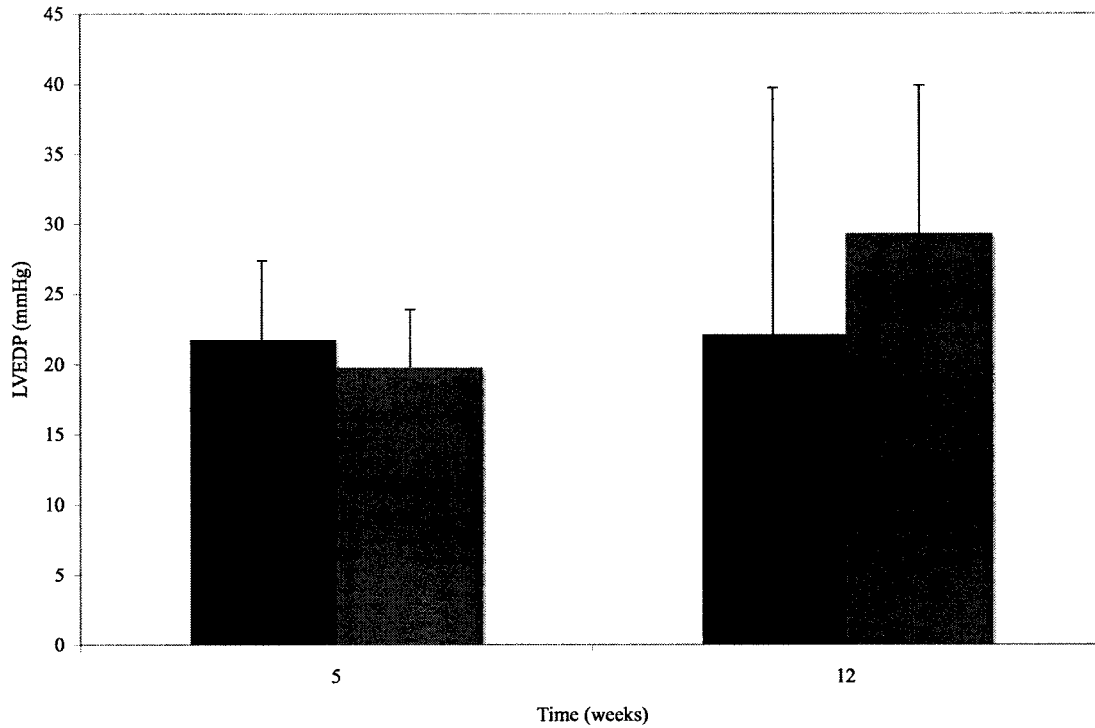


**Figure 4-10.** Comparison of LVEDP of individual dogs; Control dogs = C# (--◇--); Treatment dogs = T# (—□—).

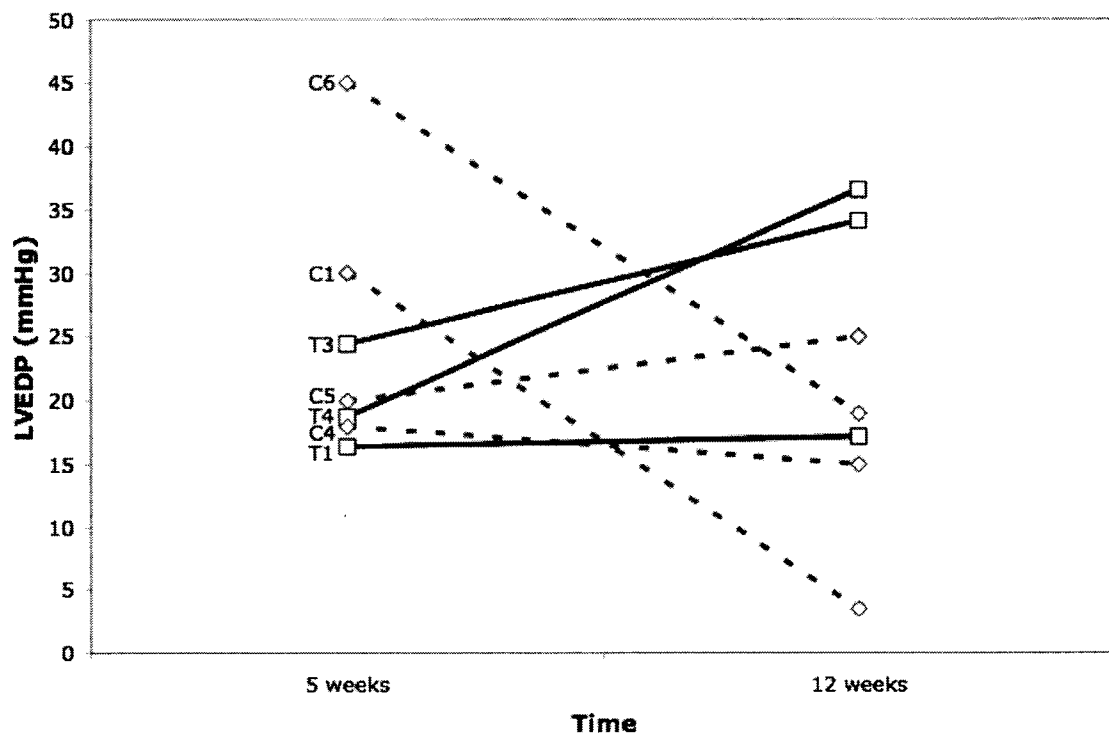


**Figure 4-11.** Representative section of epicardium (10x). Clear spaces (arrows) are areas of mesh dropout. These areas are surrounded by a mild to moderate inflammatory reaction.

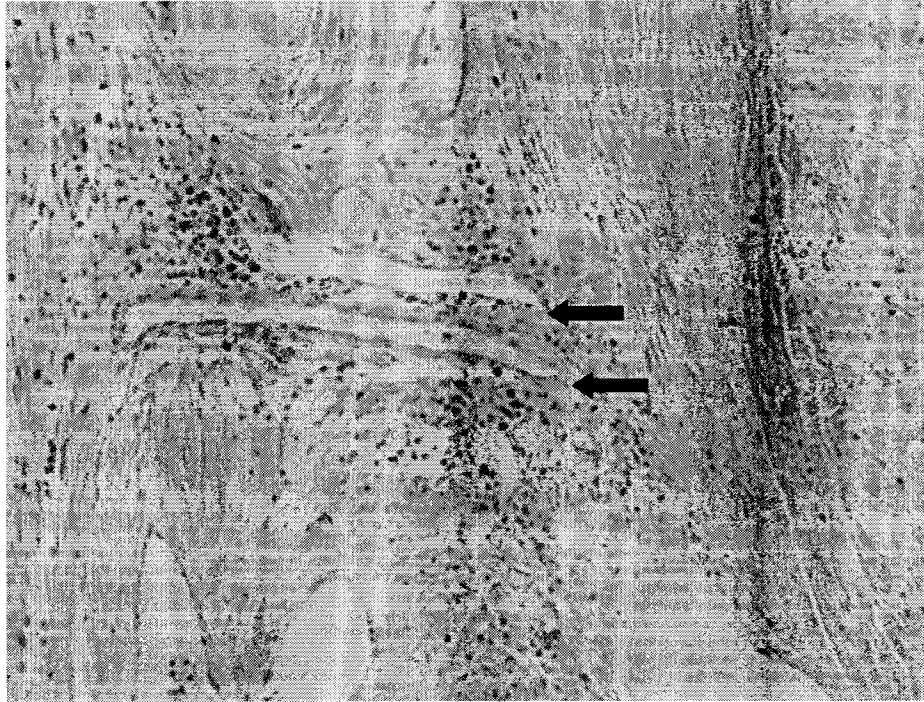
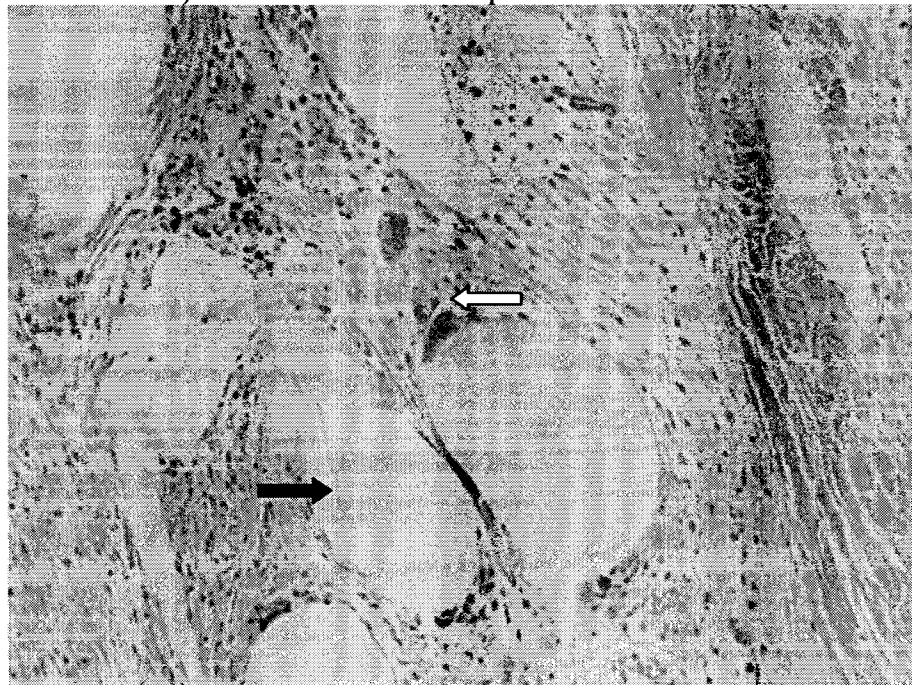


**Figure 4-12.** Representative section of epicardium (10x). Fragments of mesh can be seen in the clear spaces (black arrow). A moderate inflammatory reaction with multinucleated giant cells (white arrow) surrounds these clear spaces.



## CONCLUSIONS AND FUTURE DIRECTIONS

A main focus of my degree program was to investigate the effect prosthetic cardiac binding would have in treating heart failure. This project was a natural progression of work previously performed at Colorado State University. Multiple experiments evaluating dynamic and adynamic cardiomyoplasty have been evaluated at this institution for almost ten years.<sup>1-5</sup> The model of heart failure used in my project was developed at Colorado State University and the adjustments made to the protocol have resulted in a simpler model with a reduced mortality rate.<sup>6</sup> Also, the study design was a reflection of a previous experiments performed to evaluate dynamic and adynamic cardiomyoplasty.<sup>2-5</sup> Using similar study design and the same model of heart failure, allows us to compare results between techniques.<sup>7</sup> Preliminary assessment finds that dynamic cardiomyoplasty appears to be superior to adynamic cardiomyoplasty and prosthetic cardiac binding as it can provide a myocardial sparing effect (Figure 1).

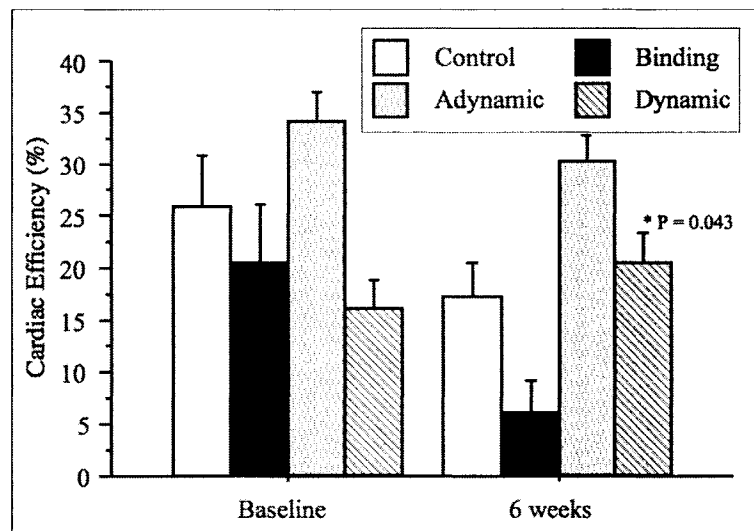


**Figure 5-1. Comparison of cardiac efficiency over time for control dogs and dogs undergoing dynamic cardiomyoplasty, adynamic cardiomyoplasty, and prosthetic cardiac binding. A significant improvement of cardiac efficiency was only present in the dogs receiving dynamic cardiomyoplasty.**

To evaluate the efficacy of a particular treatment there are many ways of assessing heart function. Aside from routine echocardiographic and hemodynamic parameters, it is felt that determination of cardiac energetic parameters and creation of pressure-volume loops provide the most information about cardiac performance. Myocardial oxygen consumption ( $MVO_2$ ) is an important indicator of cardiac performance reflecting oxygen supply and demand. It is a valuable physiological tool as  $MVO_2$  provides a quantifiable link between myocardial performance and total metabolism.

One of the particular objectives of my project was the determination of myocardial oxygen consumption and cardiac efficiency to state whether or not prosthetic cardiac binding had a myocardial sparing effect. From the results it appears that prosthetic cardiac binding is an ineffectual interventional treatment of Adriamycin-induced cardiomyopathy in dogs. The study design also instituted treatment after heart failure was already established. This is not a typical protocol as most studies evaluating prosthetic cardiac binding or ventricular constraint place the wrap prior to induction of heart failure. It is likely that we would have seen better results had the wrap been placed prior to induction of heart failure as in other studies. This method may be applicable for pilot, feasibility, or acute studies, but surgical treatments ultimately need to be challenged in a setting that more accurately reflects the course of treatment of human heart failure.

If prosthetic cardiac binding was successful in limiting progressive ventricular dilatation and providing a myocardial sparing effect to reverse ventricular remodeling this could improve support for clinical interest in this method. The procedure is relatively less invasive when compared to other surgical treatments of heart failure as it

avoids both cardiopulmonary bypass and skeletal muscle harvest. If even minor benefit could be attained, then certainly prosthetic cardiac binding could be utilized as an adjunctive treatment. Most clinical patients that have received the Acorn Cardiac Support Device (Acorn Cardiovascular Inc., St. Paul, MN) do so in concert with other cardiac surgery, usually coronary artery bypass grafting. The CSD has been implanted in over 130 human patients with dilated cardiomyopathy with randomized clinical trials now in progress.<sup>8-9</sup>

I believe our lack of success with prosthetic cardiac binding when compared to the optimistic results reported for CSD is primarily related to the material utilized for the ventricular wrap and the model of heart failure that was chosen. Even if our hemodynamic data were more encouraging, the significant epicardial response to polypropylene mesh is most concerning. To investigate this further, an experiment would be needed that would directly compare the epicardial reaction to polypropylene, polytetrafluoroethylene, and polyester wraps in normal dogs and in dogs with Adriamycin-induced cardiomyopathy. Further histological comparison should also be performed between dogs with Adriamycin-induced cardiomyopathy with and without the presence of cardiac binding. Hopefully this would provide more information with regards to the increase in myocardial degradation in areas of epicardial inflammation. As for the model of heart failure, I believe that the adjustments to the protocol improve this method of inducing dilated cardiomyopathy. It is a simpler and shorter protocol that limits morbidity to the animal and would be more economical. Yet, it seems that Adriamycin-induced dilated cardiomyopathy is too severe a model to be helped by prosthetic cardiac binding, particularly once heart failure has been established.

My familiarity with the technical aspects of measurement of myocardial oxygen consumption and consequent interpretation of those measurements came in the first two projects of this dissertation. Although my first chapter has little to do with treatment of heart failure, I learned about cardiac instrumentation of small laboratory animals. This was performed to assess the effect of a novel inhalant anesthetic agent. Myocardial blood flow was determined through the use of colored microsphere technology. Sevoflurane caused minimal and predictable cardiovascular effects in ferrets, without increasing myocardial metabolic demands. As large animal models are expensive and challenging, the ferret has been shown to be an excellent small animal model for cardiovascular research.

Similar methodology for assessment of cardiac performance was utilized in the second experiment in an effort to determine the mechanism for cardiac dysfunction in dogs with gastric dilatation-volvulus syndrome. Extensive instrumentation was required, but this time in dogs. Although the specific cause of cardiac abnormalities in dogs with GDV still eludes us, it was determined that alteration of splanchnic blood flow negatively influences cardiac efficiency, independent of changes in loading conditions. We speculate that reduction of cardiac efficiency could be an early event that occurs in GDV that may predispose these dogs to further cardiac injury.

In order to determine myocardial oxygen consumption in the main project, coronary blood flow was measured directly by thermodilution using a Baim coronary sinus catheter. Problems with this technique occurred in several dogs at various time points in the project. Specifically there were problems with the catheter, problems with data acquisition, and errors on my part due to technical inexperience.

If I were to improve on the study design of this prosthetic binding project, I would change several specific things. First, there was no baseline hemodynamic data. The first cardiac catheterization occurred after heart failure had already been induced. This wasn't as critical when specifically comparing treatment dogs to control dogs from 5 to 12 weeks. However, it limited my ability to draw conclusions from adjustments to the Adriamycin protocol for induction of heart failure. Also the small number of dogs utilized in this project was a significant problem. The mortality of our control dogs was within the expected limits; however the 50% mortality rate of our treatment dogs was unacceptable. One dog did die from pulmonary thromboembolism, which was most likely secondary to the duration of use of multiple lumen catheters in this dog. After this incident occurred, we removed the triple-lumen jugular catheters in the remaining dogs immediately after surgery. If we exclude this dog, our mortality rate for our treatment dogs would be 40%, which is closer to mortality rates reported in other studies.<sup>6</sup> Small numbers of animals are typically used in this type of study due to budget constraints. Housing and care of research dogs is expensive as is every anesthetic procedure they undergo. Ideally, I would have liked to have doubled the number of dogs used. Therefore, even with a 40% mortality rate, we would likely have 14 or 15 dogs that would complete the study and allow more in-depth statistical comparison of the data.

Another change I would have performed in hindsight would be the routine sedation of the dogs for the echocardiographic examinations. There is a general reluctance to sedate the animals to avoid interference with echocardiographic parameters. However, often the research dogs are extremely excitable, and rather than sedate the dogs, we chose to abort several exams. Consequently, there are gaps in our data that

could have been avoided, specifically with regards to parameters reflecting diastolic function, such as IVRT and E:A ratios.

If I were to further investigate prosthetic cardiac binding, I would consider a much longer study. Although potentially cost prohibitive, a 12-month study would clarify the issue of constriction caused by the presence of the wrap. A study that investigated various materials for pericardial substitutes, followed dogs out 3, 6, 9 and 12 months to assess the degree of reaction caused.<sup>11</sup> And as the reported clinical cases of constrictive pericarditis associated with polypropylene demonstrated, problems did not arise until an average of 11 months after the original surgery.<sup>12</sup> Of all the things I have learned from this study, I am most intrigued by the epicardial reaction and the apparent association with increased myocardial degenerative changes. Although it is unlikely that I would further investigate prosthetic cardiac binding in this model of heart failure, I would be interested in evaluating the long-term effects of complete ventricular wraps made from both polypropylene and polyester.

Work in the area of surgical support for heart failure has continued at Colorado State University (CSU). From the overall negative experience with polypropylene cardiac binding, continued research in this area this institution has been redirected back toward the use of skeletal muscle for cardiac assistance. Globally, a renewed interest has developed in dynamic cardiomyoplasty. A new stimulation protocol has been developed to avoid the muscle degeneration that results from chronic electrical stimulation.<sup>13-14</sup> The rate of muscle stimulation is based on a set heart rate cut-off thus providing the muscle wrap periods of rest when the patient is sleeping or otherwise undergoing minimal exertion. Other investigations are focusing on better preservation of the latissimus dorsi

muscle through preconditioning, heat shock therapy, and improved perfusion.<sup>15-18</sup>

Cellular cardiomyoplasty is a new approach aimed at regenerating cardiac muscle tissue.

Cells are implanted in the myocardium to grow new muscle fibers in damage areas in order to improve contractility.<sup>19</sup> And finally, there has also been a renewed interest in dynamic aortomyoplasty.

Dynamic aortomyoplasty is a surgical technique similar to cardiomyoplasty, but the latissimus dorsi muscle is wrapped around the aorta instead of the ventricles and it is stimulated to contract during diastole every other heart beat. Following harvest, the muscle is wrapped around a segment of the thoracic aorta. Intramuscular electrodes are implanted in the latissimus dorsi and sensing electrodes are attached to the ventricle. Both sets of electrodes are then connected to a cardiomyostimulator which is implanted in the patient. Following a latency period, the muscle undergoes a period of training to transform type II fast-twitch to type I slow-twitch muscle fibers to provide fatigue resistance to the chronically stimulated muscle. After an 8 to 12 week conditioning period, the cardiomyostimulator is programmed to provide optimal muscle contraction for the individual patient. The muscle is typically stimulated to contract every second or third heart beat during diastole. Additional and more important goals of dynamic aortomyoplasty, aside from improving stroke volume, include reduction of afterload prior to systole and enhancement of coronary blood flow during diastole.

Advantages of dynamic aortomyoplasty purported over other surgical procedures are that it is technically easier to perform and it can be performed without cardiopulmonary bypass or aortic cross-clamping. It has also been successfully performed with thoracoscopy in isolated studies.<sup>20</sup> Aortomyoplasty makes use of a

biologic power source which is more economical than mechanical devices and it avoids risk of infection or thromboembolism encountered with implants such as intra-aortic balloon pumps (IABP) or ventricular assist devices. Dynamic aortomyoplasty may be preferable to dynamic cardiomyoplasty as, although muscle harvest is similar, aortomyoplasty avoids significant manipulation of the already diseased heart which may reduce intraoperative morbidity. It has been suggested that aortomyoplasty could be used in place of cardiomyoplasty for NYHA class IV patients to reduce operative risk.<sup>21</sup> Other suggested indications for aortomyoplasty are to use this technique as a bridge to cardiac transplantation or as an adjunct to dynamic cardiomyoplasty.<sup>22</sup> Contraindications for dynamic aortomyoplasty are aortic wall calcification, aortic valve regurgitation, and Marfan's disease.<sup>23</sup>

Dynamic aortomyoplasty was first described in 1990 by Chachques et al, in an experimental model of acute heart failure in goats.<sup>24</sup> This technique was found to significantly increase subendocardial viability index (SVI) in normal hearts and after induction of heart failure. Larger increases in SVI were observed if a pericardial patch was used to enlarge the ascending aorta. Chachques also demonstrated chronic diastolic augmentation with dynamic aortomyoplasty.<sup>25</sup> Hemodynamic studies were performed on goats 12 and 24 months after receiving aortomyoplasty which found significant increase in SVI at the basal state and after induction of acute heart failure. Histologically, aortic wall anatomy was preserved and tight adhesions had formed between the aortic adventitia and latissimus dorsi.

Dynamic aortomyoplasty was first performed in a clinical patient in 1992 and as of 1997 had been performed in 28 patients with significant improvement in NYHA

functional class and quality of life. Trainini evaluated 15 aortomyoplasty patients by comparing preoperative hemodynamic data compared to data collected at 6 and 12 months postoperatively.<sup>26</sup> A significant decrease in the number of yearly hospitalizations, NYHA functional class, right ventricular diameter, and left atrial diameter was found. There were also marked improvements in a 6-minute walking test, cardiac index, peak oxygen consumption, shortening fraction, and ejection fraction. It was suggested that the ideal candidate for aortomyoplasty is a patient that is not sick enough for mechanical ventricular assist or heart transplantation, but for whom medical management is not abating clinical signs.<sup>26</sup> However, more long-term hemodynamic and functional evaluations are required to support dynamic aortomyoplasty as a surgical alternative for patients with heart failure.

The value of aortomyoplasty for dilated cardiomyopathy is still mostly undetermined. A feasibility study of aortomyoplasty in dogs with naturally occurring DCM was conducted in 1996.<sup>27</sup> No hemodynamic studies were performed on these dogs, but echocardiographic parameters suggested some degree of ventricular unloading. We are currently examining dynamic aortomyoplasty at CSU. Our own feasibility and pilot project was begun in Summer 2004. It is an acute study to further evaluate difference between ascending (Figure 1) and descending dynamic aortomyoplasty (Figure 2) in normal dogs. Our objectives are to learn how to perform different surgical variations of dynamic aortomyoplasty in the normal dog and to determine which technique is most feasible and effective.

We anticipate that data obtained from this study will aid in obtaining funding for a larger project investigating dynamic aortomyoplasty. The objective of this study is to

evaluate dynamic descending aortomyoplasty as an interventional treatment for cardiomyopathy. Results from this study would allow us to compare the effect of dynamic aortomyoplasty to the results from the previous studies that have evaluated dynamic cardiomyoplasty, adynamic cardiomyoplasty, and prosthetic cardiac binding in a similar model.

## References

1. Orton EC, Monnet E, Brevard SM, et al. Dynamic cardiomyoplasty for treatment of idiopathic dilatative cardiomyopathy. *J Am Vet Med Assoc* 1994;205:1415-1419
2. Monnet E, Orton EC. Myocardial oxygen consumption is affected by dynamic cardiomyoplasty in dogs with Adriamycin-induced cardiomyopathy. *J Card Surg* 1998;13:475-483
3. Monnet E, Orton EC, Jacobs G, et al. Fluoroscopic determination of latissimus dorsi muscle shortening fraction after dynamic cardiomyoplasty. *Pacing Clin Electrophysiol* 1998;21:1741-1746
4. Monnet E, Orton EC, Child G, et al. Neuromuscular function of the latissimus dorsi muscle in goats after dynamic cardiomyoplasty. *Pacing Clin Electrophysiol* 1999;22:125-1633
5. Monnet E. Adynamic cardiomyoplasty: Effect on cardiac efficiency and contractile reserve in dogs with Adriamycin-induced cardiomyopathy. *J Card Surg* 2002;17:60-69
6. Monnet E, Orton EC. A canine model of heart failure by intracoronary Adriamycin injection: hemodynamic and energetic results. *J Cardiac Failure* 1999;5:255-264
7. Monnet E, MacPhail CM, Orton EC, et al. Dynamic cardiomyoplasty, adynamic cardiomyoplasty, or cardiac binding: What is the optimal procedure for the treatment of heart failure? *Basic Appl Myol* 2004;14:256.
8. Raman JS, Byrne MJ, Power JM, et al. Ventricular constraint in severe heart failure halts decline in cardiovascular function associated with experimental dilated cardiomyopathy. *Ann Thorac Surg* 2003; 76:141-147
9. Oz MC, Konertz WF, Kleber FX, et al. Global experience with the Acorn cardiac support device. *J Thorac Cardiovasc Surg* 2003;126:983-991
10. Bristow MR, Mason JW, Billingham ME, et al. Doxorubicin cardiomyopathy: Evaluation by phonocardiography, endomyocardial biopsy, and cardiac catheterization. *Ann Intern Med* 1978;88:168-175
11. Meus PJ, Wernly JA, Campbell CD, et al. Long-term evaluation of pericardial substitutes. *J Thorac Cardiovasc Surg* 1983;85:54-58
12. Chen RF, Lai CP. Constrictive pericarditis associated with Marlex mesh. Two case reports. *Tex Heart Inst J* 2001;28:63-64

13. Rigatelli G, Rigatelli G, Barbiero M, et al. "Demand" stimulation of latissimus dorsi heart wrap: experience in humans and comparison with adynamic girdling. *Ann Thorac Surg* 2003;76:1587-1592
14. Rigatelli G, Carraro U, Barbiero M, et al. A review of the concept of circulatory bioassist focused on the "new" demand dynamic cardiomyoplasty: the renewal of dynamic cardiomyoplasty? *Angiology* 2003;54:301-306
15. Ianuzzo CD, Ianuzzo SE, Felid M, et al. Cardiomyoplasty: preservation of the latissimus dorsi muscle. *J Card Surg* 1995;10:104-110
16. Ianuzzo CD, Ianuzzo SE, Locke M, et al. Preservation of the latissimus dorsi muscle during cardiomyoplasty surgery. *J Card Surg* 1996;11:99-108
17. Monnet E. Bipediculated skeletal muscle flap to assist the failing heart. Unpublished data.
18. Guadagnoli M, Monnet E, Chachques JC. Can the Vineberg procedure improve blood supply of the muscle flap during dynamic cardiomyoplasty? A pilot study. Unpublished data
19. Chachques JC, Acar C, Herreros J, et al. Cellular cardiomyoplasty: clinical application. *Ann Thorac Surg* 2004;77:11212-1130.
20. Mesana TG, Mouly-Bandini A, Ferzoco SJ, et al: Dynamic aortomyoplasty: clinical experience and thoracoscopic surgery feasibility study. *J Card Surg* 1998;13:60-69.
21. Bolotin G, van Der Veen FH, Lorusso R, et al: Aortomyoplasty. *Basic Appl Myol* 1998;8:59-65.
22. Takahashi R, Yozu R, Kurosaka Y, et al: Assisted circulation using cardiomyoplasty together with aortomyoplasty. *Artif Organs* 1993;17:914-918.
23. Chachques JC, Grandjean PA, and Carpentier A: Dynamic aortomyoplasty. In Carpentier MD, Chachques JC, Grandjean PA (eds.): *Cardiomyoplasty*. Futura Publishing, Mount Kisco, NY, 1991, pp 199-208.
24. Chachques JC, Grandjean PA, Cabrera Fischer EI, et al: Dynamic aortomyoplasty to assist left ventricular failure. *Ann Thorac Surg* 1990;49:225-230.
25. Chachques JC, Haab F, Cron C, et al: Long-term effects of dynamic aortomyoplasty. *Ann Thorac Surg* 1994;58:128-134.
26. Trainini J, Cabrera Fischer EI, Barisani J, et al: Dynamic aortomyoplasty in treating end-stage heart failure. *J Heart Lung Transplant* 2002;21:1068-1073.

27. White RN, Cobb MA, Brownlie SE, et al: Skeletal muscle extra-aortic counterpulsation in dogs with dilated cardiomyopathy. *J Small Anim Pract* 1997;38:554-560.

**Figure 5-2.** Intraoperative photograph of ascending dynamic aortomyoplasty.



**Figure 5-3.** Intraoperative photograph of descending dynamic aortomyoplasty.

